

# PACIFIC EARTHQUAKE ENGINEERING RESEARCH CENTER

## **Comparison of the Response of Small- and Large-Component Cripple Wall Specimens Tested under Simulated Seismic Loading**

**A Report for the “Quantifying the Performance of  
Retrofit of Cripple Walls and Sill Anchorage in Single-  
Family Wood-Frame Buildings” Project**

**Brandon Schiller**

**Tara Hutchinson**

University of California San Diego

**Kelly Cobeen**

Wiss, Janney, Elstner Associates, Inc.

PEER Report 2020/21

Pacific Earthquake Engineering Research Center  
Headquarters, University of California at Berkeley

November 2020

#### Disclaimer

The opinions, findings, and conclusions or recommendations expressed in this publication are those of the author(s) and do not necessarily reflect the views of the study sponsor(s), the Pacific Earthquake Engineering Research Center, or the Regents of the University of California.

#### Disclaimer

The opinions, findings, and conclusions or recommendations expressed in this publication are those of the author(s) and do not necessarily reflect the views of the study sponsor(s), the Pacific Earthquake Engineering Research Center, or the Regents of the University of California.

# **Comparison of the Response of Small- and Large-Component Cripple Wall Specimens Tested under Simulated Seismic Loading**

**A Report for the “Quantifying the Performance of  
Retrofit of Cripple Walls and Sill Anchorage in  
Single-Family Wood-Frame Buildings” Project**

**Brandon Schiller**

**Tara Hutchinson**

University of California San Diego

**Kelly Cobeen**

Wiss, Janney, Elstner Associates, Inc.

PEER Report No. 2020/21  
Pacific Earthquake Engineering Research Center  
Headquarters at the University of California, Berkeley

November 2020



## ABSTRACT

This report is one of a series of reports documenting the methods and findings of a multi-year, multi-disciplinary project coordinated by the Pacific Earthquake Engineering Research Center (PEER and funded by the California Earthquake Authority (CEA). The overall project is titled “*Quantifying the Performance of Retrofit of Cripple Walls and Sill Anchorage in Single-Family Wood-Frame Buildings,*” henceforth referred to as the “PEER–CEA Project.”

The overall objective of the PEER–CEA Project is to provide scientifically based information (e.g., testing, analysis, and resulting loss models) that measure and assess the effectiveness of seismic retrofit to reduce the risk of damage and associated losses (repair costs) of wood-frame houses with cripple wall and sill anchorage deficiencies as well as retrofitted conditions that address those deficiencies. Tasks that support and inform the loss-modeling effort are: (1) collecting and summarizing existing information and results of previous research on the performance of wood-frame houses; (2) identifying construction features to characterize alternative variants of wood-frame houses; (3) characterizing earthquake hazard and ground motions at representative sites in California; (4) developing cyclic loading protocols and conducting laboratory tests of cripple wall panels, wood-frame wall subassemblies, and sill anchorages to measure and document their response (strength and stiffness) under cyclic loading; and (5) the computer modeling, simulations, and the development of loss models as informed by a workshop with claims adjusters.

This report is a product of *Working Group 4: Testing*, whose central focus was to experimentally investigate the seismic performance of retrofitted and existing cripple walls. Two testing programs were conducted; the University of California, Berkeley (UC Berkeley) focused on large-component tests; and the University of California San Diego (UC San Diego) focused on small-component tests. The primary objectives of the tests were to develop descriptions of the load-deflection behavior of components and connections for use by Working Group 5 in developing numerical models and collect descriptions of damage at varying levels of drift for use by Working Group 6 in developing fragility functions. This report considers two large-component cripple wall tests performed at UC Berkeley and several small-component tests performed at UC San Diego that resembled the testing details of the large-component tests.

Experiments involved imposition of combined vertical loading and quasi-static reversed cyclic lateral load on cripple wall assemblies. The details of the tests are representative of era-specific construction, specifically the most vulnerable pre-1945 construction. All cripple walls tested were 2 ft high and finished with stucco over horizontal lumber sheathing. Specimens were tested in both the retrofitted and unretrofitted condition. The large-component tests were constructed as three-dimensional components (with a 20-ft × 4-ft floor plan) and included the cripple wall and a single-story superstructure above. The small-component tests were constructed as 12-ft-long two-dimensional components and included only the cripple wall. The pairing of small- and large-component tests was considered to make a direct comparison to determine the following: (1) how closely small-component specimen response could emulate the response of the large-component specimens; and (2) what boundary conditions in the small-component specimens led to the best match the response of the large-component specimens.

The answers to these questions are intended to help identify best practices for the future design of cripple walls in residential housing, with particular interest in: (1) supporting the realistic design of small-component specimens that may capture the response large-component specimen response; and (2) to qualitatively determine where the small-component tests fall in the range of lower- to upper-bound estimation of strength and deformation capacity for the purposes of numerical modelling. Through these comparisons, the experiments will ultimately advance numerical modeling tools, which will in turn help generate seismic loss models capable of quantifying the reduction of loss achieved by applying state-of-practice retrofit methods as identified in *FEMA P-1100 Vulnerability-Base Seismic Assessment and Retrofit of One- and Two-Family Dwellings*. To this end, details of the test specimens, measured as well as physical observations, and comparisons between the two test programs are summarized in this report.

## **ACKNOWLEDGMENT AND DISCLAIMER**

### **ACKNOWLEDGMENT**

This research project benefited from the interaction of many researchers and practitioners. The authors are grateful for the technical input and advice from all members of the PEER–CEA Project Team including Principal Investigator, Yousef Bozorgnia, Project Coordinator, Grace Kang, and members of the Working Groups, Jake Baker, Henry Burton, Greg Deierlein, Seb Ficcadenti, Bret Lizundia, Curt Haselton, Charlie Kircher, Thor Matteson, Frank McKenna, Vahid Mahdavifar, Silvia Mazzoni, Gilberto Mosqueda, Sharyl Rabinovici, Evan Reis, Chia-Ming Uang, John van de Lindt, Dave Welch, and Farzin Zareian. In addition, the authors are grateful for the technical input and advice from the members of the Project Review Panel, which includes: Colin Blaney, Doug Hohbach, John Hooper, and Charlie Scawthorn.

The authors would also like to thank Dr. Chris Latham, Darren McKay, Noah Aldrich, Michael Sanders, Abdullah Hamid, Andrew Sanders, Sergio Suarez, Carla Tutolo, Derek McDanell, Edna Mariela, William Deeley, Selena Nichols, Armando Godoy-Velasquez, and all undergraduate students staffed at UC San Diego Powell Structural Labs for their continuous work in supporting the execution of the experimental program discussed herein.

### **DISCLAIMER**

This research study was funded by the California Earthquake Authority (CEA). The support of the CEA is gratefully acknowledged. The opinions, findings, conclusions, and recommendations expressed in this publication are those of the authors and do not necessarily reflect the views of the CEA, Pacific Earthquake Engineering Research Center (PEER), members of the Project Team, or the Regents of the University of California.



# CONTENTS

<b>ABSTRACT</b> .....	<b>iii</b>
<b>ACKNOWLEDGMENT and DISCLAIMER</b> .....	<b>v</b>
<b>TABLE OF CONTENTS</b> .....	<b>vii</b>
<b>LIST OF TABLES</b> .....	<b>xi</b>
<b>LIST OF FIGURES</b> .....	<b>xiii</b>
<b>1 INTRODUCTION</b> .....	<b>1</b>
<b>1.1 General</b> .....	<b>1</b>
<b>1.2 Purpose of This Report</b> .....	<b>2</b>
<b>1.3 Organization of This Report</b> .....	<b>3</b>
<b>2 OVERVIEW OF TEST SPECIMENS</b> .....	<b>5</b>
<b>2.1 Small-Component Specimens</b> .....	<b>5</b>
2.1.1 Small-Component Specimen A-1 .....	6
2.1.2 Small-Component Specimen A-2 .....	9
2.1.3 Small-Component Specimen A-3 .....	11
2.1.4 Small-Component Specimen A-4 .....	13
2.1.5 Small-Component Specimen A-20 .....	15
2.1.6 Small-Component Specimen A-5 .....	17
2.1.7 Small-Component Specimen A-19 .....	20
2.1.8 Small-Component Specimen Summary .....	24
<b>2.2 Large-Component Specimens</b> .....	<b>24</b>
2.2.1 Large-Component Specimen AL-1 .....	26
2.2.2 Large-Component Specimen AL-2.....	26
<b>3 LOAD-DEFLECTION RESPONSE COMPARISON</b> .....	<b>29</b>
<b>3.1 Load-Deflection Response</b> .....	<b>29</b>
<b>3.2 Overlays of Small- and Large-Component Response</b> .....	<b>34</b>
<b>3.3 Comparison of Lateral Strength</b> .....	<b>38</b>
<b>3.4 Comparison of Drift Ratios</b> .....	<b>40</b>
<b>3.5 Comparison of Post-Peak Drift Capacity</b> .....	<b>42</b>

3.6	<b>Comparison of Other Response Characteristics.....</b>	<b>44</b>
<b>4</b>	<b>COMPARISON OF UPLIFT BEHAVIOR.....</b>	<b>45</b>
4.1.1	Comparison of Anchor Bolt Loads.....	45
4.1.2	Comparison of Uplift Displacements.....	50
4.1.3	Comparison of Damage Associated with Uplift and Slip at Anchor Bolts.....	50
4.1.4	Discussion of Uplift and Slip at Anchor Bolts.....	54
<b>5</b>	<b>COMPARISON OF OBSERVATIONS AND DAMAGE.....</b>	<b>55</b>
<b>5.1</b>	<b>Comparison of Observations and Damage at 1.4% Drift Ratio.....</b>	<b>55</b>
5.1.1	Comparison of Observations and Damage at 1.4% Drift Ratio for Unretrofitted Specimens.....	55
5.1.2	Comparison of Damage at 1.4% Drift Ratio for Specimens with Retrofit.....	66
<b>5.2</b>	<b>Comparison of Observations and Damage at Lateral Strength.....</b>	<b>72</b>
5.2.1	Comparison of Damage at Lateral Strength for Unretrofitted Specimens.....	72
5.2.2	Comparison of Damage at Lateral Strength for Specimens with Retrofit.....	85
<b>5.3</b>	<b>Comparison of Observations and Damage at 20% Residual Lateral Force.....</b>	<b>91</b>
5.3.1	Comparison of Observations and Damage at 20% Residual Lateral Force for Unretrofitted Specimens.....	91
5.3.2	Comparison of Observations and Damage at 20% Residual Lateral Strength for Specimens with Retrofit.....	105
<b>6</b>	<b>DISCUSSION.....</b>	<b>115</b>
<b>6.1</b>	<b>Cripple Wall Lateral Strength.....</b>	<b>115</b>
<b>6.2</b>	<b>Cripple Wall Drift at Lateral Capacity.....</b>	<b>116</b>
<b>6.3</b>	<b>Cripple Wall Post-Peak Load-Deflection Behavior.....</b>	<b>116</b>
<b>6.4</b>	<b>Cripple Wall Boundary Conditions for Future Testing.....</b>	<b>117</b>
<b>6.5</b>	<b>Cripple Wall Uplift Behavior.....</b>	<b>117</b>
<b>6.6</b>	<b>Comparison of Observed Damage.....</b>	<b>118</b>
<b>7</b>	<b>CONCLUSIONS.....</b>	<b>119</b>
<b>7.1</b>	<b>Overarching Conclusions.....</b>	<b>119</b>

7.2	<b>Future Research Needs</b> .....	121
<b>REFERENCES</b> .....		125
<b>APPENDIX A</b> .....		127
A.1	<b>Introduction</b> .....	127
A.2	<b>Testing Group A: Cripple Wall Components</b> .....	127
	A.3.1 Testing Group A: Small Components.....	128
	A.3.2 Testing Group A: Large Components.....	129
A.4	<b>Testing Group B: Load Path Connections</b> .....	130
A.5	<b>Testing Group C: Combined Materials in Occupied Stories</b> .....	131
A.6	<b>Future Testing</b> .....	131
<b>APPENDIX B</b> .....		133
B.1	<b>Introduction</b> .....	133
B.2	<b>Foreword</b> .....	133
B.3	<b>Objectives and Benefits</b> .....	133
B.4	<b>Physical Testing Recommendations</b> .....	134
	B.4.1 Test House Configuration.....	135
	B.4.2 Pre-Test Survey.....	136
	B.4.3 Documentation of Full-Scale Test House Design.....	136
	B.4.4 Damage States of Interest .....	137
	B.4.5 Testing Protocol.....	137
	B.4.6 Documentation of Testing.....	137
B.5	<b>Recommended Concurrent Work</b> .....	137
	B.5.1 Numerical Modeling.....	137
	B.5.2 Damage Assessment .....	138
	B.5.3 Loss Modeling .....	138
B.6	<b>Considerations regarding Cost and Schedule</b> .....	138
B.7	<b>Conclusions</b> .....	138



## LIST OF TABLES

Table 2.1	Small-component test specimen summary.....	24
Table 3.1	Comparison of unretrofitted cripple wall lateral strength.....	39
Table 3.2	Comparison of retrofitted cripple wall lateral strength.....	39
Table 3.3	Comparison of cripple wall lateral strength with and without retrofit.....	40
Table 3.4	Comparison of cripple wall global drift ratios at lateral strength. ....	41
Table 3.5	Comparison of cripple wall relative drift ratios at capacity.....	41
Table 4.1	Comparison of uplift displacements. ....	50
Table A.3	Small-component complete testing matrix. ....	128
Table A.2	Large-component test matrix. ....	129
Table A.3	Load path connection test matrix.....	130
Table A.4	Combined materials in occupied stories test matrix. ....	131



## LIST OF FIGURES

Figure 2.1	Diagram of small-component test specimen geometry.....	6
Figure 2.2	Illustration of top boundary condition A: (top) plan view detail; and (bottom) top of wall detail. ....	7
Figure 2.3	Illustration of bottom boundary condition a. ....	7
Figure 2.4	Specimen A-1 pre-test photographs of top boundary condition A and bottom boundary condition a: (a) exterior elevation; (b) interior elevation; (c) north exterior corner; and (d) south interior corner.....	8
Figure 2.5	Illustration of top boundary condition B: (top) plan view detail and (bottom) top of wall detail. ....	9
Figure 2.6	Specimen A-2 pre-test photographs with top boundary condition B and bottom boundary condition a: (a) exterior elevation; (b) interior elevation; (c) south exterior corner; and (d) south interior corner.....	10
Figure 2.7	Illustration of top boundary condition C.....	11
Figure 2.8	Specimen A-3 pre-test photographs of top boundary condition C and bottom boundary condition a: (a) exterior elevation; (b) interior elevation; (c) south exterior corner; and (d) south interior corner.....	12
Figure 2.9	Illustration of return wall for bottom boundary condition b. ....	13
Figure 2.10	Specimen A-4 pre-test photographs with top boundary condition B and bottom boundary condition b: (a) exterior elevation; (b) interior elevation; (c) south exterior corner; and (d) south interior corner.....	14
Figure 2.11	Illustration of return wall for bottom boundary condition d. ....	15
Figure 2.12	Specimen A-20 pre-test photographs of existing 2-ft-tall cripple wall with stucco over horizontal sheathing exterior finish and bottom boundary condition d: (a) exterior elevation; (b) interior elevation; (c) south exterior corner; and (d) south interior corner. ....	16
Figure 2.13	Diagram of <i>FEMA P-1100</i> retrofit [2018] (applied to Specimen A-5). ....	17
Figure 2.14	Specimen A-5 anchor bolt retrofit: (a) framing face corner retrofit detail; and (b) framing face retrofit detail.....	18
Figure 2.15	Specimen A-5 retrofit with plywood sheathing. ....	18
Figure 2.16	Retrofitted Specimen A-5 pre-test photographs with top boundary condition B and bottom boundary condition a: (a) exterior elevation; (b) interior elevation; (c) north exterior corner; and (d) south interior corner. ....	19
Figure 2.17	Diagram of <i>FEMA P-1100</i> retrofit [2018] (as applied to Specimen A-19). ....	20

Figure 2.18	Specimen A-19 anchor bolt retrofit: (a) framing face corner retrofit detail; (b) view of stud bay; and (c) view of added 4 × 4 stud attachment. ....	21
Figure 2.19	Specimen A-19 retrofit plywood sheathing. ....	22
Figure 2.20	Retrofitted Specimen A-19 pre-test photographs with top boundary condition B and bottom boundary condition c: (a) exterior elevation; (b) interior elevation; (c) south exterior corner; and (d) south interior corner. ....	23
Figure 2.21	Overview of large-component Specimen AL-1. ....	25
Figure 2.22	Bottom of stucco detail for Specimens AL-1 and AL-2. ....	26
Figure 2.23	Overview of large-component seismic retrofit elements: (a) view of stud bay with retrofit anchor bolt and steel plate washer (Specimen AL-2); (b) view of A-35 clip at cripple wall top plate; and (c) view of crawlspace and retrofit plywood. ....	27
Figure 3.1	Specimen A-1 load-displacement plots showing global drift (left) and relative drift (right). ....	30
Figure 3.2	Specimen A-2 load-displacement plots showing global drift (left) and relative drift (right). ....	30
Figure 3.3	Specimen A-3 load-displacement plots showing global drift (left) and relative drift (right). ....	31
Figure 3.4	Specimen A-4 load-displacement plots showing global drift (left) and relative drift (right). ....	31
Figure 3.5	Specimen A-20 load-displacement plots showing global drift (left) and relative drift (right). ....	32
Figure 3.6	Specimen A-5 load-displacement plots showing global drift (left) and relative drift (right). ....	32
Figure 3.7	Specimen A-19 load-displacement plots showing global drift (left) and relative drift (right). ....	33
Figure 3.8	Specimen AL-1 hysteresis curves. ....	33
Figure 3.9	Specimen AL-2 hysteresis curves. ....	34
Figure 3.10	Comparison of lateral force versus <i>relative</i> drift for large-component Specimen AL-1 and small-component Specimen A-1. ....	35
Figure 3.11	Comparison of lateral force versus <i>relative</i> drift for large-component Specimen AL-1 and small-component Specimen A-2. ....	35
Figure 3.12	Comparison of lateral force versus <i>relative</i> drift for large-component Specimen AL-1 and small-component Specimen A-3. ....	36
Figure 3.13	Comparison of lateral force versus <i>relative</i> drift for large-component Specimen AL-1 and small-component Specimen A-4. ....	36

Figure 3.14	Comparison of lateral force versus <i>relative</i> drift for large-component Specimen AL-1 and small-component Specimen A-20.....	37
Figure 3.15	Comparison of lateral force versus <i>relative</i> drift for large-component Specimen AL-2 and small-component Specimen A-5.....	37
Figure 3.16	Comparison of lateral force versus <i>relative</i> drift for large-component Specimen AL-2 and small-component Specimen A-19.....	38
Figure 3.17	Envelope of lateral force– <i>relative</i> lateral displacement hysteresis for existing specimens. (average of push and pull directions presented).....	43
Figure 3.18	Envelope of lateral force– <i>relative</i> lateral displacement hysteresis for retrofitted specimens. (average of push and pull directions presented).....	43
Figure 4.1	Specimen A-1 anchor bolt loads.....	46
Figure 4.2	Specimen A-2 anchor bolt loads.....	46
Figure 4.3	Specimen A-3 anchor bolt loads.....	46
Figure 4.4	Specimen A-4 anchor bolt loads.....	47
Figure 4.5	Specimen A-20 anchor bolt loads.....	47
Figure 4.6	Specimen AL-1 anchor bolt loads.....	47
Figure 4.7	Specimen A-5 anchor bolt loads.....	48
Figure 4.8	Specimen A-19 anchor bolt loads.....	49
Figure 4.9	Specimen AL-2 anchor bolt loads.....	49
Figure 4.10	Specimen AL-1 anchor bolts with nuts and washers removed following completion of testing.....	52
Figure 4.11	Specimen AL-2 anchor bolts with nuts and washers removed following completion of testing.....	52
Figure 4.12	Specimen AL-2 retrofit blocks at end of testing showing no signs of splitting.....	53
Figure 4.13	Specimen AL-2 showing the only block that experienced splitting.....	53
Figure 5.1	Specimen A-1 damage state of at -1.4% global drift ratio @ $\Delta = -0.336$ in.: (a) exterior elevation; (b) interior elevation; (c) bottom of exterior wall displacement; (d) south top exterior and corner view; (e) north exterior and corner view; and (f) top of wall displacement.....	56
Figure 5.2	Specimen A-2 damage state of at -1.4% drift @ $\Delta = -0.336$ in.: (a) exterior elevation; (b) top of exterior wall; (c) bottom of exterior wall; (d) bottom corner of south-end interior; (e) north-end exterior corner view; and (f) north-end interior corner view.....	57

Figure 5.3	Specimen A-3 damage state at -1.4% drift @ $\Delta = -0.336$ in.: (a) exterior elevation; (b) top of the exterior wall; (c) bottom of exterior wall; (d) bottom of interior wall; (e) north-end of exterior corner; and (f) south-end of exterior corner.....	59
Figure 5.4	Specimen A-4 damage state of at -1.4% drift @ $\Delta = -0.336$ in.: (a) exterior elevation; (b) top of exterior wall; (c) bottom of exterior wall; (d) bottom of north-end exterior corner; (e) bottom of interior wall; and (f) north-end of exterior corner.....	61
Figure 5.5	Specimen A-19 damage state of at -1.4% drift ratio @ $\Delta = -0.336$ in.: (a) top of south-end exterior of wall; (b) bottom of south-end exterior of wall; (c) bottom of south-end interior corner of wall; (d) bottom interior of wall (south panel); (e) middle exterior of wall; and (f) bottom of north-end exterior corner of wall.....	63
Figure 5.6	Specimen AL-1 damage state of at 1.4% drift ratio: (a) bottom of northwest corner; (b) middle of northwest corner; (c) northwest corner detail; and (d) bottom of southwest corner. ....	65
Figure 5.7	Specimen A-5 damage state at +1.4% drift @ $\Delta = +0.336$ in.: (a) exterior elevation; (b) top of exterior wall; (c) bottom of exterior wall; (d) plywood panel joint; (e) close-up of top of the south-end interior wall; and (f) north-end exterior corner. ....	67
Figure 5.8	Specimen A-19 damage state at -1.4% drift ratio @ $\Delta = -0.336$ in.: (a) top of south-end exterior of wall; (b) bottom of south-end exterior of wall; (c) bottom of south-end interior corner of wall; (d) bottom interior of wall (south panel); (e) middle exterior of wall; and (f) bottom of north-end exterior corner of wall.....	69
Figure 5.9	Specimen AL-2 damage state at 1.4% drift ratio: (a) bottom of northwest corner; (b) bottom of southwest corner; (c) bottom of south-end of wall; and (d) middle of southeast corner.....	71
Figure 5.10	Specimen A-1 damage state of at lateral strength @ +3% drift, $\Delta = +0.72$ in.: (a) exterior elevation; (b) top of the exterior wall; (c) bottom of exterior wall; (d) close-up of stud; (e) north-end corner of wall; and (f) close-up of top of south-end interior corner. ....	74
Figure 5.11	Specimen A-2 damage state at lateral strength @ -4% drift, $\Delta = -0.96$ in.: (a) exterior elevation; (b) top of exterior wall; (c) bottom of exterior wall; (d) close-up of studs; (e) close-up of north-end corner; and (f) close-up of bottom south-end exterior corner.....	76

Figure 5.12	Specimen A-3 damage state of at lateral strength @ +4% drift, $\Delta = +0.96$ in.: (a) exterior elevation; (b) top of exterior wall (c) bottom of exterior wall; (d) close-up of south-end wall; (e) close-up of north-end corner of wall; and (f) north-end exterior corner.....	78
Figure 5.13	Specimen A-4 damage state of at lateral strength @ -5% drift, $\Delta = -1.20$ in.: (a) exterior elevation; (b) top of exterior wall; (c) bottom of exterior wall; (d) close-up of stud; (e) close-up of exterior south-end corner; and (f) north-end exterior corner. ....	80
Figure 5.14	Specimen A-20 damage state of at lateral strength @ +3% drift ratio, $\Delta = +0.72$ in.: (a) top of north-end exterior of wall; (b) bottom of north-end exterior of wall; (c) bottom of south-end interior corner of wall; (d) middle of south-end interior corner of wall; (e) south-end corner of wall; and (f) bottom of south-end corner of wall.....	82
Figure 5.15	Specimen AL-1 damage state of at lateral strength @ 3% drift ratio, $\Delta = +0.72$ in.: (a) gap between stucco and foundation; (b) cracking and flaring of stucco; (c) bottom of northwest corner; (d) stucco spall at floor line; (e) bottom of south-west end of wall; and (f) separation of stucco and lumber sheathing. ....	84
Figure 5.16	Specimen A-5 damage state of at lateral strength @ +5% drift, $\Delta = +1.20$ in.: (a) exterior elevation; (b) top of exterior wall; (c) bottom of exterior wall; (d) close-up of plywood panel joint; (e) close-up of south-end exterior corner; (d) bottom of south-end interior wall corner.....	86
Figure 5.17	Specimen A-19 damage state of at lateral strength @ +8% drift ratio, $\Delta = +1.92$ in.: (a) exterior elevation; (b) south-end exterior corner of wall; (c) north-end exterior of wall; (d) bottom interior of wall (south and middle panels); (e) bottom interior of wall (north panel); (f) bottom interior of wall (south and middle panels); and (g) bottom interior of wall (north panel).....	88
Figure 5.19	Specimen AL-2 damage state of at lateral strength @ 3% drift ratio, $\Delta = +0.72$ in.: (a) bottom of southwest corner; (b) southwest corner detail; (c) bottom of northwest corner; (d) middle of southwest corner; (e) gap between stucco and foundation; and (f) middle of north-end of crawlspace.....	90
Figure 5.20	Specimen A-1 damage state at 60% post-peak reduction of lateral strength @ +12% drift, $\Delta = +2.88$ in.: (a) close-up of studs and sill plate; (b) exterior top of the wall; (c) north-end interior corner; and (d) north-end bottom of corner.....	92
Figure 5.21	Specimen A-1 post-test photographs (lateral load = 0 kips, residual displacement = +4.90 in. @ +20.4% drift): (a) exterior elevation of cripple wall; (b) interior elevation of cripple wall; (c) north-end exterior corner view: and (d) south-end interior corner view.....	93

Figure 5.22	Specimen A-2 damage state of at 70% post-peak reduction of lateral strength @ +12% drift, $\Delta = +2.88$ in.: (a) north-end of interior corner bottom; (b) close-up of top of interior wall; (c) south-end of exterior bottom corner; and (d) north-end of bottom corner. ....	94
Figure 5.23	Specimen A-2 post-test photographs (lateral load = 0 kips, residual displacement = +3.45 in @ +14.4% drift): (a) exterior elevation of cripple wall; (b) interior elevation of cripple wall; (c) south-end exterior corner view; (d) north-end interior view. ....	95
Figure 5.24	Specimen A-3 damage state at 60% post-peak reduction of lateral strength @ -12% drift, $\Delta = -2.88$ in.: (a) exterior view of north-end return wall; (b) interior of bottom of south-end return wall; (c) bottom of south-end exterior corner; (d) bottom of north-end corner. ....	96
Figure 5.25	Specimen A-3 damage state at 80% post-peak reduction of lateral strength @ -12% drift, $\Delta = -2.88$ in.: (a) exterior elevation (b) bottom of north-end interior corner; (c) north-end exterior corner; and (d) top-down view of exterior. ....	97
Figure 5.26	Specimen A-4 damage state at 80% post-peak reduction of lateral strength @ -12% drift, $\Delta = -2.88$ in.: (a) exterior elevation; (b) bottom of north-end interior corner; (c) north-end exterior corner; and (d) bottom of north-end corner. ....	98
Figure 5.27	Specimen A-4 post-test photographs at lateral load = 0 kips and residual displacement = +3.43 in. @ +14.3% drift): (a) exterior elevation of cripple wall; (b) interior elevation of cripple wall; (c) north-end exterior corner view; and (d) north-end interior view. ....	99
Figure 5.28	Specimen A-20 damage state at 20% residual lateral strength at -14% drift ratio @ $\Delta = -3.36$ in. unless otherwise noted: (a) top of south-end interior of wall at +14% drift; (b) bottom of south-end interior of wall at +14% drift; (c) bottom of south-end exterior corner of wall; and (d) south-end exterior corner of wall. ....	101
Figure 5.29	Specimen A-20 post-test photographs at lateral load = 0 kips, residual displacement = +4.81 in. (+20.0% drift ratio) after monotonic push to +5.0 in. (+20.8% drift ratio): (a) exterior elevation; (b) interior elevation; (c) north-end exterior corner of wall view; and (d) south-end interior corner of wall view. ....	102
Figure 5.30	Specimen AL-1 photographs after cyclic testing to 6 to 8% drift ratio: (a) bottom of southwest corner; (b) southwest corner detail; (c) bottom of northeast corner; and (d) bottom of southeast corner detail. ....	103

Figure 5.31	Specimen AL-1 post-test photographs after monotonic push to 40% drift ratio: (a) bottom of northeast end; (b) bottom of southeast corner; (c) west-end; (d) bottom of northwest corner; (e) bottom of northeast corner; and (f) east-end of crawlspace interior. ....	104
Figure 5.32	Specimen A-5 damage state at 80% post-peak reduction of lateral strength @ -11% drift, $\Delta = -2.64$ in.: (a) interior elevation; (b) top-down view of interior; (c) close-up of exterior south-end corner; and (d) close-up of interior north-end corner. ....	106
Figure 5.33	Specimen A-5 post-test photographs at lateral load = 0 kips and residual displacement = -1.74 in. @ -7.3% drift: (a) exterior elevation of cripple wall; (b) interior elevation of cripple wall; (c) north-end exterior corner view; and (d) south-end interior corner view. ....	107
Figure 5.34	Specimen A-19 damage state at 20% residual lateral strength @ -11% drift, $\Delta = -2.64$ in.: (a) interior elevation; (b) top-down view of interior; (c) close-up of exterior south-end corner; and (d) close-up of interior north-end corner. ....	109
Figure 5.35	Specimen A-19 post-test photographs at lateral load = 0 kips and residual displacement = +4.26 in. (+17.8% drift ratio) after monotonic push to +5.0 in. (+20.8% drift ratio): (a) exterior elevation; (b) interior elevation; (c) north-end exterior of wall view; and (d) north-end interior corner of wall view. ....	110
Figure 5.36	Specimen AL-2 during the final monotonic push to 40% drift ratio: (a) bottom of northwest corner; (b) bottom of southwest corner; (c) east-end of wall; and (d) northeast-end of wall. ....	112
Figure A.1	Group A small-component test setup (2 ft and 4 ft CW) is proposed to be similar to that used in CUREE testing by Chai et al. [2002]. ....	128
Figure A.2	Group A small-component instrumentation setup (6 ft CW) is proposed to be similar to that used in CUREE testing by Chai et al. [2002]. ....	128
Figure A.3	Group A large-component test setup is proposed to be similar to that used in CUREE-CEA testing by Arnold et al. [2003] i.e., <i>CUREE EDA-03</i> and <i>CUREE EDA-07</i> . ....	129
Figure B.1	PEER–CEA Project Earthquake Damage Workshop Case Study Building 1 and Case Study Building 2 plan [Vail et al. 2020] ....	139
Figure B.2	PEER–CEA Project Earthquake Damage Workshop Case Study Building 1 exterior elevations [Vail et al. 2020]. ....	140
Figure B.3	PEER–CEA Project Earthquake Damage Workshop Case Study Building 2 exterior elevations [Vail et al. 2020]. ....	141



# 1 Introduction

## 1.1 GENERAL

This report is one of a series of reports documenting the methods and findings of a multi-year, multi-disciplinary project coordinated by the Pacific Earthquake Engineering Research Center (PEER) and funded by the California Earthquake Authority (CEA). The overall project is titled “*Quantifying the Performance of Retrofit of Cripple Walls and Sill Anchorage in Single-Family Wood-Frame Buildings,*” henceforth referred to as the “PEER–CEA Project.”

The overall objective of the PEER–CEA Project is to provide scientifically based information (e.g., testing, analysis, and resulting loss models) that measure and assess the effectiveness of seismic retrofit to reduce the risk of damage and associated losses (repair costs) of wood-frame houses with cripple wall and sill anchorage deficiencies as well as retrofitted conditions that address those deficiencies. Tasks that support and inform the loss-modeling effort are: (1) collecting and summarizing existing information and results of previous research on the performance of wood-frame houses; (2) identifying construction features to characterize alternative variants of wood-frame houses; (3) characterizing earthquake hazard and ground motions at representative sites in California; (4) developing cyclic loading protocols and conducting laboratory tests of cripple wall panels, wood-frame wall subassemblies, and sill anchorages to measure and document their response (strength and stiffness) under cyclic loading; and (5) the computer modeling, simulations, and the development of loss models as informed by a workshop with claims adjusters.

Within the PEER–CEA Project, detailed work was conducted by seven Working Groups, each addressing a particular area of study and expertise, and collaborating with the other Working Groups. The seven Working Groups are as follows:

Working Group 1: Resources Review

Working Group 2: Index Buildings

Working Group 3: Ground-Motion Selection and Loading Protocol

**Working Group 4: Testing**

Working Group 5: Analytical Modeling

Working Group 6: Interaction with Claims Adjusters and Catastrophe Modelers

Working Group 7: Reporting

This report is a product of the Working Group denoted in bolded text above.

Physical testing was carried out at the University of California San Diego (UC San Diego) and University of California, Berkeley (UC Berkeley). Leadership for WG4 was provided by Dr. Tara Hutchinson and Brandon Schiller of UC San Diego, Dr. Vahid MahdaviFar of UC Berkeley, and Kelly Cobeen.

The primary objectives of the testing identified by the project were:

- Development of descriptions of load-deflection behavior of components and connections for use by Working Group 5 (WG5) in development of numerical models, and
- Collection of descriptions of damage at varying levels of peak transient drift for use by Working Group 6 (WG6) in development of fragility functions.

To this end, WG4 developed an overall testing plan; see Appendix A of this report. It should be noted that the technical reports developed for the PEER–CEA Project are issued as PEER reports and posted at the PEER website under “Publications and Products”:  
<https://peer.berkeley.edu/publications-products>.

## 1.2 PURPOSE OF THIS REPORT

This report compares the response of the UC San Diego small-component and UC Berkeley large-component cripple wall specimens tested under simulated seismic loading. The specimens being compared were all constructed with a stucco exterior finish installed over horizontal lumber sheathing. Specimens constructed with other materials were included in the WG4 tests but are outside of the scope of this report. The intent of the UC Berkeley large-component cripple wall tests (Specimens AL-1 and AL-2) was to capture as closely as possible the effect of boundary conditions in a complete house subjected to ground motion. This included providing continuity of the exterior stucco around corners, continuity of the stucco into the superstructure story above, and continuity of the stucco down the face of the foundation (a common detail in existing homes). The UC San Diego small-component tests (Specimens A-1, A-2, A-3, A-4, A-5, A-19, and A-20) explored the effects of a range of boundary conditions applied to the 12-ft-long cripple wall components. Both programs involved an experiment investigation of both existing<sup>1</sup> and retrofitted cripple walls.

This pairing of small- and large-component tests was included in the Project testing plan so that a direct comparison could be made to determine: (1) how closely small-component testing could emulate the response seen in the large-component tests; and (2) what boundary conditions in the small-component testing best match the results of the large-component tests. The answers to these questions are intended to help identify best boundary conditions to use on small-component testing in order to emulate large-component test response, and to qualitatively understand where the small-component tests fall in the range of lower-bound to upper-bound estimation of capacity and deformation capacity for purposes of numerical modeling.

---

<sup>1</sup> An important note regarding terminology: For the present report series, cripple walls in their “as-built” configuration are referred to as either “existing”, “unretrofit”, or “unretrofitted” cripple walls, all terms being synonymous. In addition, the terms “retrofit” and “retrofitted” are both used interchangeably to describe cripple walls to which sill anchorage and bracing have been added. No other types of seismic retrofit are considered in this Project, for instance chimney, roof, garage opening or porch attachment changes. Additional information on terminology and definitions related to this Project can be found in a glossary appendix of the WG7 Project Technical Summary [Reis 2020].

Table 1.1 describes the small- and large-component tests that have been paired for purpose of this discussion. In addition, full details of the UC San Diego small-component testing and UC Berkeley large-component testing can be found in the following reports:

- A series of four reports addressing the UC San Diego small-component tests [Schiller et al. 2020(a), 2020(b), 2020(c), and 2020(d)], and
- A report addressing UC Berkeley large-component tests [Cobeen et al. 2020].

**Table 1.1 Pairing of small- and large-component test specimens.**

<b>Cripple wall description</b>	<b>Retrofit included</b>	<b>UC Berkeley large-component specimen</b>	<b>UC San Diego small-component specimens</b>
Stucco over horizontal lumber sheathing	No	AL-1	A-1 A-2 A-3 A-4 A-20
Stucco over horizontal lumber sheathing	Yes	AL-2	A-5 A-19

### 1.3 ORGANIZATION OF THIS REPORT

This report is organized as follows:

- Chapter 1 provides a general introduction.
- Chapter 2 provides an overview of the test specimens that serve as a basis of the comparison.
- Chapter 3 compares the load-deflection response of the small- and large-component test specimens.
- Chapter 4 compares the uplift behavior of the small- and large-component test specimens.
- Chapter 5 compares observations and damage incurred for small- and large-component test specimens.
- Chapter 6 discusses in broader terms the comparisons presented in Chapters 3 through 5.
- Chapter 7 provides conclusions and discusses future research needs.
- Appendix A includes the originally developed testing plan, updated to match the testing that was conducted.

- Appendix B discusses recommendations for future full-house testing, fulfilling Task 4.5 of the PEER–CEA Project Plan.

This report includes selected information extracted from the complete WG4 reports. See the completed WG4 reports for further details.

## 2 Overview of Test Specimens

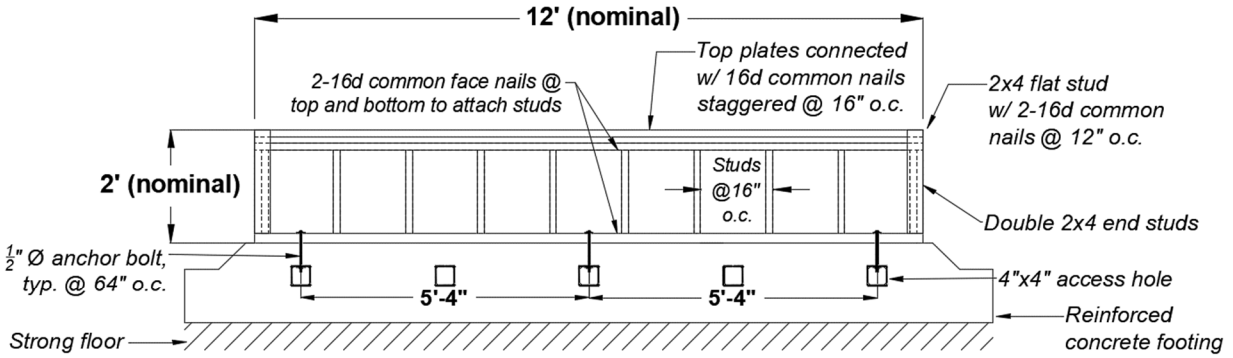
The tests specimens discussed in this report are described in detail in the separate PEER–CEA Project Reports. The purpose of this chapter is to provide a brief introduction of the test specimens. The reader is referred to other PEER–CEA Project reports for additional details.

### 2.1 SMALL-COMPONENT SPECIMENS

The small-component specimens listed in Table 1.1 were part of an extensive cripple wall small-component test program run at UC San Diego. The listed specimens were compared with the response of the UC Berkeley large-component tests with the specific task of exploring a range of specimen boundary conditions.

The listed small-component test specimens were 2-ft-high, 12-ft-long cripple walls. They had an exterior finish of stucco applied over horizontal lumber sheathing. All specimens were tested using the same displacement-controlled loading protocol. All specimens were tested with a superimposed dead load of 450 lbs per linear foot (plf); see Figure 2.1 for a diagram of the typical small-component test specimen.

The primary purpose of testing Specimens A-1, A-2, A-3, A-4, and A-20 was to explore the influence of different test specimen boundary conditions for the top, bottom, and corners of the cripple wall. The primary purpose of testing Specimens A-5 and A-19 was to study the effect of retrofitting cripple walls. Sections 2.1.1 through 2.1.4 describe the variations in boundary detailing and the seismic retrofit.



**Notes:**

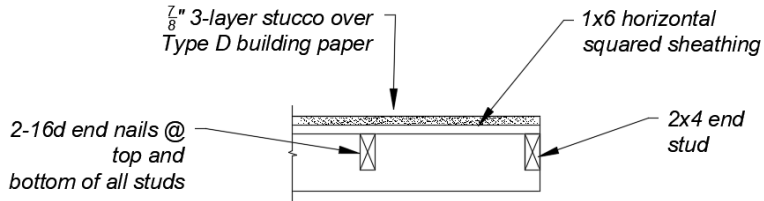
1. Sill plates are 2x6 and top-plates are 2x4.
2. Anchor bolts are  $\frac{1}{2}$ "  $\varnothing$  with  $2\frac{1}{2}$ " (min.) x  $\frac{3}{16}$ " square washer (to receive load cell on top).

**Elevation**  
**Framing Details (Interior Face)**  
**2' Tall Cripple Wall**

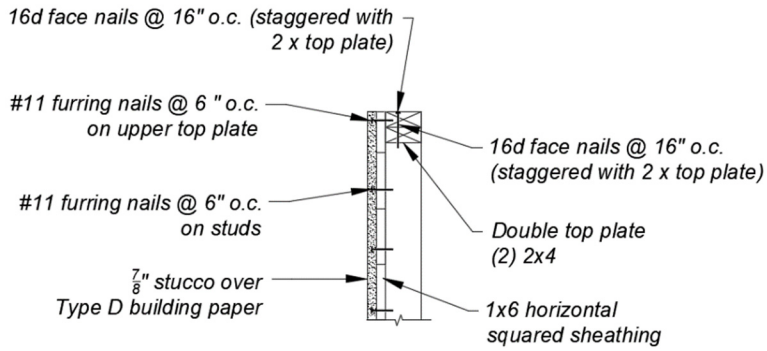
**Figure 2.1     Diagram of small-component test specimen geometry.**

**2.1.1 Small-Component Specimen A-1**

Small-component Specimen A-1 included top boundary condition A and bottom boundary condition a. Top boundary condition A represents a lower bound of stucco continuity, with the stucco ending at the panel ends and top without any wrapping around corners or supplemental fasteners; see Figure 2.2. Bottom boundary condition a has the stucco outboard of the face of the concrete foundation, while the horizontal wood sheathing is seated on the foundation; see Figure 2.3. Photographs of the specimen taken prior to testing are shown in Figure 2.4.

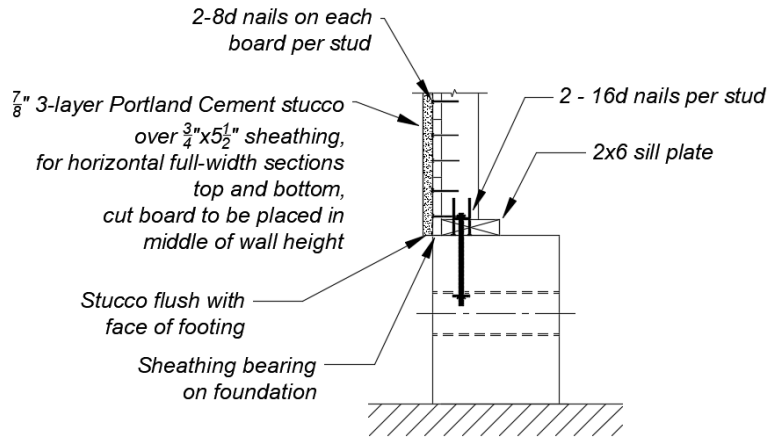


**Plan View Detail**  
**Stucco Over Horizontal Sheathing**  
**Top Boundary Condition A**



**Top of Wall Detail**  
**Stucco Over Horizontal Sheathing**  
**Top Boundary Condition A**

**Figure 2.2** Illustration of top boundary condition A: (top) plan view detail; and (bottom) top of wall detail.



**Bottom of Wall Detail**  
**Stucco Over Horizontal Sheathing**  
**Bottom Boundary Condition a**

**Figure 2.3** Illustration of bottom boundary condition a.



(a)



(b)



(c)

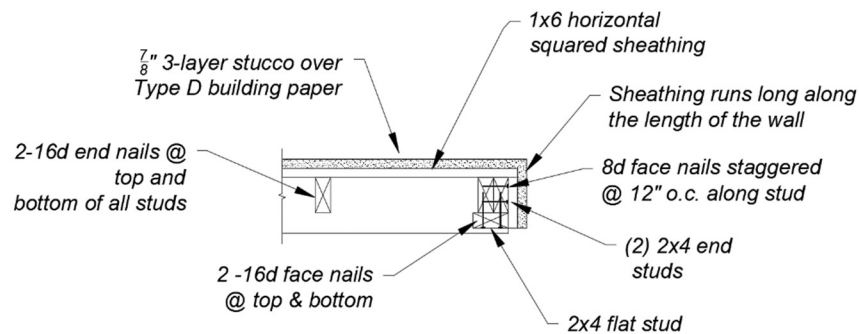


(d)

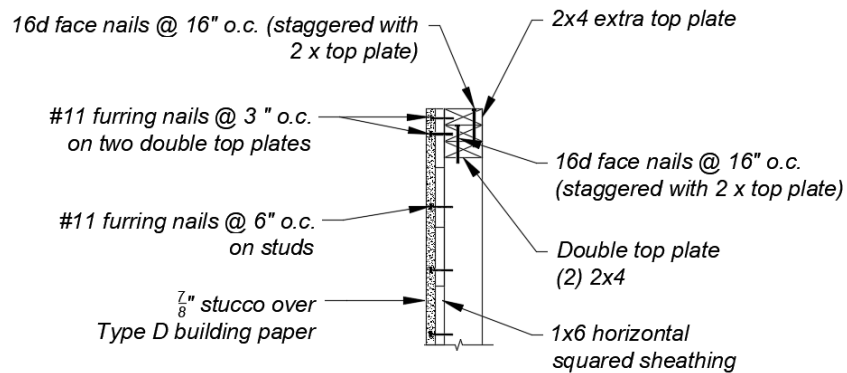
**Figure 2.4** Specimen A-1 pre-test photographs of top boundary condition A and bottom boundary condition a: (a) exterior elevation; (b) interior elevation; (c) north exterior corner; and (d) south interior corner.

### 2.1.2 Small-Component Specimen A-2

Small-component Specimen A-2 included top boundary condition B and bottom boundary condition a. Top boundary condition B included additional fastening between the stucco and the cripple wall top plates to emulate additional transfer of load into the stucco that might occur in the superstructure portion of a complete house. Top boundary condition B also included wrapping of the stucco around the end of the wall specimen. Both of these detail changes were intended to provide further continuity of the stucco, moving toward the continuity found in a complete house. Top boundary condition B is illustrated in Figure 2.5. Photographs of the specimen taken prior to testing are shown in Figure 2.6.



**Plan View Detail  
Stucco Over Horizontal Sheathing  
Top Boundary Condition B**



**Top of Wall Detail  
Stucco Over Horizontal Sheathing  
Top Boundary Condition B & C**

**Figure 2.5 Illustration of top boundary condition B: (top) plan view detail and (bottom) top of wall detail.**



(a)



(b)



(c)



(d)

**Figure 2.6** Specimen A-2 pre-test photographs with top boundary condition B and bottom boundary condition a: (a) exterior elevation; (b) interior elevation; (c) south exterior corner; and (d) south interior corner.

### 2.1.3 Small-Component Specimen A-3

Small-component Specimen A-3 included top boundary condition C and bottom boundary condition a. Top boundary condition C had the same fastening along the top of the wall as top boundary condition B. In addition, this boundary condition incorporated a return wall at each end, effectively resulting in a C-shaped wall specimen. The return walls were 2 ft long on both ends of the specimen. The first stud bay was 16 in. on center and the second was 8 in. on center. The return wall corners were framed with two 2 × 4 studs, and the return wall was tied down with two anchor bolts, one within each stud bay; see Figure 2.7. Photographs of the specimen taken prior to the test are shown in Figure 2.8.

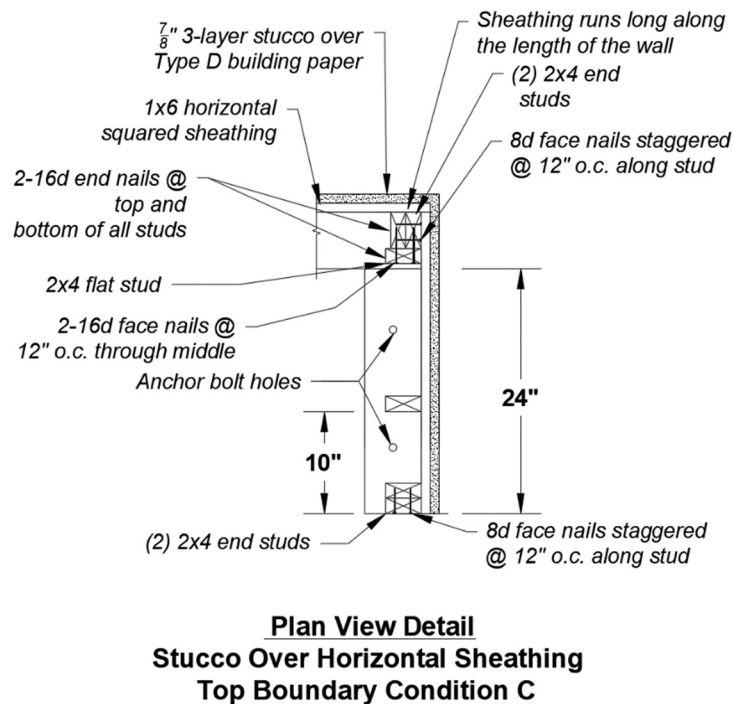


Figure 2.7 Illustration of top boundary condition C.



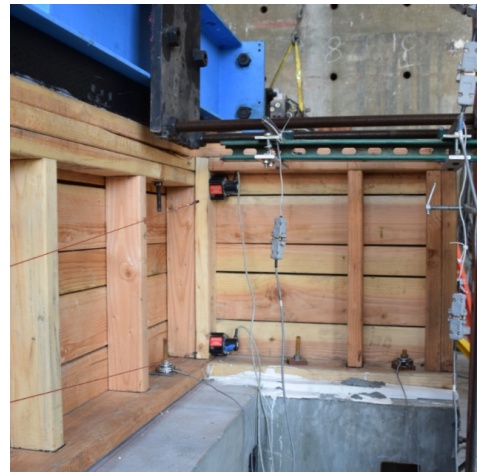
(a)



(b)



(c)



(d)

**Figure 2.8** Specimen A-3 pre-test photographs of top boundary condition C and bottom boundary condition a: (a) exterior elevation; (b) interior elevation; (c) south exterior corner; and (d) south interior corner.

### 2.1.4 Small-Component Specimen A-4

Small-component Specimen A-4 included top boundary condition B and bottom boundary condition b. With bottom boundary condition b, both the stucco and the horizontal lumber sheathing were seated on the foundation. This is illustrated in Figure 2.9, while top boundary condition B is illustrated in Figure 2.5. Photographs of Specimen A-4 are provided in Figure 2.10.

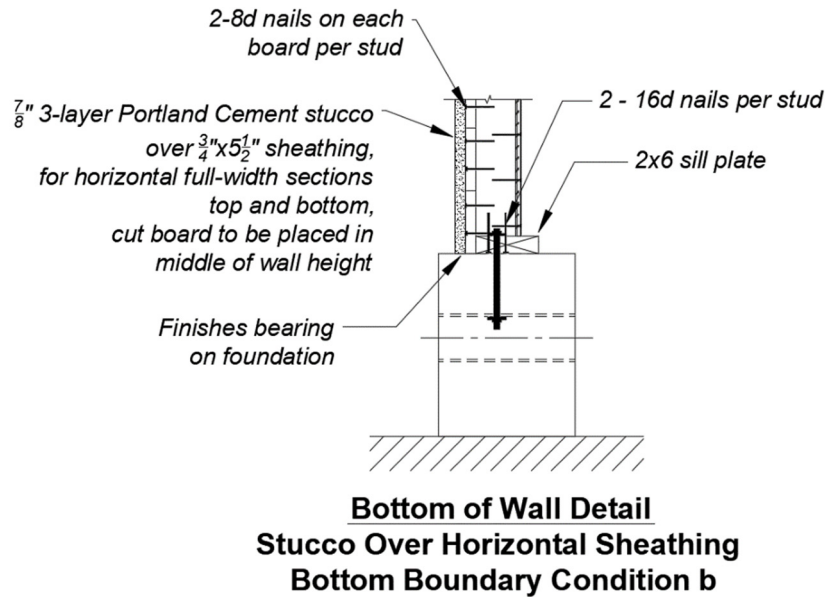


Figure 2.9 Illustration of return wall for bottom boundary condition b.



(a)



(b)



(c)



(d)

**Figure 2.10** Specimen A-4 pre-test photographs with top boundary condition B and bottom boundary condition b: (a) exterior elevation; (b) interior elevation; (c) south exterior corner; and (d) south interior corner.

### 2.1.5 Small-Component Specimen A-20

Small-component Specimen A-20 included top boundary condition B and bottom boundary condition d. With bottom boundary condition d, both finish materials (the stucco and horizontal lumber sheathing) were outboard of the foundation. In addition, the stucco extended 8 in. down the face of the footing. This is illustrated in Figure 2.11, while top boundary condition B is illustrated in Figure 2.5. These boundary conditions are the same as large-component Specimen AL-1. Photographs of Specimen A-20 are provided in Figure 2.12.

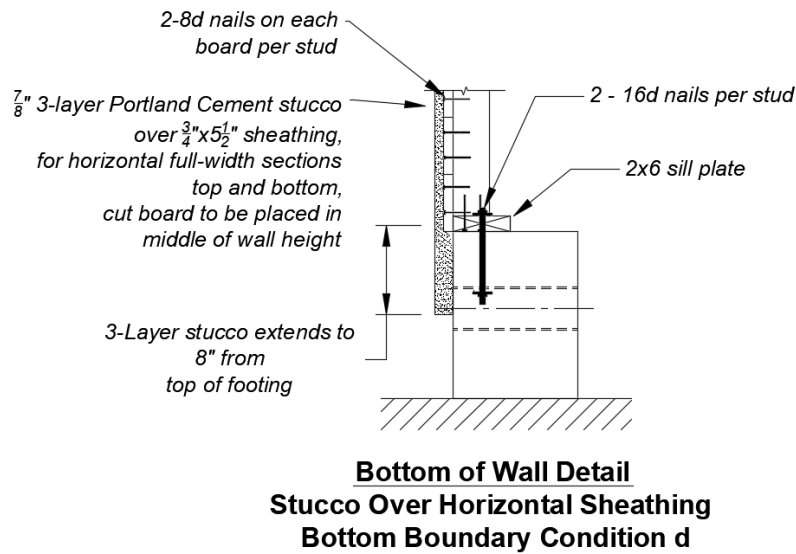


**Figure 2.11** Illustration of return wall for bottom boundary condition d.



(a)



(b)



(c)



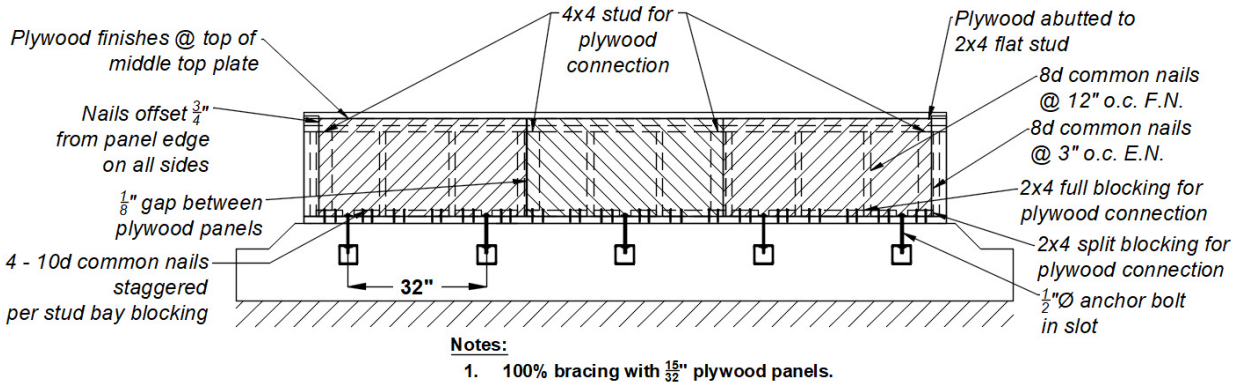
(d)

**Figure 2.12** Specimen A-20 pre-test photographs of existing 2-ft-tall cripple wall with stucco over horizontal sheathing exterior finish and bottom boundary condition d: (a) exterior elevation; (b) interior elevation; (c) south exterior corner; and (d) south interior corner.

## 2.1.6 Small-Component Specimen A-5

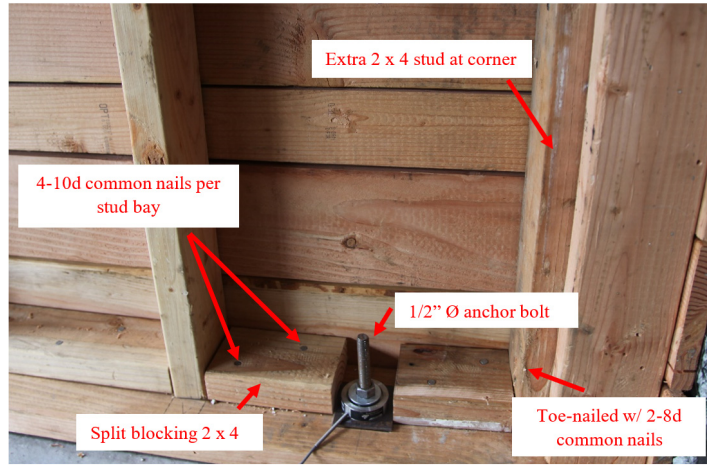
Small-component Specimen A-5 included the seismic retrofit of the cripple wall. The retrofit was installed on a test specimen with top boundary condition B and bottom boundary condition a, which matched the configuration of Specimen A-2. The retrofit was designed based on guidance from the in-progress ATC-110 design guidelines [FEMA 2018]. An engineered retrofit was designed based on materials and weights consistent with 1940s-era construction, using an  $R$  factor of 4. The retrofit involved fully sheathing the interior face of the cripple wall with 15/32-in. plywood. Prior to installation of the sheathing, 2 × 4 blocking was attached to the sill plate with 4-10d common nails per stud bay. Added blocking was split into two sections for stud bays that had anchor bolts so that the anchor bolts were seated on the sill plate. Additional 2 × 4 studs were toe-nailed in with 2-8d common nails top and bottom at each end of the wall, and two 4 × 4 studs were toe-nailed in with 2-8d common nails top and bottom in the interior of the cripple wall at each interior third.

The addition of studs and blocking plates were used so that the plywood panels could be nailed to the cripple wall. Details of the framing are shown in Figure 2.13. The interior of the framing before the application of plywood can be seen in Figures 2.14 (a) and (b). The plywood was placed in three 4-ft sections, fully sheathing the interior face of the wall. Panels were attached with 8d common nails at 4 in. on center along the edges and 12 in. on center in the field. An 1/8-in. gap was provided between panels to allow for expansion; the nails were placed 3/4 in. from the panel edge to prevent nails from tearing through the panel edges. Details of the plywood panel attachment for Specimen A-5 can be seen in Figure 2.15, and pre-test photos of the overall specimen are provided in Figure 2.16. For the 12-ft section of wall tested, five 1/2-in.-diameter anchor bolts were used. Five anchor bolts were installed in the pre-existing anchor bolt sleeves on the foundation, spaced at 32 in. on center; see Figure 2.13.

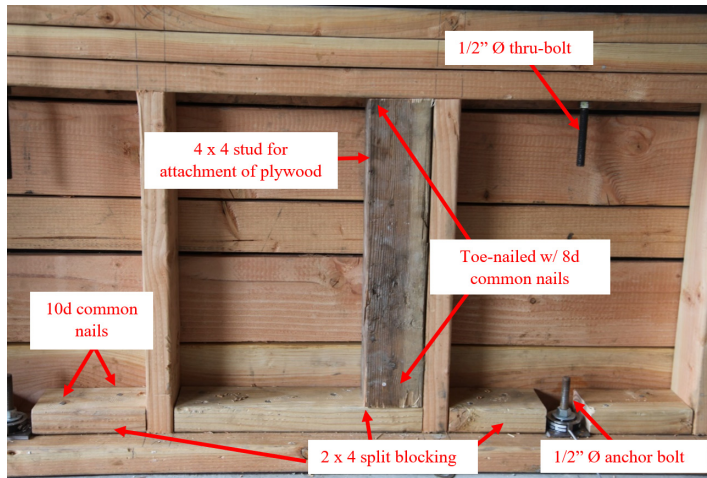


**Elevation**  
**Retrofit Framing Details (Interior Face)**  
**2' Tall Cripple Wall**  
**5 Anchor Bolt Configuration**

**Figure 2.13** Diagram of FEMA P-1100 retrofit [2018] (applied to Specimen A-5).



(a)



(b)

Figure 2.14 Specimen A-5 anchor bolt retrofit: (a) framing face corner retrofit detail; and (b) framing face retrofit detail.

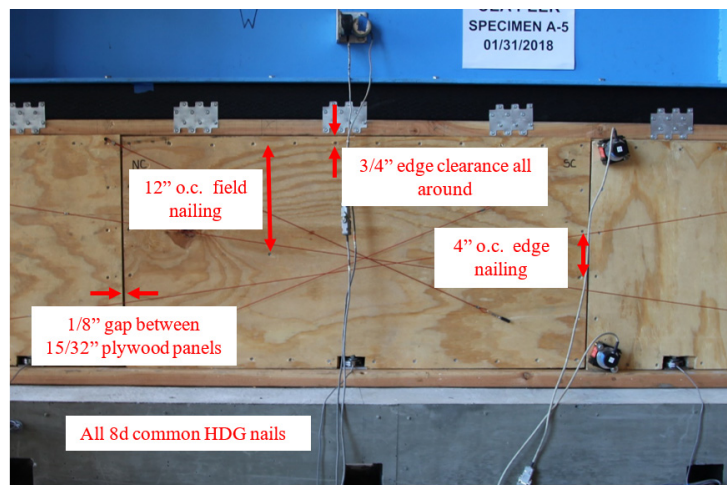


Figure 2.15 Specimen A-5 retrofit with plywood sheathing.



(a)



(b)



(c)



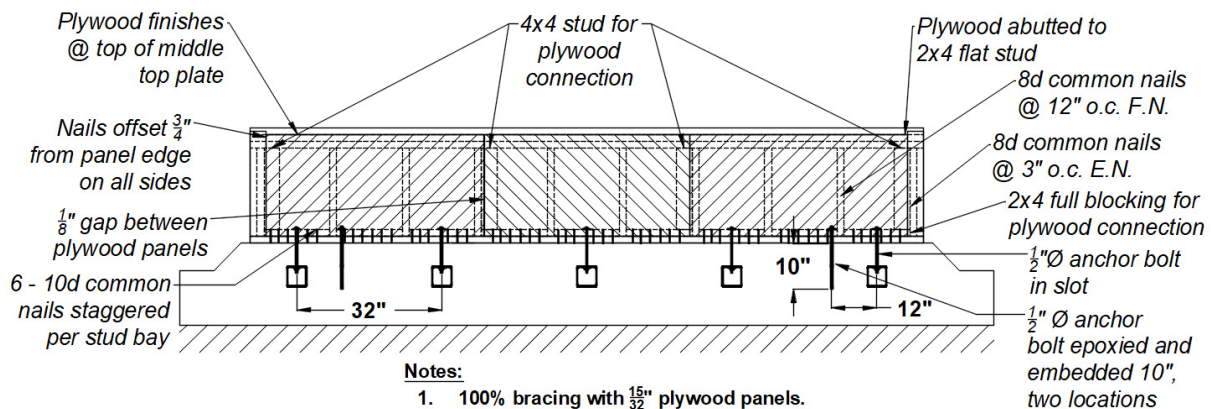
(d)

**Figure 2.16** Retrofitted Specimen A-5 pre-test photographs with top boundary condition B and bottom boundary condition a: (a) exterior elevation; (b) interior elevation; (c) north exterior corner; and (d) south interior corner.

### 2.1.7 Small-Component Specimen A-19

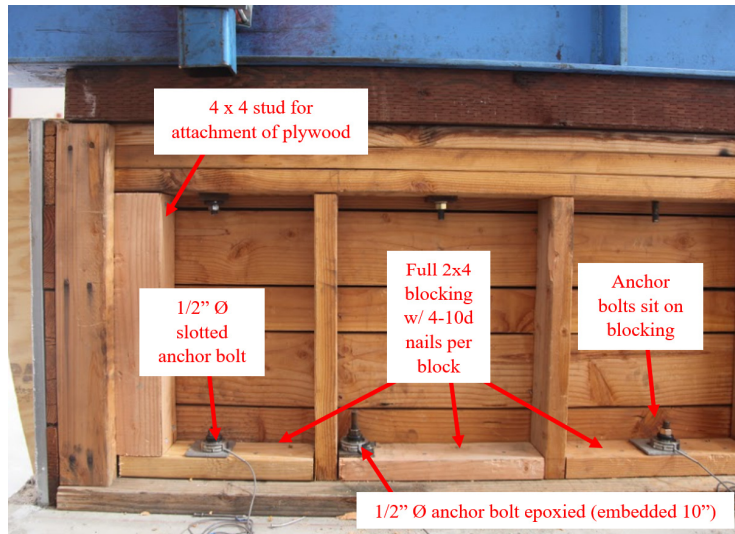
Small-component Specimen A-19 also included seismic retrofit of the cripple wall. The retrofit was installed on a test specimen with top boundary condition B and bottom boundary condition c. The retrofit was design in accordance with the finalized *FEMA P-1100* prescriptive retrofit provisions [FEMA 2018] for houses with a weight classification of “heavy” construction. The retrofit involved fully sheathing the interior face of the cripple wall with 15/32-in. plywood. Prior to sheathing, 2 × 4 blocking was attached to the sill plate with 6-10d common nails per stud bay. Full sections of blocking were used so that the anchor bolts were seated on the blocking. Additional 2 × 4 studs were toe-nailed in with 2-8d common nails top and bottom at each end of the wall, and two 4 × 4 studs were toe-nailed in with 2-8d common nails top and bottom in the interior of the cripple wall at each interior third.

The addition of studs and blocking plates were used to allow the plywood panels to be nailed to the cripple wall. Details of the framing are shown in Figure 2.17. The interior of the framing before the application of plywood can be seen in Figure 2.18(a), (b), and (c). The plywood was placed in three 4-ft sections, fully sheathing the interior face of the wall. Panels were attached with 8d common nails at 3 in. on center along the edges and 12 in. on center along the field. A 1/8-in. gap was provided between panels to allow for expansion, and the nails were placed 3/4 in. from the panel edge to prevent nails from tearing through the panel edges. Details of the plywood panel attachment for Specimen A-5 can be seen in Figure 2.19. For the 12-ft section of wall tested, five 1/2-in.-diameter anchor bolts were used. In addition, *FEMA P-1100* requires an extra 1/2-in.-diameter anchor bolt at each end of the cripple wall. Five anchor bolts were installed in the pre-existing anchor bolt sleeves on the foundation, spaced at 32 in. on center, and the additional two anchor bolts were embedded 10 in. into the foundation and epoxied with Simpson Strong-Tie SET-XP, 12 in. inward from the outer two most anchor bolts; see Figure 2.17. Photographs of Specimen A-20 are provided in Figure 2.20.

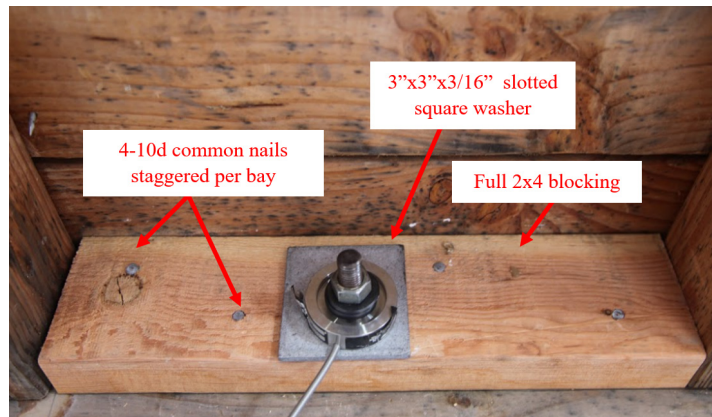


**Elevation**  
**Retrofit Framing Details (Interior Face)**  
**2' Tall Cripple Wall**  
**7 Anchor Bolt Configuration**

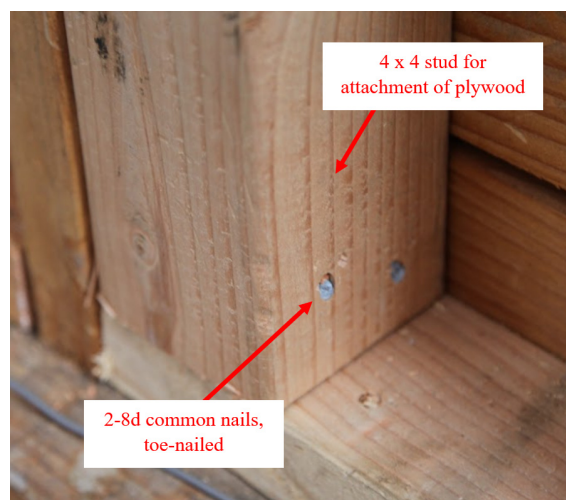
**Figure 2.17** Diagram of *FEMA P-1100* retrofit [2018] (as applied to Specimen A-19).



(a)



(b)



(c)

**Figure 2.18 Specimen A-19 anchor bolt retrofit: (a) framing face corner retrofit detail; (b) view of stud bay; and (c) view of added 4 × 4 stud attachment.**

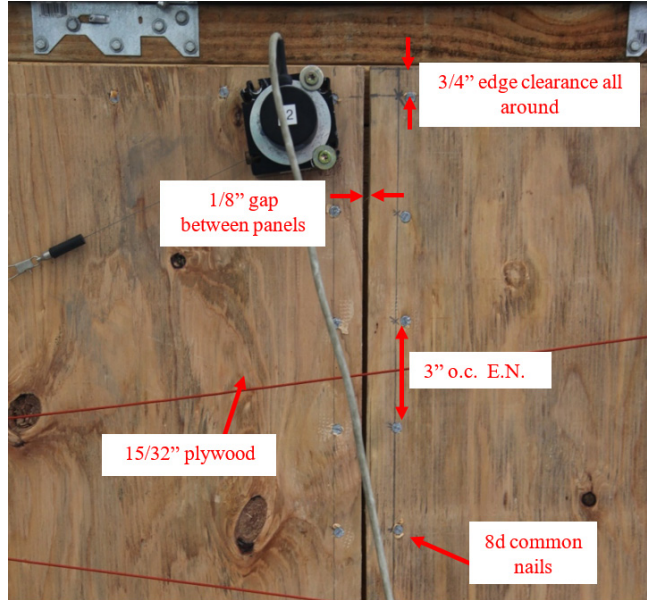


**Figure 2.19 Specimen A-19 retrofit plywood sheathing.**



(a)



(b)



(c)



(d)

**Figure 2.20** Retrofitted Specimen A-19 pre-test photographs with top boundary condition B and bottom boundary condition c: (a) exterior elevation; (b) interior elevation; (c) south exterior corner; and (d) south interior corner.

## 2.1.8 Small-Component Specimen Summary

Table 2.1 provides a summary of the small-component tests and their boundary conditions.

**Table 2.1 Small-component test specimen summary.**

Small-component specimen	Retrofit included	Top boundary condition	Bottom boundary condition	Boundary condition graphics: top, end, bottom
A-1	No	A	a	
A-2	No	B	a	
A-3	No	C	a	
A-4	No	B	b	
A-20	No	B	d	
A-5	Yes	B	a	
A-19	Yes	B	c	

## 2.2 LARGE-COMPONENT SPECIMENS

The two large-component specimens listed in Table 1.1 were part of a large-component test program run at UC Berkeley. Both tests included 2-ft-tall cripple walls. In order to include the most representative boundary conditions, the test specimens were composed of three-dimensional structures with a 20-ft × 4-ft plan dimension. The test specimens were constructed on top of a cast concrete foundation and included a 2-ft-tall cripple wall extending for the full structure perimeter,

a floor diaphragm, an 8-ft-tall superstructure, and a roof diaphragm. Figure 2.22 shows Specimen AL-1; the configuration for Specimen AL-2 was identical except that the cripple wall was retrofitted according to the *FEMA-1100* guidelines. Loading was applied parallel to the 20-ft-long walls.

This configuration allowed continuity of the stucco exterior finish around the corners, continuity of the stucco from the cripple wall into the superstructure above, and continuity of the stucco down the face of the foundation (a common detail in older stucco clad houses). Figure 2.9 illustrates extension of the stucco down the face of the foundation, which matches bottom boundary condition d from the small-component testing. The stucco used was representative of 1940s-era construction, including the application of three coats of stucco over a 1-1/2-in. 17-gauge wire mesh fastened with #11  $\times$  1-1/2-in. furring nails with 1/4-in. wads. Like the small-component specimens, the stucco in Specimens AL-1 and AL-2 was applied over 1  $\times$  6 horizontal lumber sheathing. The interior of the superstructure for both large-component specimens was finished with 1/2-in. gypsum wallboard.



Figure 2.21 Overview of large-component Specimen AL-1.

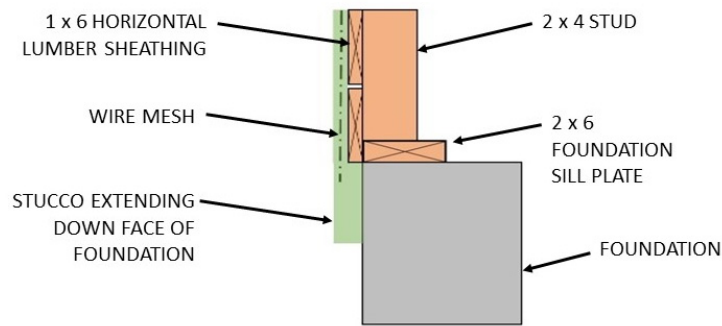


**Figure 2.22 Bottom of stucco detail for Specimens AL-1 and AL-2.**

Load was applied to the test specimen at the floor diaphragm level using a wide flange loading beam attached to the floor diaphragm with screws. The same displacement-based loading protocol was used in testing Specimens AL-1 and AL-2 as had been used for the small-component tests. The drift was defined as a ratio of the 24-in. cripple wall clear height.

### **2.2.1 Large-Component Specimen AL-1**

Large-component Specimen AL-1 was intended to represent an unretrofitted 1940s-era house. Four 1/2-in.-diameter anchor bolts were provided in each of the 20-ft long walls, approximately replicating an anchor bolt spacing of 6 ft on center, a configuration that is commonly found in older homes that had anchor bolts installed at the time of construction.

### **2.2.2 Large-Component Specimen AL-2**

Large-component Specimen AL-2 was intended to represent an existing 1940s-era house with seismic retrofit of the cripple walls and anchorage. The retrofit was designed in accordance with the prescriptive vulnerability-based provisions of *FEMA P-1100*, Volume 1 [FEMA 2018]. The retrofit included increasing the number of anchor bolts from four to ten on each 20-ft wall. The ten anchor bolts include eight that are intended to provide shear and an additional anchor bolt at each end of each wall, intended to provide supplemental uplift capacity. The retrofit also included 19 ft of 15/32-in. plywood sheathing applied on the interior face (crawl space face) of each 20-ft wall, nailed with 8-penny common nails at 3 in. on center. Finally, the retrofit included fourteen A-35 shear clips on each wall, providing shear transfer between the cripple wall top plates and the floor diaphragm above. The retrofit was installed in accordance with *FEMA P-1100*. Figure 2.23 shows the installed retrofit elements.



(a)



(b)



(c)

**Figure 2.23** Overview of large-component seismic retrofit elements: (a) view of stud bay with retrofit anchor bolt and steel plate washer (Specimen AL-2); (b) view of A-35 clip at cripple wall top plate; and (c) view of crawlspace and retrofit plywood.



## 3 Load-Deflection Response Comparison

This chapter provides comparison of the load-deflection response of the small- and large-component tests. Load-deflection plots of each test are provided in Section 3.1. Overlays of the small- and large-component tests are provided in Section 3.2. Discussion of the response is provided in Sections 3.3 through 3.6, including comparisons of lateral strength, deflection at lateral strength, post-peak response, and other characteristics of note.

### 3.1 LOAD-DEFLECTION RESPONSE

The load-deflection response of the small-component tests is provided in Figures 3.1 through 3.7. Figures 3.1 through 3.5 illustrate the response of unretrofitted small-component test specimens. Figures 3.6 and 3.7 illustrate the response of retrofitted small-component test specimens.

Two plots are provided for each specimen, one identified as global drift, and one identified as relative drift. The global drift includes all sources of displacement. The relative drift removes displacement due to sliding between the foundation sill plate and the foundation. This sliding was found to be a notable portion of the full displacement in some test specimens. The global displacement plots give the best indication of the overall movement of the specimens at given load levels. The relative displacements provide the best comparison with the large component tests, which did not experience any measureable slip between the foundation sill plate and the foundation. The relative displacements are also the most applicable for numerical modeling of the cripple walls.

The load-deflection responses of the five unretrofitted specimens varied considerably and provide a large range in expected performance of the stucco over horizontal sheathing finish. Specimen A-1 had the lowest lateral strength in push directions of loading of the five specimens considered. This cripple wall contained no stucco return around the corners; this stucco return was shown to have a large effect on the strength capacity of the cripple wall. The cripple wall that best matched the boundary conditions of Specimen AL-1 was Specimen A-20. With both specimens, all finish materials (stucco and horizontal lumber sheathing) were orientated outboard of the foundation and were able to freely rotate as the specimen displaced. The lateral strength of Specimen A-20 was 22% higher than Specimen A-1. The lateral strength of A-20 was 22% less than that of Specimen A-2. Specimens A-1, A-2, and A-3 all orientated the stucco outboard of the foundation, with the sheathing bearing on the top of the foundation. Of the unretrofitted specimens, A-4 had the largest lateral strength. The lateral strength of Specimen A-4 was 57% higher than Specimen A-20. With Specimen A-4, all of the finish materials were bearing on the foundation.

The orientation of the finish materials relative to the foundation significantly affected the lateral strength of the specimens. By inhibiting the in-plane rotation of the finish materials due to the bearing of the materials on the foundation, the cripple walls gained strength. In addition, the drift capacity of the specimens was also significantly affected by the orientation of the finish materials. The drift capacity increased when more materials were bearing on the foundation. This is due to the imposed displacement being taken on by the sheathing fasteners more than the stucco furring nails. After reaching strength, the specimens with the stucco outboard of the foundation had large drops in strength in subsequent drift cycles; see Figure 3.2, 3.3, and 3.5.

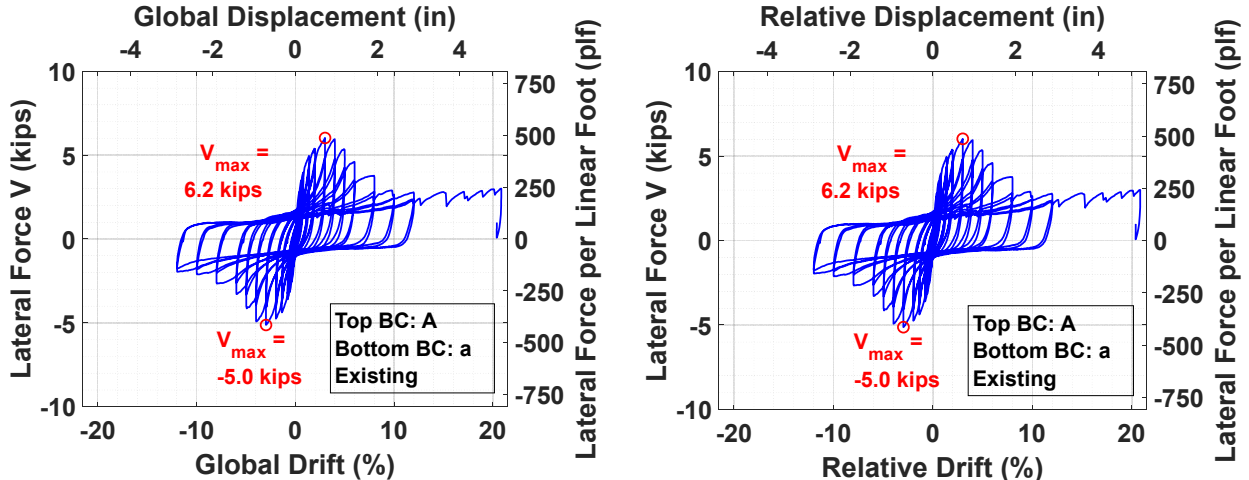


Figure 3.1 Specimen A-1 load-displacement plots showing global drift (left) and relative drift (right).

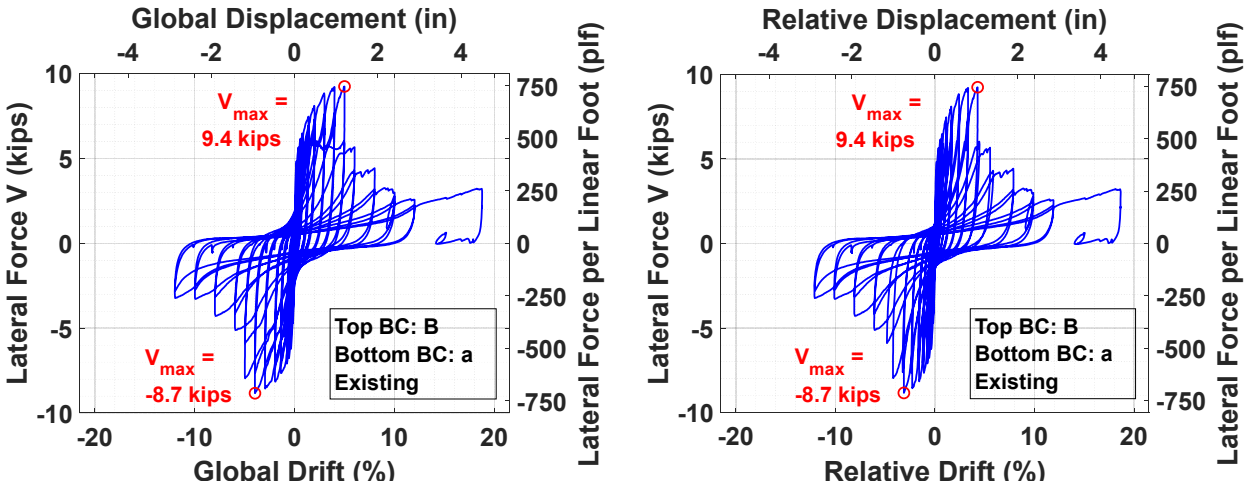


Figure 3.2 Specimen A-2 load-displacement plots showing global drift (left) and relative drift (right).

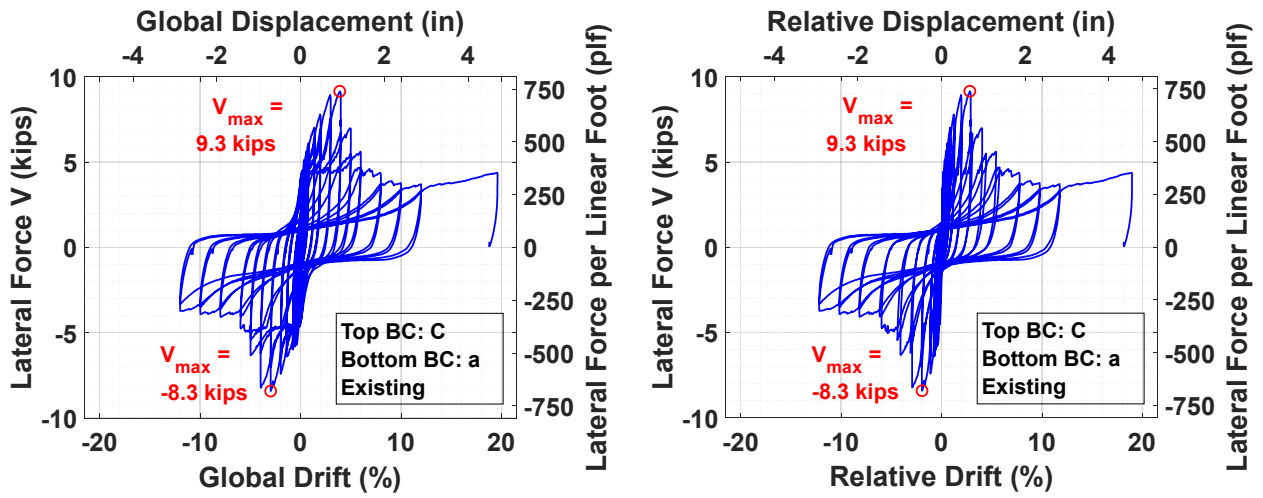


Figure 3.3 Specimen A-3 load-displacement plots showing global drift (left) and relative drift (right).

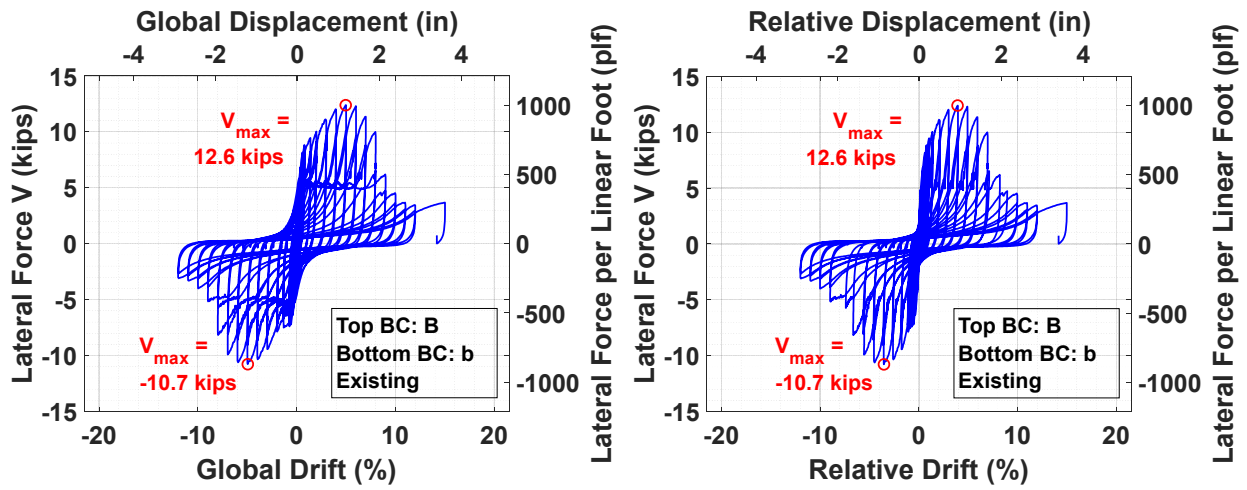


Figure 3.4 Specimen A-4 load-displacement plots showing global drift (left) and relative drift (right).

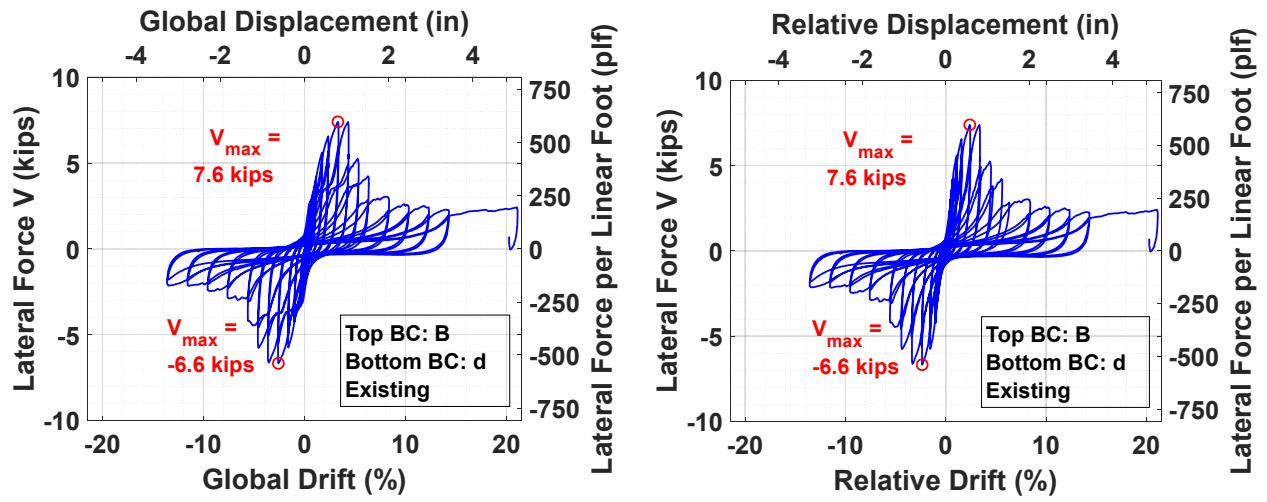


Figure 3.5 Specimen A-20 load-displacement plots showing global drift (left) and relative drift (right).

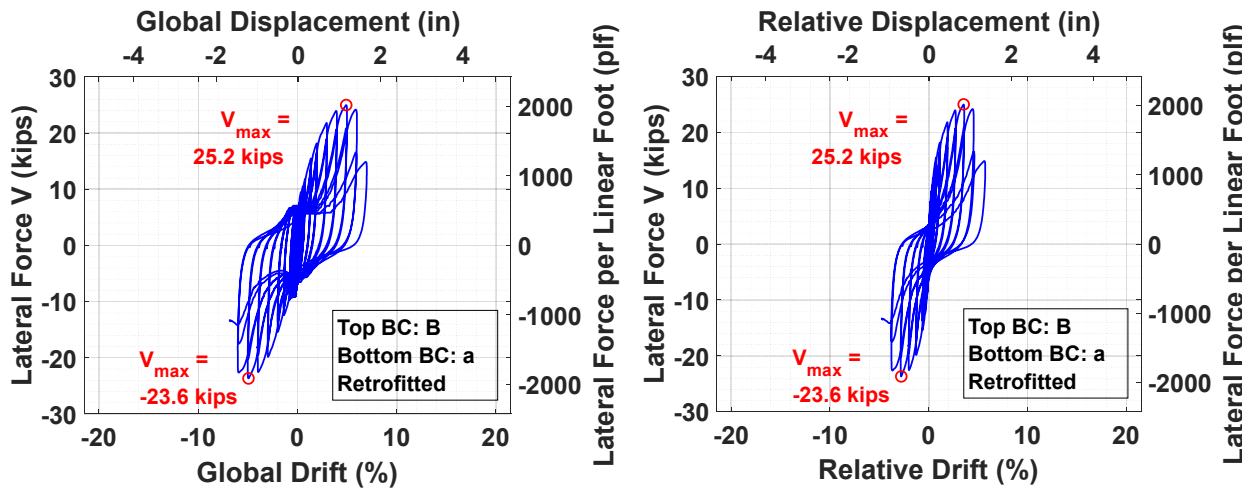


Figure 3.6 Specimen A-5 load-displacement plots showing global drift (left) and relative drift (right).

The most dramatic differences between the global and relative drifts can be seen in Figures 3.6 and 3.7 for retrofitted Specimens A-5 and A-19. In both cases, about one-third of the displacement at peak capacity came from slip observed at the interface between the foundation sill plate and the foundation. Further discussion of this can be found in Chapter 4.

The load-deflection behavior of the large-component tests is provided in Figures 3.8 and 3.9. Two plots are provided for each specimen. One includes both the hysteresis loops and the end monotonic push. The second provides an enlarged view of the hysteresis loops. Because no measurable slip occurred between the foundation sill plate and the foundation in the large-component tests, the global and relative drift do not need to be differentiated.

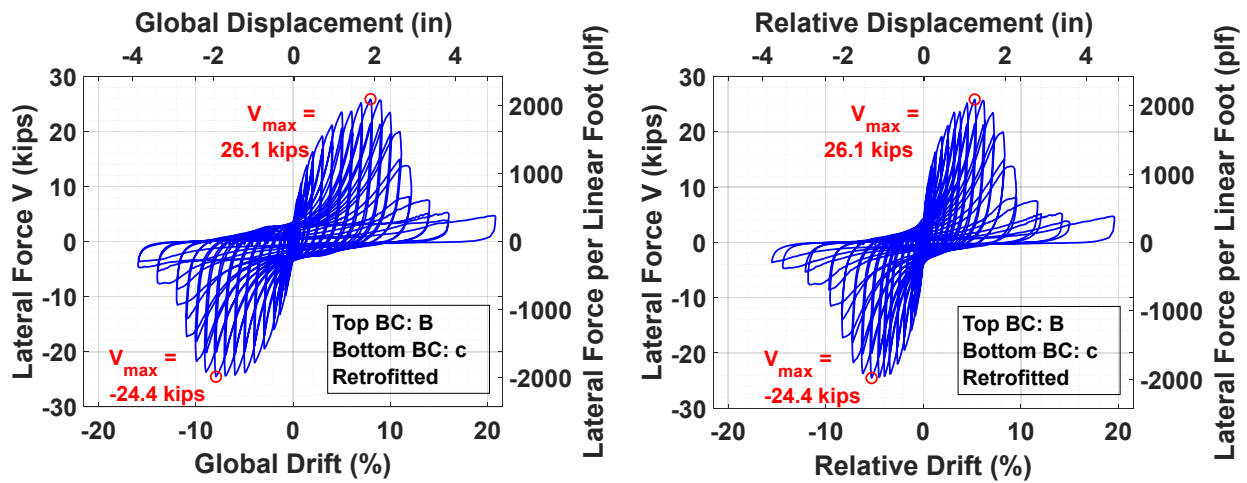


Figure 3.7 Specimen A-19 load-displacement plots showing global drift (left) and relative drift (right).

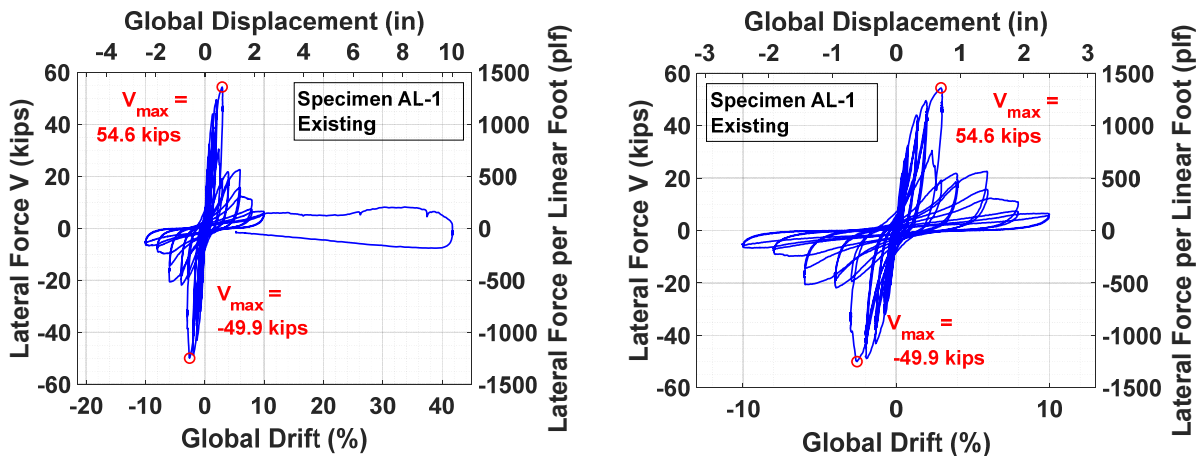


Figure 3.8 Specimen AL-1 hysteresis curves.

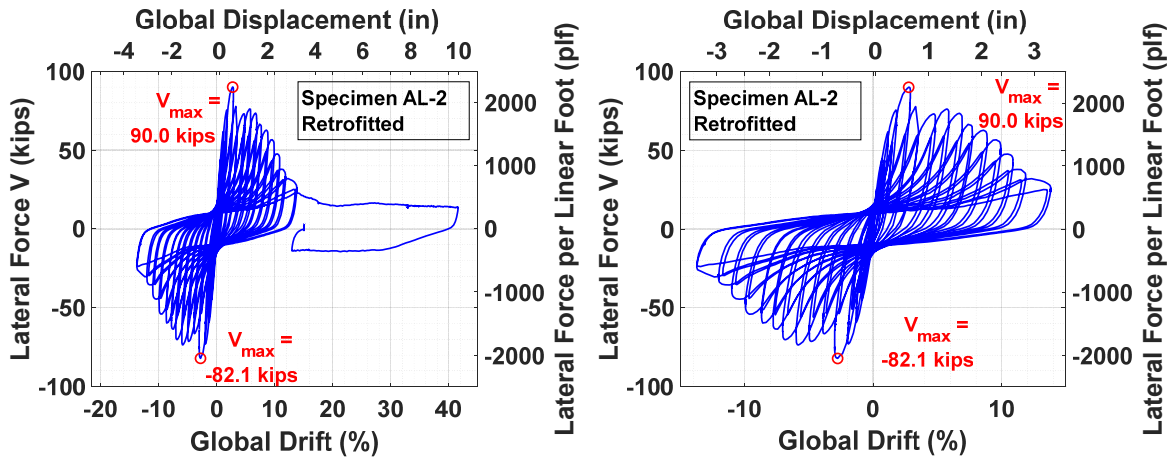


Figure 3.9 Specimen AL-2 hysteresis curves.

### 3.2 OVERLAYS OF SMALL- AND LARGE-COMPONENT RESPONSE

The comparison of response of the small- and large-component test specimens can best be seen with overlays of the load-deflection plots. Figures 3.10 through 3.14 show the overlays of small-component Specimens A-1 through A-4 and A-20 relative to large-component specimen Specimen AL-1. These are shown only for the relative displacement (as discussed in Section 3.1) because this most directly reflects the displacement demands imposed on the cripple wall itself. The overlaid hysteresis plots are shown with the monotonic push included and the monotonic push excluded to allow comparison of the cyclic loading portion of the response.

For Specimens A-1, A-2, A-3 and A-20, the character of the post-peak response is generally similar to Specimen AL-1, even though there is significant variation in the peak capacity. For Specimen A-4, the character of the load-deflection response is markedly different and more in line with the response of the retrofitted specimens. The drop in capacity over many loading cycles tended to be more limited. This will be discussed below.

Figures 3.15 and 3.16 show the overlays of small-component Specimens A-5 and A-19 relative to large-component Specimen AL-2. These are shown only for the relative displacement (as discussed in Section 3.1) because this most directly reflects the displacement demands imposed on the cripple wall itself. The overlaid hysteresis plots are shown with the monotonic push included and the monotonic push excluded to allow comparison of the cyclic loading portion of the response. Both Specimens A-5 and A-19 provide a good match to the lateral strength of Specimen AL-2, although the displacements at lateral strength vary. For Specimen A-5, a significant drop in lateral strength occurred just after reaching peak capacity, after which testing stopped. Both Specimens A-19 and AL-2 had a very slow drop in post-peak lateral strength, allowing the testing to extend to very large drift ratios.

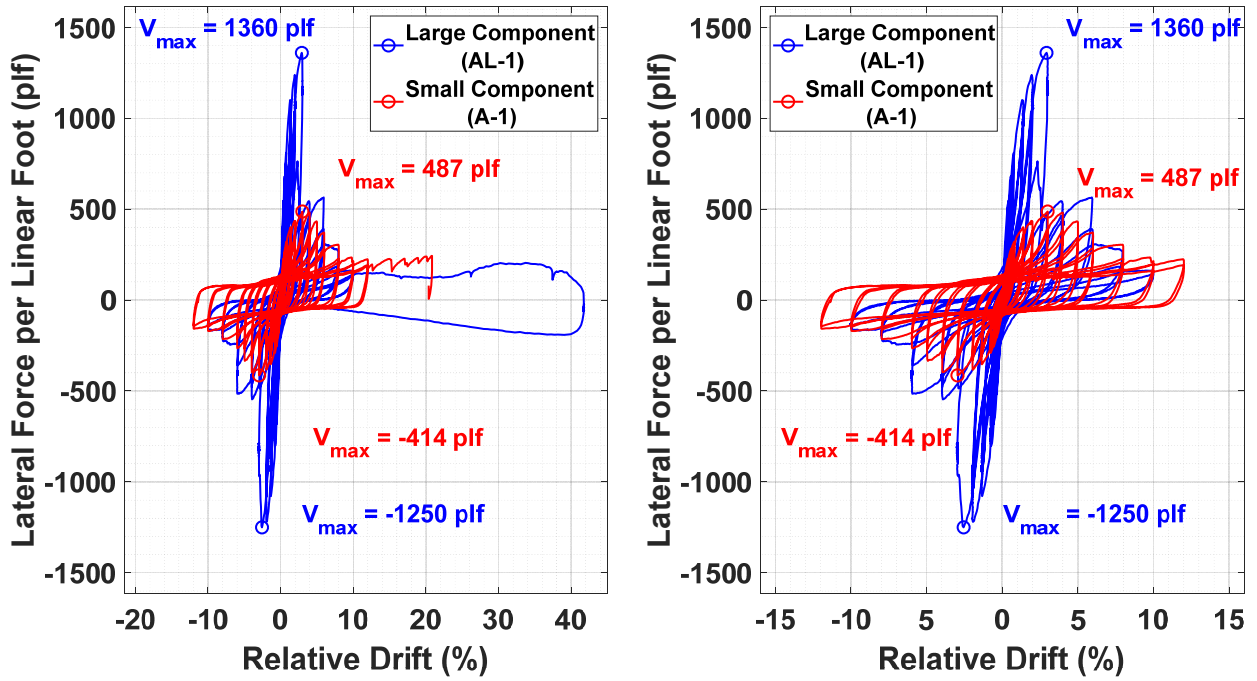


Figure 3.10 Comparison of lateral force versus *relative drift* for large-component Specimen AL-1 and small-component Specimen A-1.

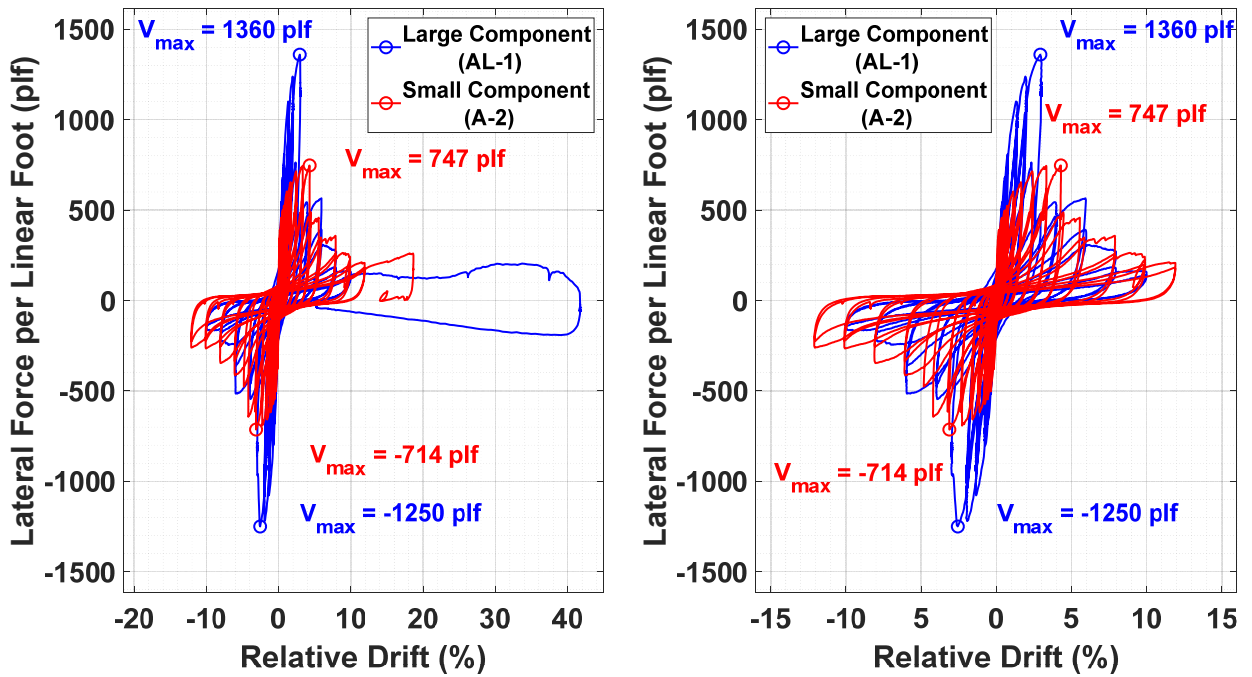


Figure 3.11 Comparison of lateral force versus *relative drift* for large-component Specimen AL-1 and small-component Specimen A-2.

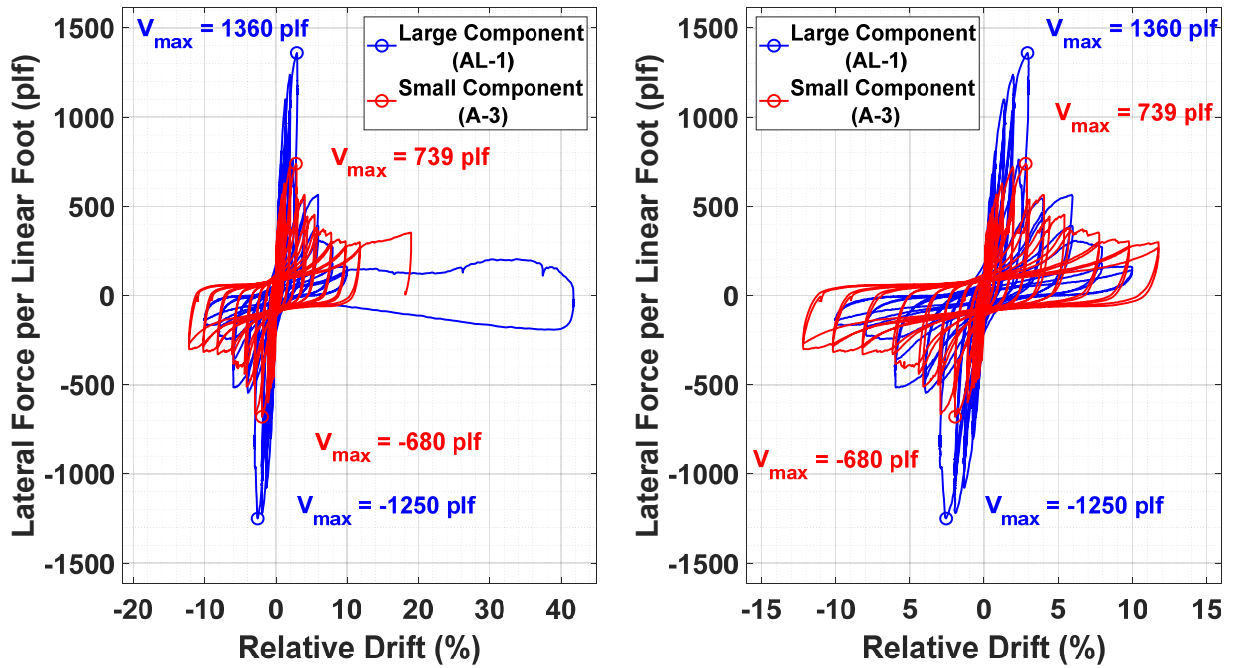


Figure 3.12 Comparison of lateral force versus *relative drift* for large-component Specimen AL-1 and small-component Specimen A-3.

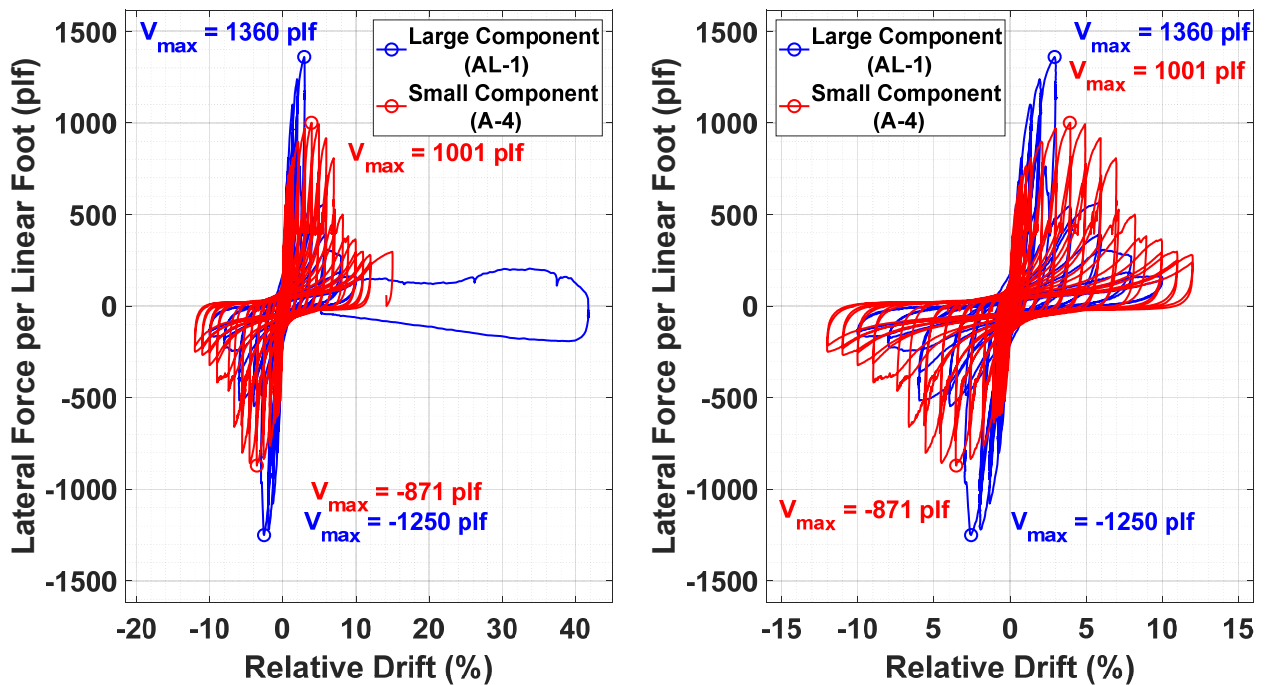


Figure 3.13 Comparison of lateral force versus *relative drift* for large-component Specimen AL-1 and small-component Specimen A-4.

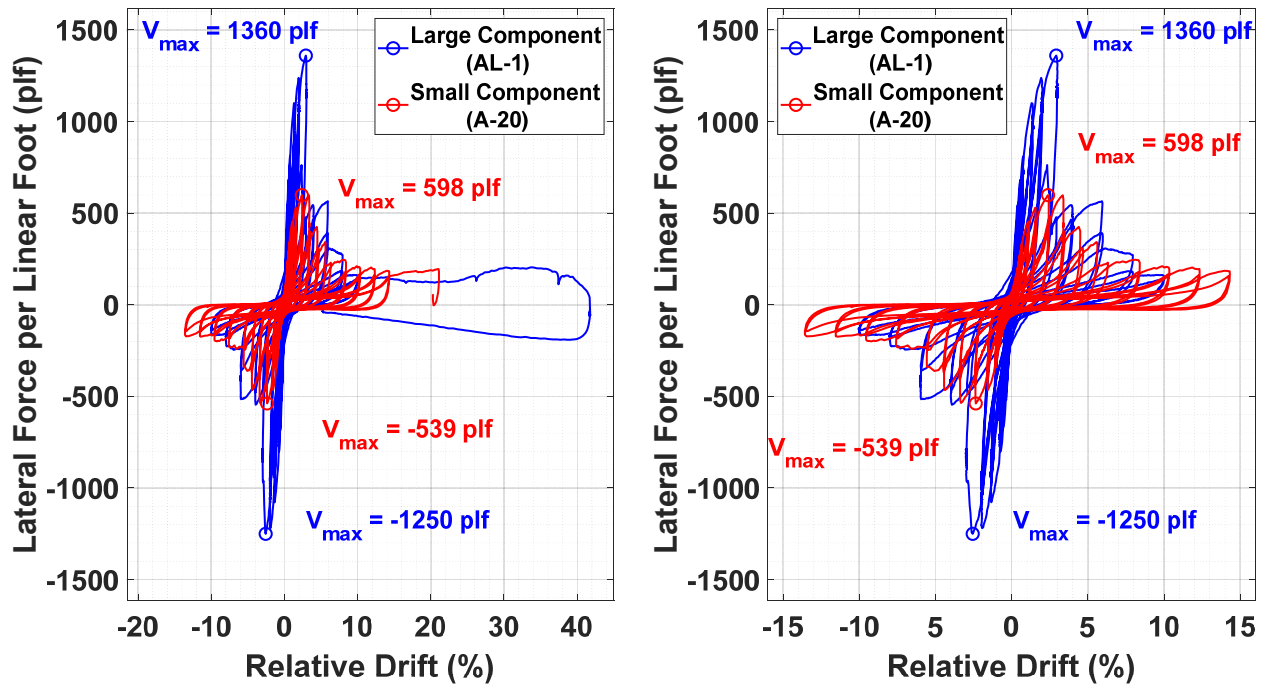


Figure 3.14 Comparison of lateral force versus *relative drift* for large-component Specimen AL-1 and small-component Specimen A-20.

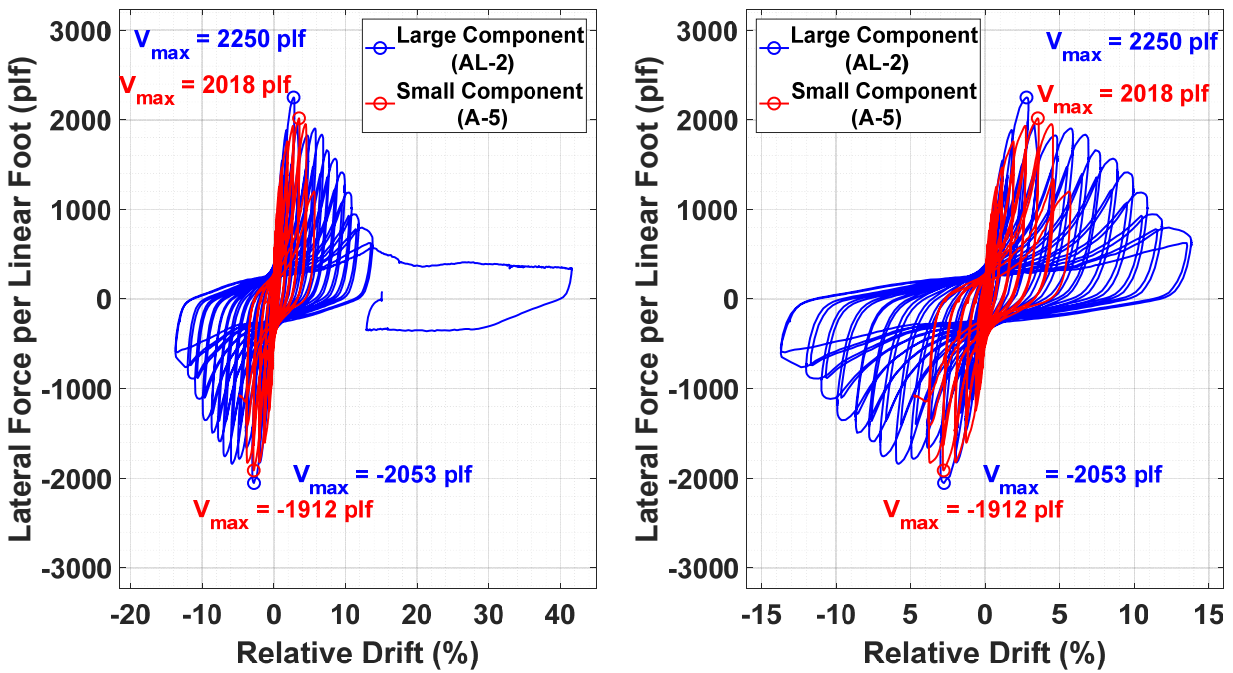


Figure 3.15 Comparison of lateral force versus *relative drift* for large-component Specimen AL-2 and small-component Specimen A-5.

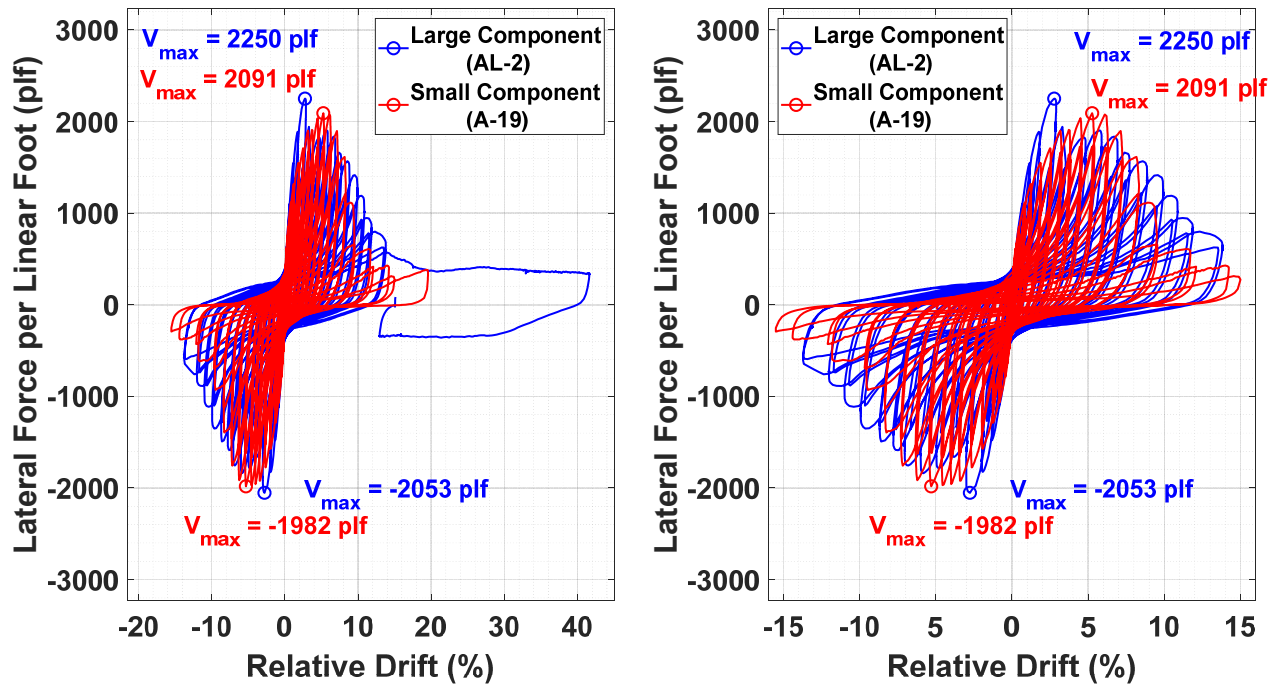


Figure 3.16 Comparison of lateral force versus *relative* drift for large-component Specimen AL-2 and small-component Specimen A-19.

### 3.3 COMPARISON OF LATERAL STRENGTH

One of the primary descriptors for the performance of cripple walls is lateral strength (peak capacity). Because of the differences in the lengths and configurations of the small- and large-component tests, comparisons are best made based on a pound per linear foot basis. This reflects the small-component forces divided by 12 ft and the large-component forces divided by 40 ft. Table 3.1 compares lateral strength per linear foot for large-component Specimen AL-1 and small-component Specimens A-1, A-2, A-3, A-4, and A-20. The lateral strength provided is the average of the positive and negative quadrants. These tests represent the unretrofitted condition.

As anticipated, Specimen A-1, without continuity at the boundaries, had the lowest lateral strength. Specimens A-2 and A-3 had very similar lateral strengths, both noticeably larger than Specimen A-1. A comparison of Specimens A-2 and A-3 seems to suggest that the 2-ft-long return walls of Specimen A-3 did not provide lateral strength that was significantly different than that provided with the 6-in. stucco return. Specimen A-4, in which both the stucco and horizontal lumber sheathing were seated on top of the concrete foundation, had the highest lateral strength of the small-component specimens; this strength was approximately twice the strength of Specimen A-1 and 30% higher compared to Specimen A-2. The bearing of the finish materials on the foundation had a large effect on the strength capacities of the specimens.

**Table 3.1 Comparison of unretrofitted cripple wall lateral strength.**

Specimen	Specimen type	Top and bottom boundary conditions	Average lateral strength (plf)
A-1	Small	A, a	465
A-2	Small	B, a	730
A-3	Small	C, a	710
A-4	Small	B, b	935
A-20	Small	B, d	570
AL-1	Large	Not applicable	1300

**Table 3.2 Comparison of retrofitted cripple wall lateral strength.**

Specimen	Specimen type	Specimen top and bottom boundary conditions	Average lateral strength (plf)
A-5	Small	B, a	1965
A-19	Small	B, c	2035
AL-2	Large	Not applicable	2150

The configuration of Specimen A-20 most closely matched Specimen AL-1 in that the stucco was extended down the face of the foundation, and all finish materials were positioned outboard of the foundation. It should be noted that for Specimen A-20 the bond between the extension of the stucco and the foundation had been damaged prior to testing. The lateral strength provided by Specimen A-20 was at the lower end of lateral strength for small-component specimens, approximately half of the Specimen AL-1 lateral strength. The overlay of the load-deflection plots can be seen in Figure 3.14. The high lateral strength of Specimen AL-1 was dependent on the bond between the stucco and the foundation, with a significant drop in lateral strength occurring immediately after the bond was broken. This was a significant contributor to the higher lateral strength for Specimen AL-1; it is not clear whether the use of a large component versus small also contributed to the higher lateral strength. Specimen A-20 is described to have had a weaker bond due to the pre-existing damage, with slip between the stucco and foundation occurring early on in the testing, producing a lower lateral strength than it might have had the bond been stronger.

Table 3.2 compares the capacity per linear foot for large-component Specimen AL-2 and small-component Specimens A-5 and A-19. The capacity is defined as the average of the positive and negative quadrant capacities. These tests represent the retrofitted condition. Compared to the lateral strength of the small- and large-component tests without retrofit, the unit shear capacities with retrofit are very similar. This may be in part attributed to a plywood nailing detail in Specimen AL-2 that is thought to have kept the retrofit from achieving its full intended capacity; see Section

3.6. Based on comparisons of the large-component test lateral strengths discussed in Cobeen et al. [2020], it is estimated that with the corrected top plate nailing detail (since revised in *FEMA P-1100*) the peak capacity might have been between 400 and 800 plf higher. In addition, the rotation of the plywood panels for Specimen AL-2 was inhibited by the sill plate and the floor joists, whereas the plywood panels in both of the small-component tests were only restrained by the sill plate. Due to this, the plywood panels in the small-component tests were able to rotate and uplift more freely than those in the large-component test; this increased the drift capacity and the lateral strength contribution of the small-component retrofit.

Table 3.3 compares the lateral strength of test specimens with and without retrofit to identify the increase in strength provided by retrofit. The small-component tests show significantly larger increases in lateral capacity with retrofit. This difference could be driven by a few different factors. Included is the concern that a sheathing nailing detail used in Specimen AL-2, resulting in the capacity contribution of the plywood retrofit sheathing being reduced. Even with a higher capacity for Specimen AL-2, however, the ratio for AL-2 would appear to remain less than the ratio for the small-component test, suggesting that the small-component test inherently report a larger increase in capacity with retrofit. Regardless, very significant increases in cripple wall lateral strength occurred with the addition of the cripple wall seismic retrofit.

**Table 3.3 Comparison of cripple wall lateral strength with and without retrofit.**

Specimens	Specimen type	Average lateral strength for the unretrofitted specimen (plf)	Average lateral strength for the retrofitted specimen (plf)	Ratio of lateral strength with and without retrofit
A-5	Small	730	1965	2.7
A-19	Small	730	2035	2.8
AL-2	Large	1300	2150	1.7

### 3.4 COMPARISON OF DRIFT RATIOS

Drift ratios at lateral strength (peak capacity) indicate the ductility and displacement capacity of the test specimen. Tables 3.4 and 3.5 summarize and compare the drift ratios at lateral strength for the small- and large-component specimens. The drift ratios are defined as a ratio of the displacement divided by the cripple wall clear height of 24 in. The drift ratios from the positive and negative quadrants are averaged. Table 3.4 provides global drift, including the slip between foundation sill plate and foundation for the small-component test specimens. The values in Table 3.5 have the slip removed so that the noted drifts are imposed over the height of the cripple wall.

**Table 3.4 Comparison of cripple wall global drift ratios at lateral strength.**

Specimen	Specimen type	Retrofit included	Specimen top and bottom boundary conditions	Average drift ratio at lateral strength (%)
A-1	Small	No	A,a	3.0
A-2	Small	No	B,a	4.5
A-3	Small	No	C,a	3.5
A-4	Small	No	B,b	5.0
A-20	Small	No	B,d	3.0
AL-1	Large	No	-	2.8
A-5	Small	Yes	B,a	5.0
A-19	Small	Yes	B,c	8.0
AL-2	Large	Yes	-	2.8

**Table 3.5 Comparison of cripple wall relative drift ratios at capacity.**

Specimen	Specimen type	Retrofit included	Top and bottom boundary conditions	Average relative drift ratio at lateral strength (%)
A-1	Small	No	A, a	3.0
A-2	Small	No	B, a	3.7
A-3	Small	No	C, a	2.5
A-4	Small	No	B, b	3.7
A-20	Small	No	B, d	2.4
AL-1	Large	No	-	2.8
A-5	Small	Yes	B, a	3.2
A-19	Small	Yes	B, c	5.3
AL-2	Large	Yes	-	2.8

The values in Table 3.5 are the most relevant for use in comparing the response of the cripple walls. There is a fair amount of variation in relative drift ratio at lateral capacity over both groups for both the unretrofitted and retrofitted specimens. In both groups, the large-component specimen had the lowest or near lowest drift ratio at lateral strength.

Within the group without retrofit, it is of interest that Specimen A-20, with the bottom boundary condition most similar to Specimen AL-1, had a relative drift ratio at lateral strength that

is similar but slightly less than Specimen AL-1. This is in spite of questions regarding the level of bond achieved between the stucco and foundation in Specimen A-20. Specimen A-20 is considered the baseline for the small-component tests without retrofit. The relative drift ratio was 15% lower than Specimen AL-1.

The other low relative drift ratio in the group without retrofit is Specimen A-3 with the 2-ft-tall foot return walls. Although this specimen had a peak lateral strength similar to Specimen A-2 with the 6 in. returns, the drift ratio data suggests that the 2-ft returns might have played a role in reducing drift. Besides Specimen A-3, all other unretrofitted small-component cripple walls with at least one finish material bearing on the foundation had a larger drift ratio at strength than Specimen AL-1. Specimens A-5 and AL-2 had a similar relative drift ratio at lateral strength, but Specimen A-19 had a relative drift ratio at lateral strength almost twice that of Specimen AL-2.

### **3.5 COMPARISON OF POST-PEAK DRIFT CAPACITY**

The overlaying of envelope curves provides a convenient way to compare the post-peak behavior of multiple test specimens. Figure 3.17 compiles envelope curves for unretrofitted test specimens. To allow direct comparison, the force axis reflects unit loads in pounds per linear foot of cripple wall. This is accomplished by dividing the small-component forces by 12 ft, and the large-component forces by 40 ft. The figures use the relative displacement, rather than global displacement, and drift ratios from the UC San Diego tests, since sliding of the small-component specimens was appreciable for certain specimens.

As shown in Figure 3.17, Specimens A-2, A-20, and AL-1 experienced a notable post-peak drop in lateral force. In contrast, Specimen A-1 had a lower lateral strength but did not exhibit the same type of post-peak drop in lateral force. While the lateral strengths varied widely, the general character of the post-peak lateral force for 6% drift (1.5 in.) and higher is relatively similar. All specimens retained 15–20% of lateral strength to drift ratios of between 20 and 40% in the final monotonic pushes. The slope of the post-peak drop in lateral force is one of the important parameters in numerical modeling. For the group of curves shown in Figure 3.17, Specimen AL-1 is noted to have both a more significant drop immediately post-lateral strength and a more rapid drop in post-peak capacity.

Figure 3.18 compiles envelope curves for test specimens with retrofit, again reflecting unit loads in pounds per linear foot of cripple wall. This figure shows that although the three specimens have very similar lateral strengths, the lateral strengths occur at widely varying drift ratios. While Specimen AL-2 experienced a limited drop in lateral force following lateral strength, Specimens A-5 and A-19 did not experience this drop. The overall character of the envelope curves following lateral strength are also widely varying, with Specimen A-5 showing a rapid drop-off, Specimen A-19 showing a more moderate drop-off, and Specimen AL-2 showing the most moderate drop-off. The variability of drift ratios at peak capacity and rates of drop-off shown for these three specimens create challenges for numerical modeling studies.

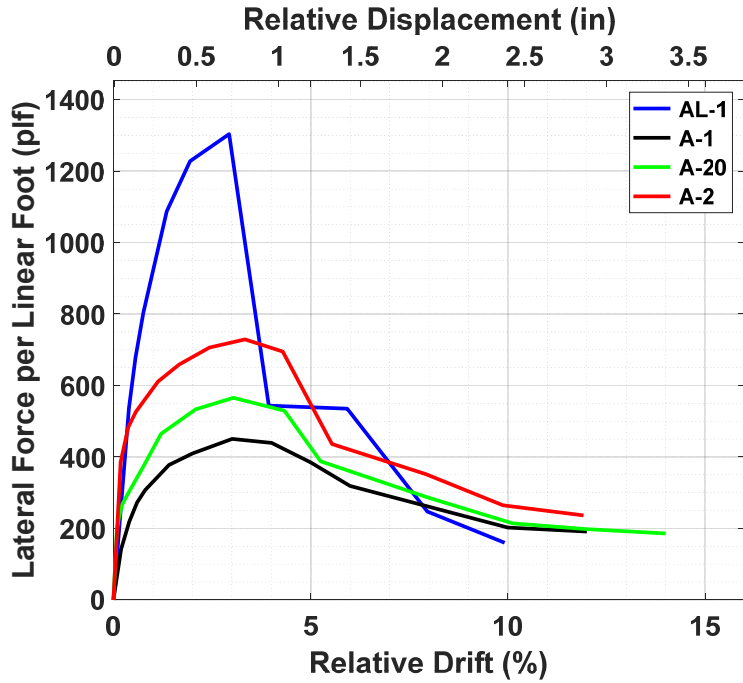


Figure 3.17 Envelope of lateral force–*relative* lateral displacement hysteresis for existing specimens. (average of push and pull directions presented)

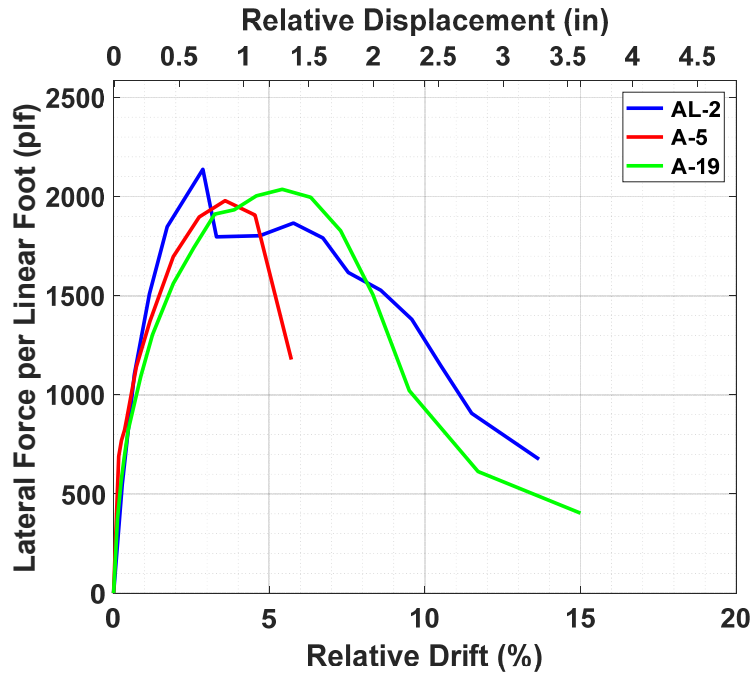


Figure 3.18 Envelope of lateral force–*relative* lateral displacement hysteresis for retrofitted specimens. (average of push and pull directions presented)

### 3.6 COMPARISON OF OTHER RESPONSE CHARACTERISTICS

This section addresses several additional items noted in comparing the load-deflection response of all specimens. In the final monotonic push, Specimen AL-2 developed a slip plane between the upper and lower cripple wall top plates. This resulted in the diaphragm and upper top plate breaking free of the lower top plate and cripple wall studs, and the diaphragm was pushed a significant distance relative to the cripple wall. This slip is largely attributed to the staggering of sheathing nails between the upper and lower top plates, combined with light nailing interconnecting the plates. This failure mechanism would not have been observed in the small-component testing because both of the top plates were secured with lag screws to the loading beam. This serves as a reminder that testing representing the complete structure can reveal additional mechanisms. As a result of this failure mechanism, the details for plywood sheathing installation in *FEMA P-1100* were revised to require full edge nailing in the upper of the two top plates to avoid this failure mode.

## 4 Comparison of Uplift Behavior

One of the most significant differences seen between the small- and large-component testing was in uplift behavior. Uplift behavior was prominent and drove some damage mechanisms in the small-component tests. In contrast, uplift behavior was limited and not associated with damage mechanisms in the large-component tests. The following sections compare the results of recorded data and observed behavior.

### 4.1.1 Comparison of Anchor Bolt Loads

Anchor bolt uplift forces were measured in all of the test specimens. Anchor bolt forces for the unretrofitted small-component specimens are shown in Figures 4.1 through 4.5. Anchor bolt forces for unretrofitted large-component Specimen AL-1 are shown in Figure 4.6. All of the anchor bolts were given a nominal level of preload prior to start of testing. The data in Figures 4.1 through 4.6 reflects the change in anchor bolt tension force over the duration of testing. For simplicity, the discussion that follows refers to these as anchor bolt forces, but they are more precisely recognized as the *change* in anchor bolt forces. It should be noted that there was a range in initial tension for anchor bolts in the small-component tests. Specimens A-1 and A-4 had anchor bolts initially tensioned between 4000 and 5000 lbs. The anchor bolts for Specimens A-2 and A-3 were initially tensioned around 1000 lbs. For all other small- and large-component tests, the anchor bolts were tensioned to around 200 pounds prior to testing.

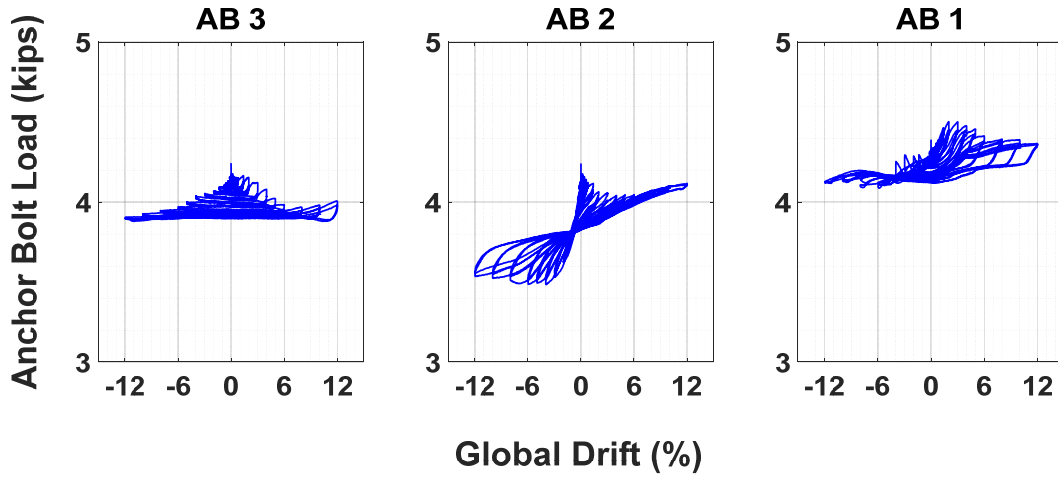


Figure 4.1

Specimen A-1 anchor bolt loads.

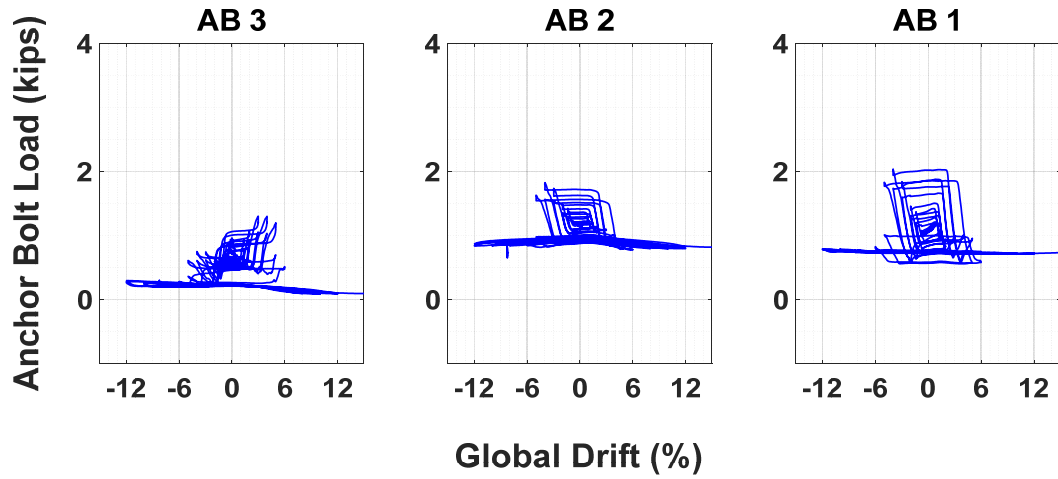


Figure 4.2

Specimen A-2 anchor bolt loads.

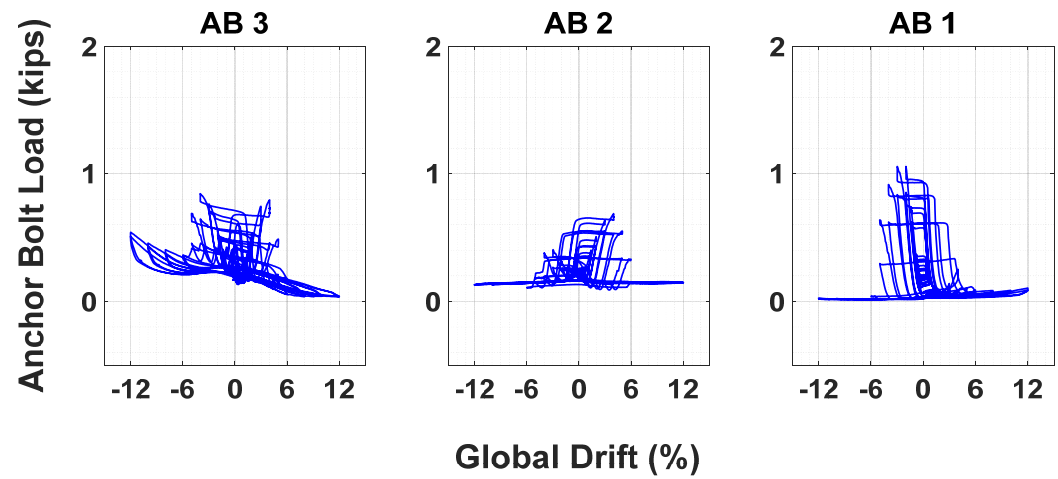


Figure 4.3

Specimen A-3 anchor bolt loads.

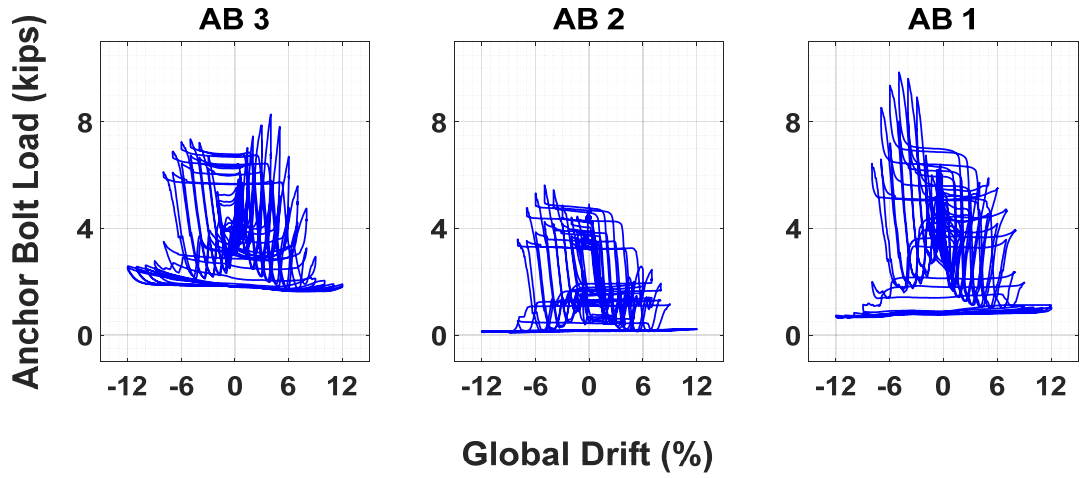


Figure 4.4 Specimen A-4 anchor bolt loads.

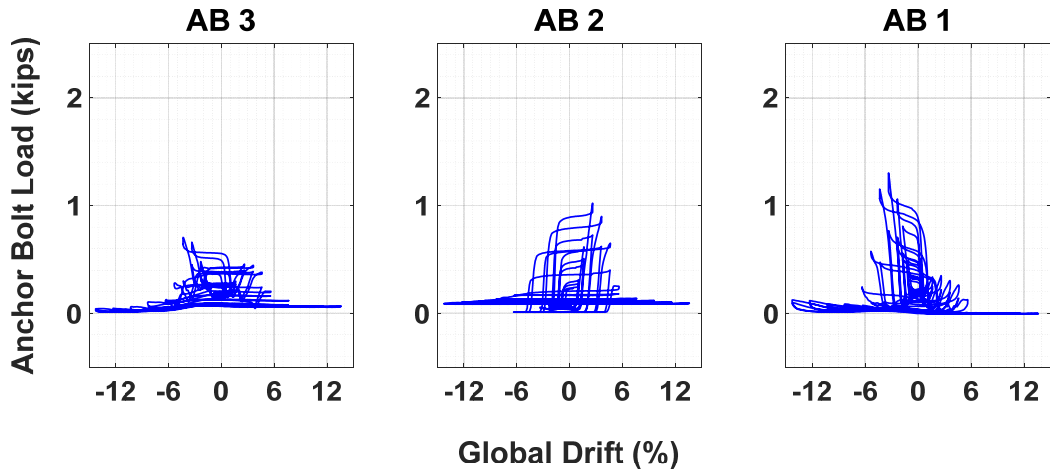


Figure 4.5 Specimen A-20 anchor bolt loads.

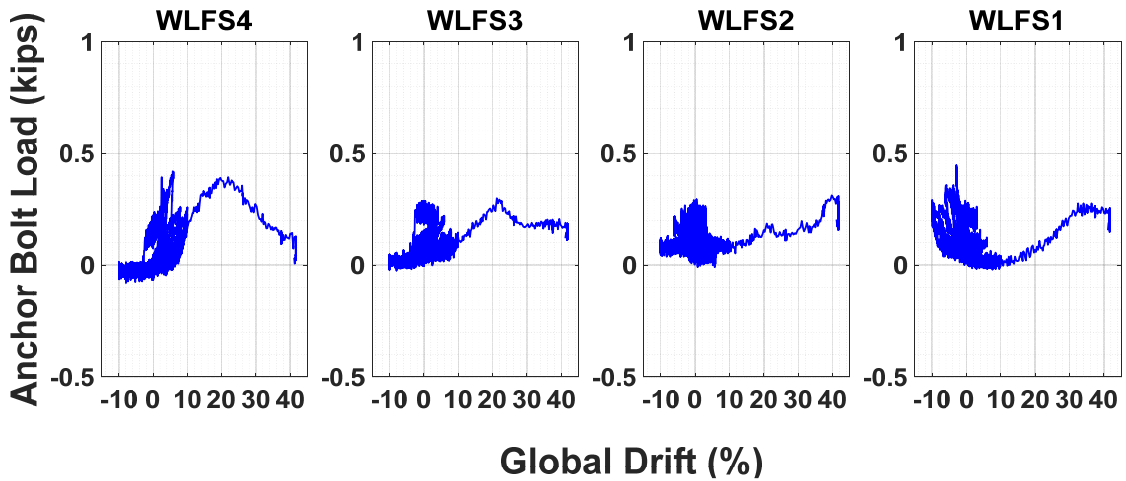


Figure 4.6 Specimen AL-1 anchor bolt loads.

Among the group of unretrofitted specimens, Specimen A-4 had by far the highest anchor bolt tension forces, with an estimated maximum of 9850 lbs. This anchor bolt force suggests that the mechanisms occurring in the anchorage for this particular specimen are very different compared to the other test specimens. All of the finish materials in Specimen A-4 were seated on the foundation, thus restricting movement due to the bearing of the finish materials. When the cripple wall displaced, the finish materials could only uplift when they rotated. In effect, this produced large increases in the anchor bolt loads throughout the test. The tension in the outermost anchor bolts for Specimen A-4 increased as much as 5000 lbs, while all the other unretrofitted small-component specimens experienced increases less than 1000 lbs. It should be noted that Specimen A-4 was the strongest of the unretrofitted small-component specimens tested, and the tension developed in the anchor bolts increased with increasing specimen strength. The weakest cripple wall tested, Specimen A-1, only experienced a 100 lbs increase in anchor bolt tension throughout the entire test.

The maximum increases in anchor bolt forces for the balance of the small-component test specimens ranged between 500 and 1100 lbs. This can be compared to the unretrofitted large-component test specimen, which had a maximum anchor bolt tension force of approximately 400 lbs. A comparison between Specimen A-20 and the other unretrofitted small-component tests (with the exception of Specimen A-4) showed that the sheathing bearing on the foundation or outboard of the foundation had little affect on the tension developed in the anchor bolts. With the exception of Specimen A-4, all of the anchor bolt changes in force can be categorized as low to moderate. In general, the small-component specimen maximum anchor bolt forces are larger than they are for the large-component specimen.

Anchor bolt forces for the retrofitted small-component specimens are shown in Figures 4.7 and 4.8. Anchor bolt forces for retrofitted large-component Specimen AL-2 are shown in Figure 4.9. Again, this data reflects the change in anchor bolt force over the duration of the test.

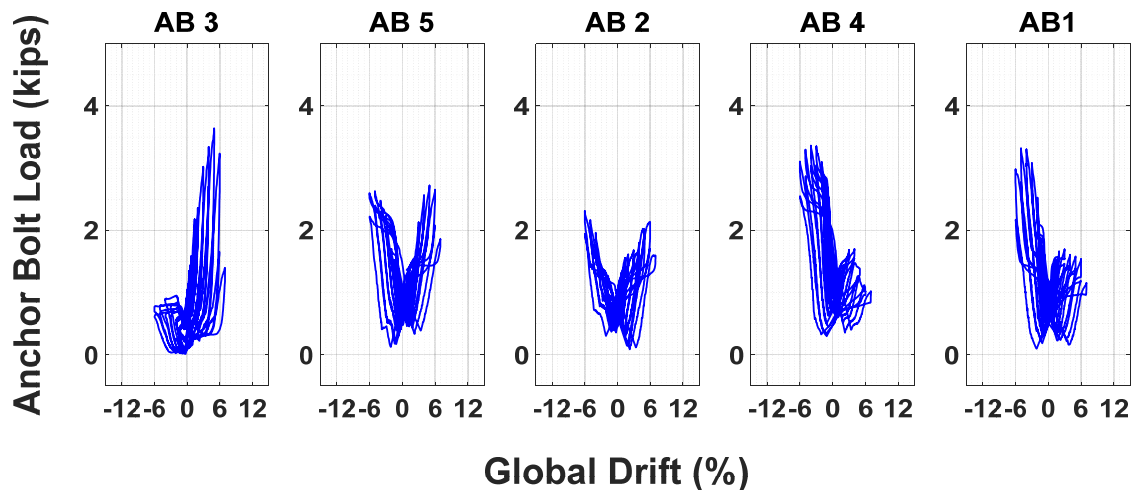


Figure 4.7 Specimen A-5 anchor bolt loads.

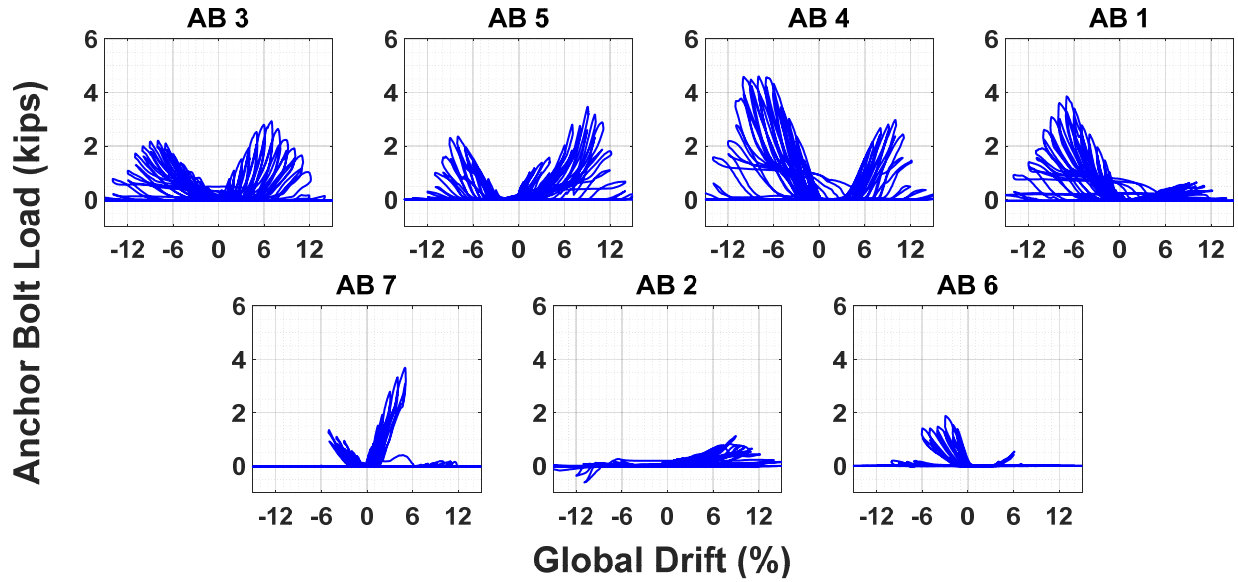


Figure 4.8 Specimen A-19 anchor bolt loads.

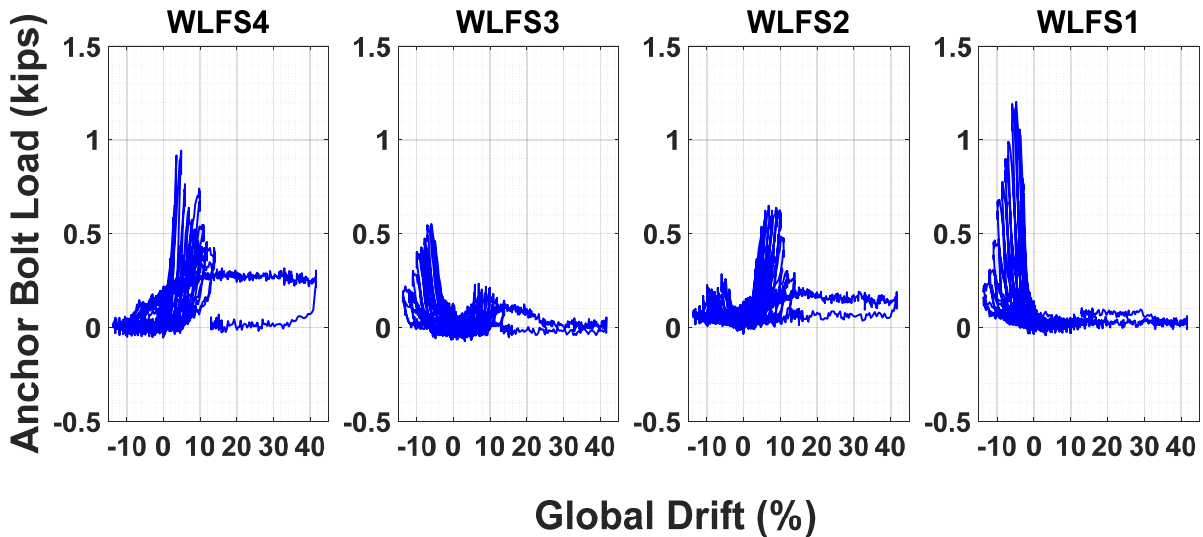


Figure 4.9 Specimen AL-2 anchor bolt loads.

The retrofitted small-component test specimen maximum anchor bolt tension forces are estimated to be 3800 lbs for Specimen A-5 and 4600 lbs for Specimen A-19. This can be compared to the retrofitted large-component test specimen with a maximum anchor bolt tension force of approximately 1200 lbs. The range in maximum anchor bolt tension for the retrofitted small-component tests were similar to each other. Increases in anchor bolt tension ranged from 900 to 4400 lbs for both specimens. The small-component specimen maximum anchor bolt forces are again larger compared to the large-component specimen. The differences in anchor bolts tensions were partially due to the lower level of uplift restraint of the plywood on the small-component specimens. As the plywood uplifts, the uplift forces were transferred through the blocking into the sill plate, increasing the tension in the anchor bolts.

While this testing considered a limited number of test specimens, it appears that there is a pattern of the maximum anchor bolt tension forces being significantly lower with the large-component testing. This could be a logical result of both the increased size of the specimen and the continuity of finish materials

#### 4.1.2 Comparison of Uplift Displacements

Uplift of the foundation sill plate off of the foundation was recorded during the course of the small-component testing. Peak uplift forces are provided in Table 4.1. Uplift between the foundation sill plate and foundation was not recorded during testing of the large-component specimens. Visual observations indicated that the uplift remained near zero for both Specimen AL-1 and AL-2. This near-zero uplift is consistent with small-component test results for Specimens A-1 and A-2, and the uplift was still modest for Specimens A-3 and A-20. Similar to the anchor bolt loads, the uplift for Specimen A-4 is larger than the rest of the unretrofitted specimens. This increased uplift was primarily attributed to the bearing of the stucco on the foundation. The uplift values are significantly higher for both retrofitted small-component test specimens compared to the observed near zero uplift for large-component Specimen AL-2. The uplift for the retrofitted small-component specimens primarily occurred due to the lack of restraint of the plywood to uplift when rotating. As previously stated, the plywood added to Specimen AL-2 was sandwiched between the sill plate and the floor joists, which inhibited uplift of the plywood and uplifted the entire specimen. The retrofitted small-component tests uplifted more because the plywood panels were able to uplift when rotating, causing the entire specimen to uplift.

**Table 4.1 Comparison of uplift displacements.**

Specimen	Specimen type	Retrofitted	Peak push uplift (in.)	Peak pull uplift (in.)
A-1	Small	No	0.06	0.01
A-2	Small	No	0.02	0.03
A-3	Small	No	0.22	0.07
A-4	Small	No	0.36	0.27
A-20	Small	No	0.16	0.17
A-5	Small	Yes	0.30	0.33
A-19	Small	Yes	0.64	0.92

#### 4.1.3 Comparison of Damage Associated with Uplift and Slip at Anchor Bolts

For the testing of unretrofitted small-component specimen, the peak uplift ranged from 0.01 in. to 0.36 in. Excluding Specimen A-4, the range was 0.01 in. to 0.22 in. The amount of displacement of the sill plate relative to the foundation as well as uplift of the specimen increased with cripple walls that had higher lateral strength. There was little difference in the damage of the unretrofitted specimens as a result of increased displacement of the sill plate relative to the foundation or uplift

of the specimen. Consequently, specimens that had experienced more uplift experienced more rotation and uplift of the studs. Along with increased uplift and rotation of the studs, the sheathing boards at the corners of the specimens experienced more cracking compared to the specimens that experienced little uplift and displacement of the sill plate. In all cases, the damage to the stucco finish was the same as well as the loss of capacity being attributed to the stucco detaching from the sill plate and bottom of the studs.

During testing of retrofitted small-component specimens, the increased uplift and displacement of the sill plate relative to the foundation had more observable effects on the damage to the specimens. The damage was primarily concentrated in the retrofit. Most notable was the increased uplift and cracking of the blocking. For both Specimens A-5 and A-19, several of the 2 × 4 blocks split during testing. This cracking occurred where the plywood fasteners were connected to the blocking. At low-displacement amplitudes, the blocking would uplift; however, at larger displacement amplitudes, the blocking cracked in many locations, particularly at the ends of the specimen where the uplift was the greatest. The damage to the finish materials was consistent with the unretrofitted specimens. Despite the increased uplift of the specimen, there was no additional damage caused to the specimen.

The increased sliding of the sill plate and the increased lateral strength of the walls increased damage to the sill plate. By the end of the test, increased ovality to the anchor bolt holes in the sill plate was visible. It should be noted that the tops of the foundations were smooth trowel finished, ultimately having less resistance sliding compared to a rough finish. For the retrofitted specimens considered herein, the damage to the sill plate did not produce much of an effect on the performance of or damage to the cripple wall. With some of the stronger retrofitted specimens tested in the program (not addressed herein), the added uplift and displacement of the sill plate produced cross-grain cracks in the sill plate and fractures in the anchor bolts.

As noted previously, there was negligible uplift between the foundation and foundation sill plate during the testing of unretrofitted large-component Specimen AL-1. There was a maximum horizontal slip between the foundation and foundation sill plate of 0.04 in. Following completion of testing, portions of the finish materials were selectively removed to allow detailed observations of the conditions underlying the materials and any hidden damage. Full details can be found in Appendix D of the large-component test report [Cobeen et al. 2020]. The nuts and cut washers were removed from a number of the anchor bolts to allow detailed observation of the anchor bolt and surrounding foundation sill plate. There was no apparent indication of slip, crushing of wood, or other similar behavior in any of the locations examined. The sill plate wood was observed to be slightly smoother under the cut washer, indicating very limited wood crushing. It is not clear if this is a result of the testing or the initial tensioning of the bolts; see Figure 4.10.

During the testing of retrofitted large-component Specimen AL-2, as previously noted there was negligible uplift between the foundation and foundation sill plate, with a maximum horizontal slip between the foundation and foundation sill plate of 0.12 in. Following testing, the nuts and cut washers were removed from a number of the anchor bolts to allow detailed observation of the anchor bolt and the 2 × 4 blocks connected to the foundation sill plate and foundation using anchor bolts; see Figure 4.11. There was no apparent indication of slip, crushing of wood, or other similar behavior in any of the locations examined. The 2 × 4 blocking wood was again observed to be slightly smoother under the cut washer, indicating very limited wood crushing. Splitting of blocking at anchor bolts had been observed in the small-component testing, therefore significant

attention was paid to the condition of the blocking at anchor bolts in Specimen AL-2. Where access openings in the plywood sheathing permitted, photos were taken from above looking for splitting of the block that might fracture the top surface. No splitting was observed in the blocks that were accessible; see Figure 4.12.

Plywood cripple wall sheathing was removed in selected locations to allow for more complete access to observe splitting of the blocking. Figure 4.13(a) shows an overview of the framing with the plywood removed. Figure 4.13(b) shows a block with no splitting. Figure 4.13 (c) and (d) shows the one block in which splitting had occurred in both the vertical and the top faces of the block. This block was located near the middle of the north wall.



**Figure 4.10** Specimen AL-1 anchor bolts with nuts and washers removed following completion of testing.



**Figure 4.11** Specimen AL-2 anchor bolts with nuts and washers removed following completion of testing.

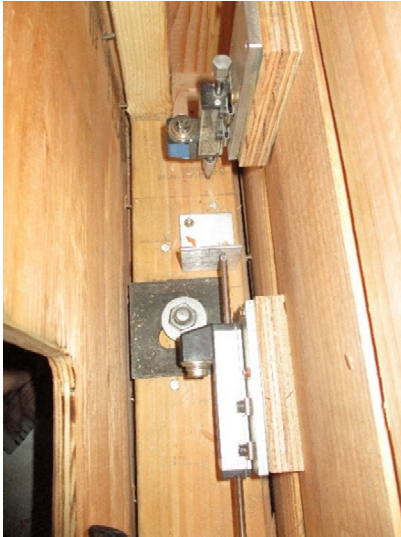


**Figure 4.12 Specimen AL-2 retrofit blocks at end of testing showing no signs of splitting.**



**(a)**



**(b)**



**(c)**



**(d)**

**Figure 4.13 Specimen AL-2 showing the only block that experienced splitting.**

#### **4.1.4 Discussion of Uplift and Slip at Anchor Bolts**

Differences were observed between the large and small-component tests with regard to anchor bolt forces, uplift of the foundation sill plate off of the foundation, and damage mechanisms related to the anchor bolts. Among the group of unretrofitted small-component test specimens, the maximum anchor bolt loads for Specimen A-4 were significantly different and appear to indicate different mechanisms at work. These mechanisms were primarily a result of having both the stucco and the sheathing bearing on the foundation. While many of the other specimens had the sheathing bearing on the foundation, the stucco was positioned outboard. Based on the small-component test results, the positioning of the stucco had the greatest effect on the strength, drift capacity, end uplift, and anchor bolt tension of any of the differences in the boundary conditions.

Larger uplift displacement and anchor bolt forces occurred in the small-component specimens compared to the large-component specimens, particularly those that had been retrofitted. Resulting damage and uplift displacements did not appear to reduce the lateral strength achieved. Uplift displacements may have influenced the larger drift levels at peak displacement experienced by some of the small-component specimens. Based on the lack of uplift seen in the large-component specimens, it may be desirable in future testing of small-components to consider detailing to mitigate displacement at anchorages, thereby better matching large-component response. It is likely that this could be accomplished by ensuring that all anchor bolt holes in the foundation sill plate are oversized by 1/16-in. instead of the 1/4 in. that was used for all small-component tests.

## 5 Comparison of Observations and Damage

The following discussion highlights observed behavior and damage judged to be of the interest in comparing the small- and large-component tests. Three points in the load-deflection response are included in this comparison. The first point is at a 1.4% drift ratio; damage and other behaviors observed up to and including this drift ratio are discussed. The second point is at lateral strength (peak capacity), and the final point is at a post-peak point where only 20% of the lateral strength remains. Further information regarding behaviors at other drift levels can be found in the PEER–CEA Project WG4 test reports.

### 5.1 COMPARISON OF OBSERVATIONS AND DAMAGE AT 1.4% DRIFT RATIO

This section discusses observations and damage up to the 1.4% drift ratio. Understanding the physical damage characteristics of cripple walls at low-level drift amplitudes is important to be able to make distinctions between what is a serviceable structure and what is a structure that requires repairs before it becomes serviceable again. While the range of 0% to 1.4% drift ratio is not a definitive criterion for what drift amplitudes constitute a serviceable wood-frame dwelling, it provides a good range of drift amplitudes to categorize damage at small displacements. In the following section, existing test specimens are discussed first, to be followed by the retrofitted specimens.

#### 5.1.1 Comparison of Observations and Damage at 1.4% Drift Ratio for Unretrofitted Specimens

##### 5.1.1.1 *Specimen A-1 Observations and Damage at 0.0% to 1.4% Drift Ratio*

Figures 5.1(a) to (f) show the damage state of Specimen A-1 at 1.4% drift amplitude. At this low-level amplitude, no cracks had formed on the stucco face. On the interior of the wall, the studs had started to uplift and exhibited slight rotation. This uplift and rotation can be seen in the connection of the studs to the sill plate, and the connection to the top plates. The most noticeable damage characteristics was the 1/4 in. of relative displacement between stucco and foundation face at the base of the cripple wall and the 1/8 in. of relative displacement between the stucco and framing at the top of the cripple wall. Based on visual observations, the lack of cracking on the specimen would indicate minimal to no structural damage to the wall.



(a)



(b)



(c)



(d)



(e)



(f)

**Figure 5.1 Specimen A-1 damage state of at -1.4% global drift ratio @  $\Delta = -0.336$  in.:**  
 (a) exterior elevation; (b) interior elevation; (c) bottom of exterior wall displacement; (d) south top exterior and corner view; (e) north exterior and corner view; and (f) top of wall displacement.

### 5.1.1.2 Specimen A-2 Observations and Damage at 0.0% to 1.4% Drift Ratio

Figure 5.2(a) to (f) show the damage state of Specimen A-2 at 1.4% drift ratio amplitude. At this drift ratio level, a new vertical crack started to form at the base of the stucco but had not yet propagated up the entire stucco face. In addition, both the north and south corners of the wall exhibited extensive cracking. Figure 5.2(e) and (f) shows that most of the cracks were concentrated at the bottom close to the corner and ran vertically, but additional cracks had formed on corner faces that propagated diagonally across the face. These cracks began forming at drift ratio amplitudes as low as 0.2% and continued extending at larger drift ratio amplitudes. Figure 5.2(c) shows that the stucco experienced 1/4-in. displacement relative to the foundation. This figure also shows that the stucco had detached from the foundation and a gap was beginning to form between the stucco and the foundation face. This occurred as the furring nails began to detach from the sheathing board and framing members. Like Specimen A-1, the studs had begun to rotate and uplift. At the top of the cripple wall, the displacement between the sheathing and framing was negligible.

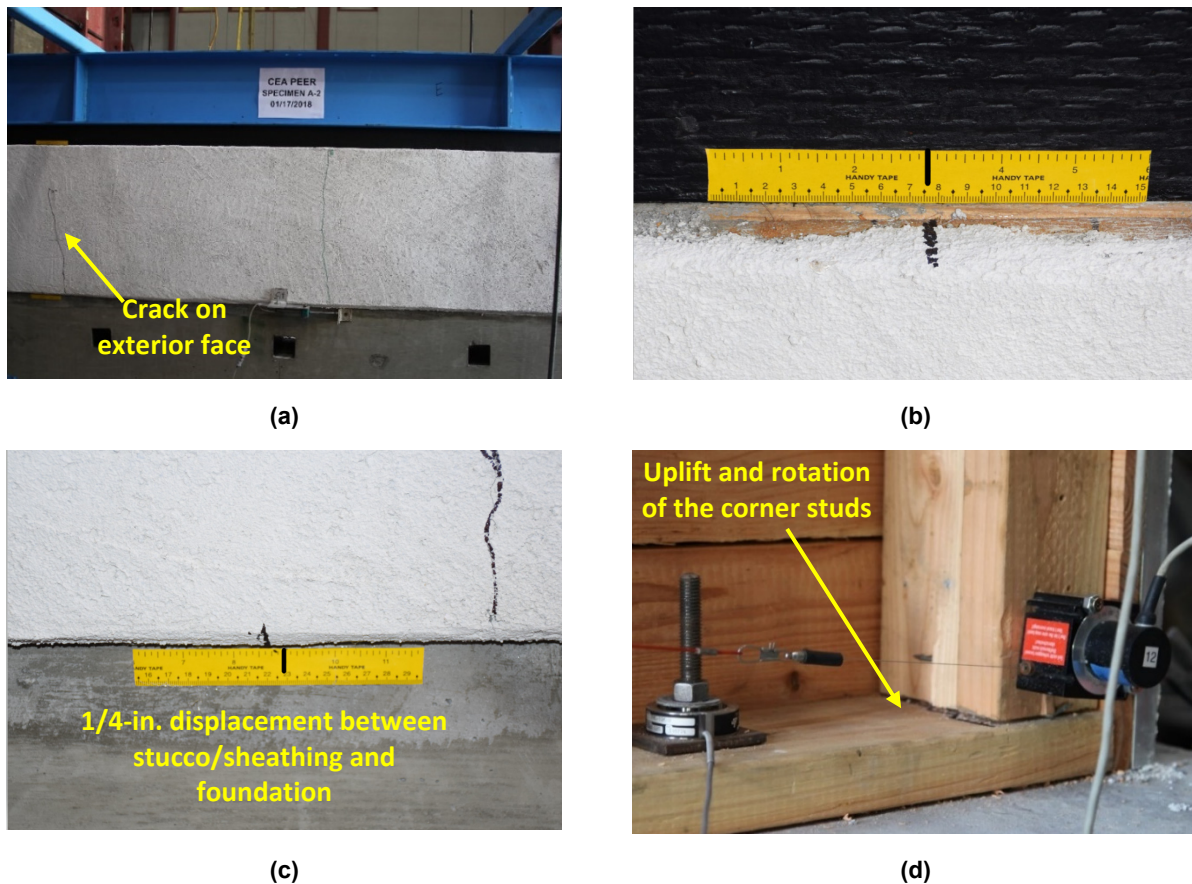
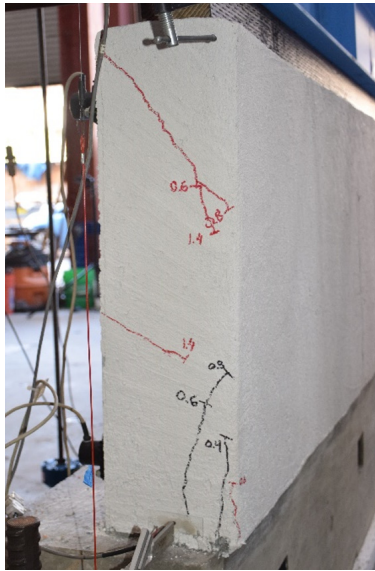
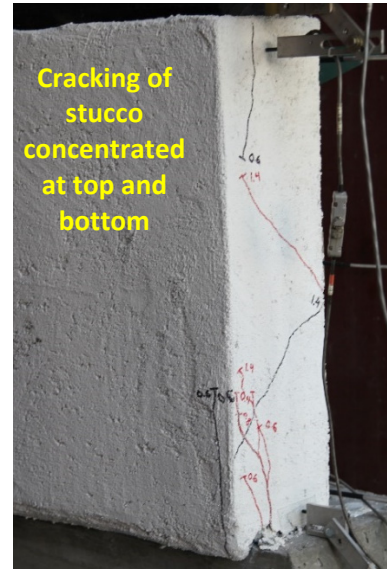


**Figure 5.2** Specimen A-2 damage state of at -1.4% drift @  $\Delta = -0.336$  in.: (a) exterior elevation; (b) top of exterior wall; (c) bottom of exterior wall; (d) bottom corner of south-end interior; (e) north-end exterior corner view; and (f) north-end interior corner view.



(e)



(f)

Figure 5.2 (continued).

### 5.1.1.3 Specimen A-3 Observations and Damage at 0.0% to 1.4% drift ratio

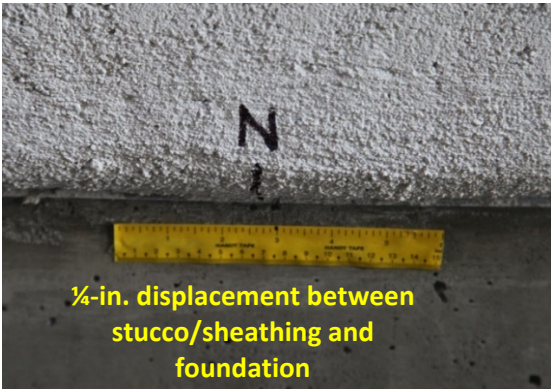
Figure 5.3(a) to (f) show the damage state of Specimen A-3 at 1.4% drift ratio amplitude. At this drift ratio level, no cracks had yet formed on the exterior face of the stucco other than a small crack running diagonally from the top of the cripple wall to the corner on the north, although many cracks began propagating vertically at the corners, as shown in Figures 5.3(e) and (f). Similar to the previous specimen, these cracks started at the 0.2% drift ratio amplitude and continued to extend in subsequent cycles of increased drift ratio amplitude. It is notable that no cracks appeared on the face of either return wall. Figure 5.3(c) shows that the stucco to foundation displacement of 3/8 in., which is higher than the previous test; the displacement of the sheathing relative to the framing did not occur, unlike the previous test. The continued reduction of relative displacement between the sheathing and framing was attributed to the presence of extended corners (end return walls), which offered additional resistance, as evidenced by the 50% reduction in displacement. Figure 5.3(d) shows significant uplift and slight rotation in the studs of the return walls.



(a)



(b)



(c)



(d)



(e)

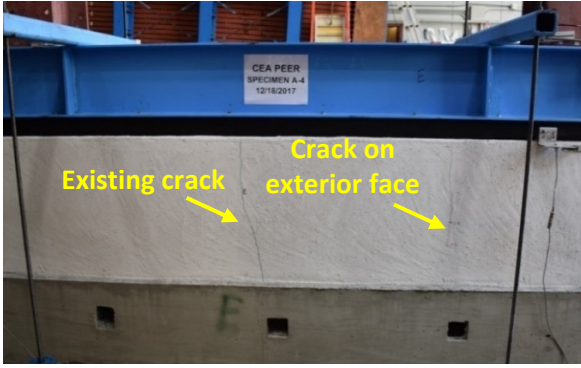


(f)

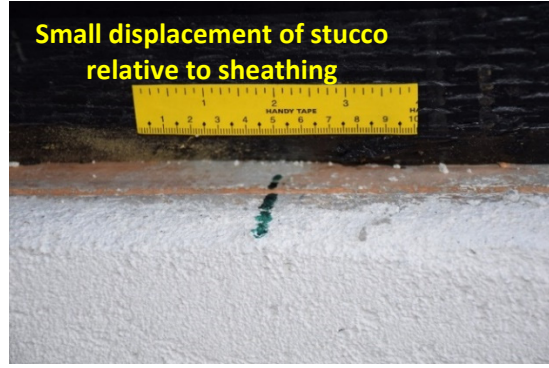
**Figure 5.3** Specimen A-3 damage state at -1.4% drift @  $\Delta = -0.336$  in.: (a) exterior elevation; (b) top of the exterior wall; (c) bottom of exterior wall; (d) bottom of interior wall; (e) north-end of exterior corner; and (f) south-end of exterior corner.

#### **5.1.1.4 Specimen A-4 Observations and Damage at 0.0% to 1.4% Drift Ratio**

Figures 5.4(a) to (f) show the damage of Specimen A-4 at 1.4% drift ratio amplitude. At this drift ratio level, cracks had started to propagate vertically on the exterior face of the stucco; see Figure 5.4(a). As with the two previous specimens, significant cracking occurred, concentrated around the corners of the wall. Specimen A-4 varied slightly though, showing more cracks on the corner faces, both vertical and diagonal, compared to the previous two cripple walls. Even at this low drift ratio amplitude, 1/8 in. of uplift occurred at the end of cripple wall; see Figure 5.4(d). Across the entire wall, the seal between the stucco and foundation broke, and a gap had started to form at the base of the wall. On the interior, uplift of the studs occurred but no visible rotation of the studs. This is due to the entire wall bearing on the foundation and resisting movement more evenly than the cripple walls, which had no bearing resistance from the stucco due to the stucco being outboard of the foundation. As with all previously tested specimens, a 1/4-in. displacement between the stucco and the foundation occurred at the base of the wall. Unlike the previous specimens, the relative displacement at the top of the cripple wall was minimal. Figure 5.4(b) shows insignificant displacement—typically less than 1/8 in—between the sheathing and framing, but this was the first instance that showed displacement between the stucco finish and the horizontal sheathing. Again, this is due to the stucco finish bearing on the foundation. As the cripple wall displaces, the bearing causes the furring nails to rotate and pull away from the sheathing boards, leading to a relative displacement between the stucco and sheathing.



(a)



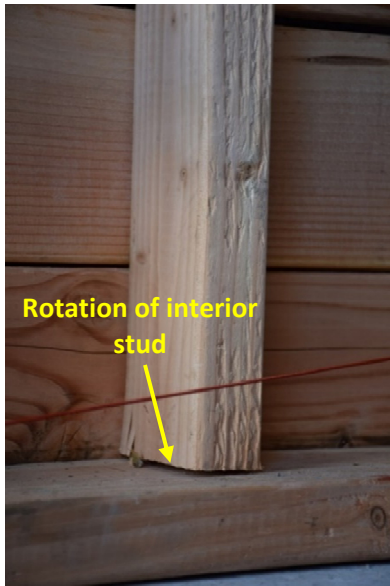
(b)



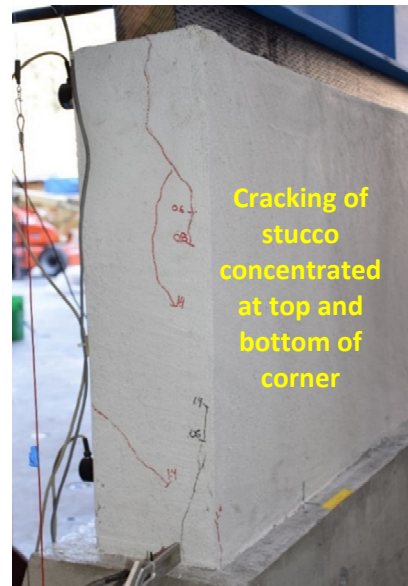
(c)



(d)



(e)



(f)

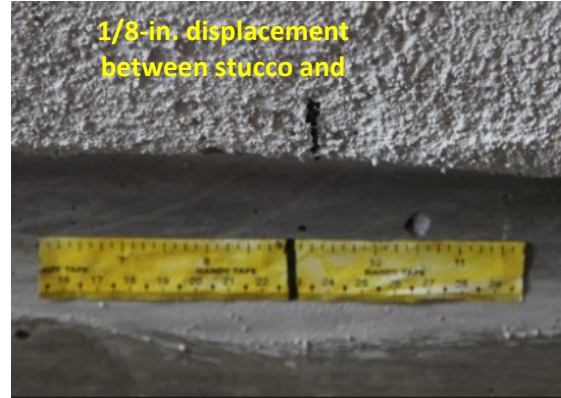
**Figure 5.4** Specimen A-4 damage state of at -1.4% drift @  $\Delta = -0.336$  in.: (a) exterior elevation; (b) top of exterior wall; (c) bottom of exterior wall; (d) bottom of north-end exterior corner; (e) bottom of interior wall; and (f) north-end of exterior corner.

#### **5.1.1.5 Specimen A-20 Observations and Damage at 0.0% to 1.4% drift ratio**

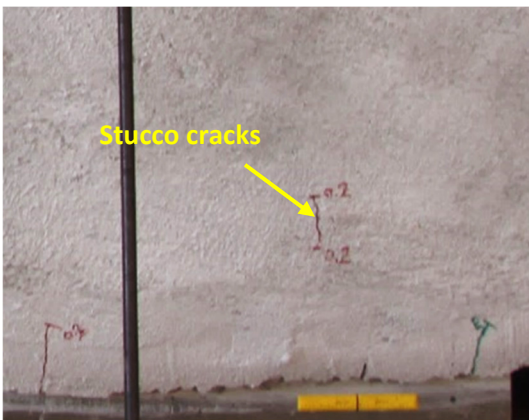
Specimen A-20 was an existing 2-ft-tall cripple wall with stucco over horizontal sheathing exterior finish and bottom boundary condition d. Figure 5.5 shows the state of the cripple wall at -1.4% (-0.336 in.). A 1/8-in. displacement between the finish materials and the framing [Figure 5.5(a)] and a 1/4-in. displacement between the finish materials and the foundation [Figure 5.5(b)] occurred. These displacements are consistent with the existing, stucco over diagonal sheathing finished Specimen (A-15). Small cracks formed at various locations along the bottom of the face of the cripple wall; see Figure 5.5(c) and (d). At this point, the stucco extension had fully detached from the footing; see Figure 5.5(e) and (f). The same cracking pattern that occurred at the bottom of the corners with the previous specimens also occurred with this specimen.



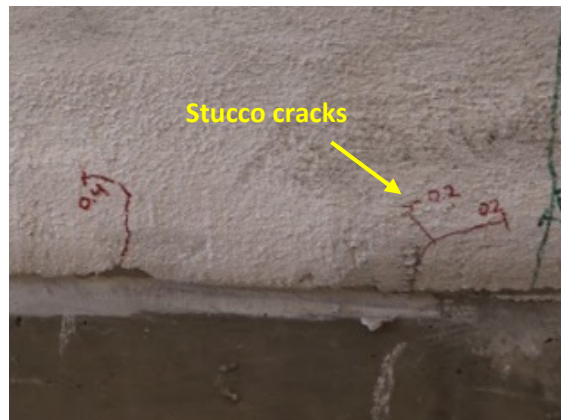
(a)



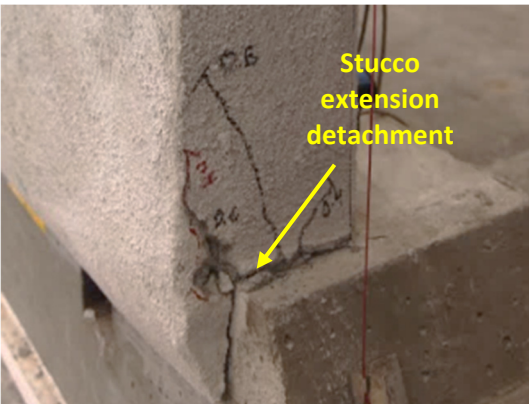
(b)



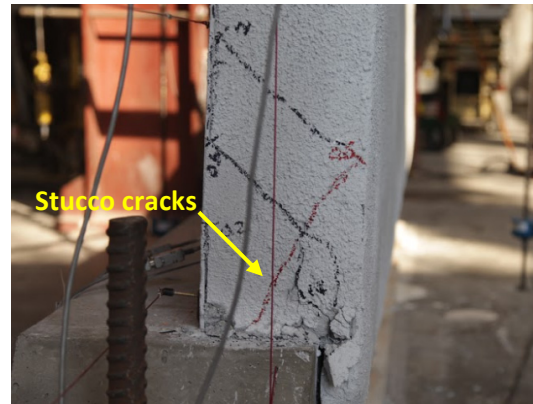
(c)



(d)



(e)



(f)

**Figure 5.5** Specimen A-19 damage state of at -1.4% drift ratio @  $\Delta = -0.336$  in.: (a) top of south-end exterior of wall; (b) bottom of south-end exterior of wall; (c) bottom of south-end interior corner of wall; (d) bottom interior of wall (south panel); (e) middle exterior of wall; and (f) bottom of north-end exterior corner of wall.

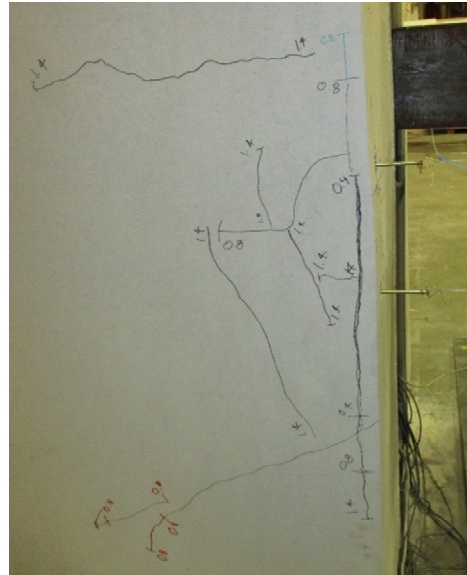
#### **5.1.1.6 Specimen AL-1 Observations and Damage at 0.0% to 1.4% drift ratio**

Prior to the start of testing, stucco wall finish cracking initiated after the installation of the stucco due to shrinkage and the application of the lead weights used for supplemental gravity load. These hairline cracks tended to follow a vertical direction and were generally uniformly distributed along the length of the specimen.

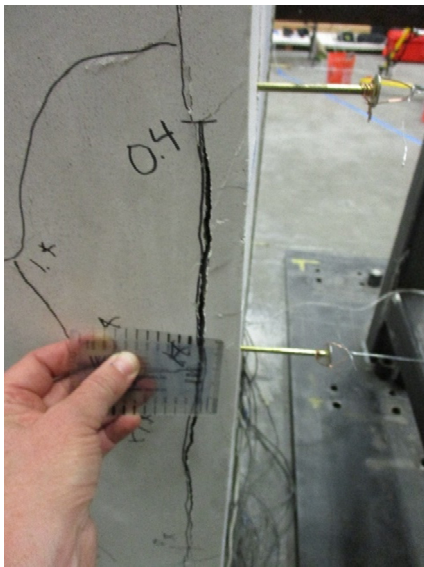
Figure 5.6 shows the damage state of Specimen AL-1 at a drift ratio of 1.4%. Stucco cracking initiated in the east and west end walls and corners at the framed floor level. At a drift ratio of 1.4%, stucco cracking at the end walls and corners had spread and began to open. While cracking in much of the north and south walls was very limited, cracking was extensive near the corners at the ends of the north and south walls. Maximum crack widths ranged from 0.075 to 0.125 in. Slight offsets in gypsum wallboard panel edges were noted on interior of the superstructure. There was no observable movement of the stucco relative to the framing and sheathing at the floor. At this drift level, the bond between the stucco and the foundation was still intact, with no measurable relative displacement occurring.



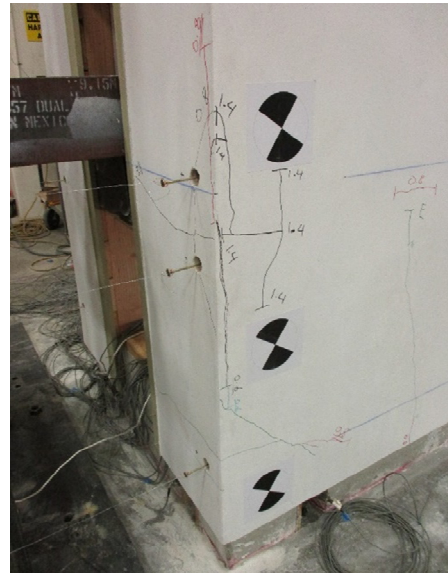
(a)



(b)



(c)



(d)

**Figure 5.6 Specimen AL-1 damage state of at 1.4% drift ratio: (a) bottom of northwest corner; (b) middle of northwest corner; (c) northwest corner detail; and (d) bottom of southwest corner.**

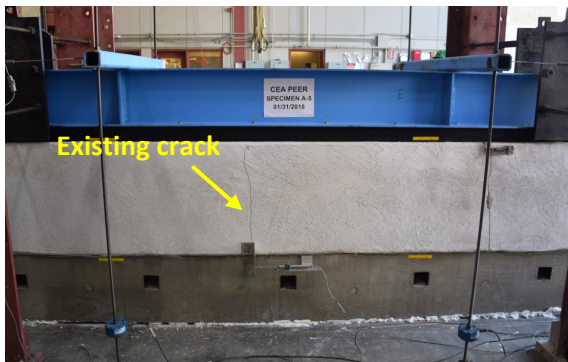
### **5.1.1.7 Discussion of Observations and Damage for Test Specimens Without Retrofit at 0.0% to 1.4% drift ratio**

In all of the small- and large-component test specimens, the cracking in the face of the stucco (the 12-ft-length for the small-component specimen and 20-ft length for the large-component specimens) was observed to be very limited and near hairline. In all of the small and large test specimens where the stucco had been returned around the corners at the specimen ends, the corners showed a concentration of stucco cracking. The damage in the large-component specimen was more extensive than the small-component specimens, with crack widths up to 1/8 in. Measurable slip and uplift were observed in the small-component tests but not in the large-component test. For the large-component specimen, the corner stucco damage was greatest at the floor level, whereas for the small-component specimens, it was greatest at the bottom of the cripple wall where it bore on the foundation.

## **5.1.2 Comparison of Damage at 1.4% Drift Ratio for Specimens with Retrofit**

### **5.1.2.1 Specimen A-5 Observations and Damage at 0.0% to 1.4% drift ratio**

Figures 5.7(a) to (f) show the damage state of Specimen A-5 at 1.4% drift ratio amplitude. At this drift ratio, no additional cracks had formed on the face of stucco. There was a large reduction in the amount of cracking at the corners of the cripple wall as compared with Specimens A-2 through A-4, as shown in Figure 5.7(f). This could be due to much of the work resisting displacement being done by the retrofit instead of the corners. As with Specimen A-2, there was a 1/4-in. displacement between the stucco and the foundation as well as disconnect between the stucco and the foundation at the base of the cripple wall. At the top of the cripple wall, a 3/16-in. displacement between the sheathing and framing formed, which is the largest of any of the previous tests. This is due to the framing members being significantly stiffened by the attachment of the plywood panels on the interior face. On the interior face, small displacements between the plywood panels had started to form as the plywood panels began to rotate. The 1/8-in. gap between abutting plywood panels remained; therefore, the wood structural panels had yet to bear on each other. Figure 5.7(e) shows that some of the nails were slightly overdriven and had started to begin pulling through the plywood. For the other nails attaching the plywood to framing, minimal rotation or pulling through was visible at this drift ratio level.



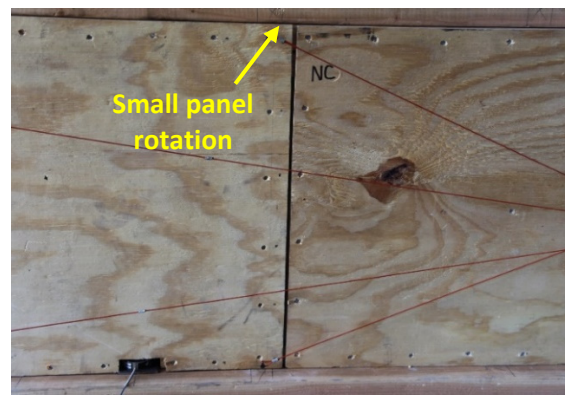
(a)



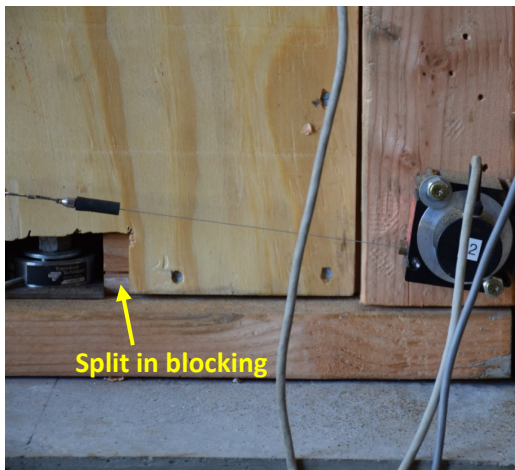
(b)



(c)



(d)



(e)



(f)

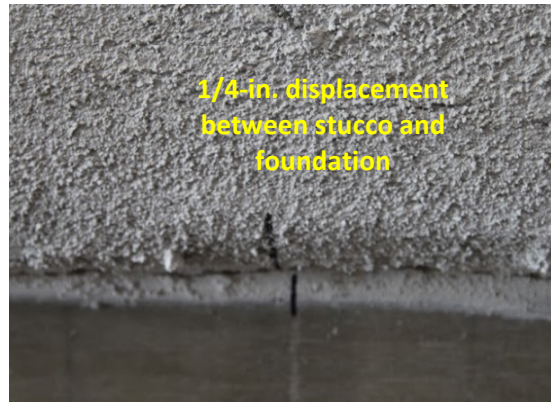
**Figure 5.7** Specimen A-5 damage state at +1.4% drift @  $\Delta = +0.336$  in.: (a) exterior elevation; (b) top of exterior wall; (c) bottom of exterior wall; (d) plywood panel joint; (e) close-up of top of the south-end interior wall; and (f) north-end exterior corner.

### **5.1.2.2 Specimen A-19 Observations and Damage at 0.0% to 1.4% drift ratio**

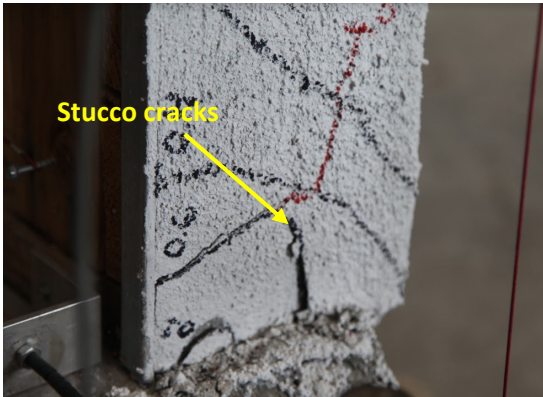
Figure 5.8 shows the state of the cripple wall at -1.4% drift ratio (-0.336 in.); the sheathing at the top of the cripple wall had been displaced by 1/8 in. relative to the framing [Figure 5.8(a)], and both finish materials had been displaced by 1/4 in. relative to the foundation; see Figure 5.8(b). Cracks had formed in the stucco at the bottom of both corners; see Figure 5.8(c) and (f). With all stucco specimens tested, there was increased cracking concentrated at the bottom of the corners due to the corners bearing on the foundation. Along the face of the specimen, a diagonal and a vertical crack had formed, as shown in Figure 5.8(e). On the interior, the damage to the plywood was the same as what occurred in the previously tested retrofitted specimens. There were small rotations of the panels, withdrawal of the nails at some locations, and rotation of many of the edge nails. Nail withdrawal began to occur at the base of the panels can be seen in Figure 5.8(d).



(a)



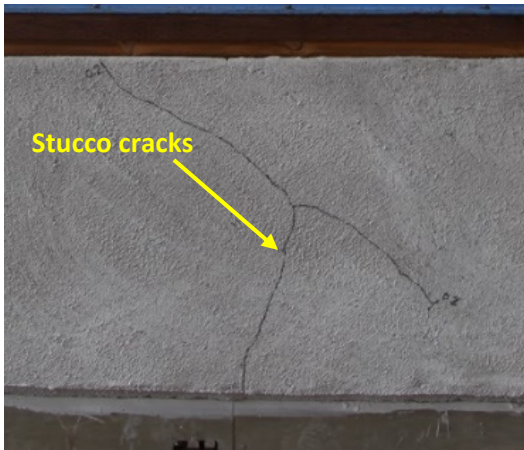
(b)



(c)



(d)



(e)



(f)

**Figure 5.8** Specimen A-19 damage state at -1.4% drift ratio @  $\Delta = -0.336$  in.: (a) top of south-end exterior of wall; (b) bottom of south-end exterior of wall; (c) bottom of south-end interior corner of wall; (d) bottom interior of wall (south panel); (e) middle exterior of wall; and (f) bottom of north-end exterior corner of wall.

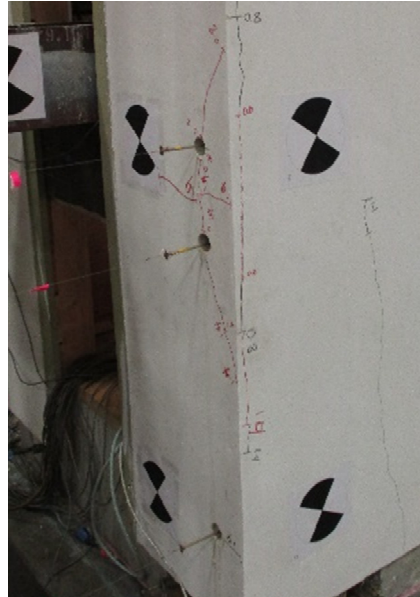
### **5.1.2.3 Specimen AL-2 Observations and Damage at 0.0% to 1.4% drift ratio**

Prior to the start of testing, stucco wall finish cracking occurred after stucco installation due to shrinkage and following application of the lead weights used for supplemental gravity loading. These hairline cracks tended to follow a vertical direction and were generally uniformly distributed along the specimen length.

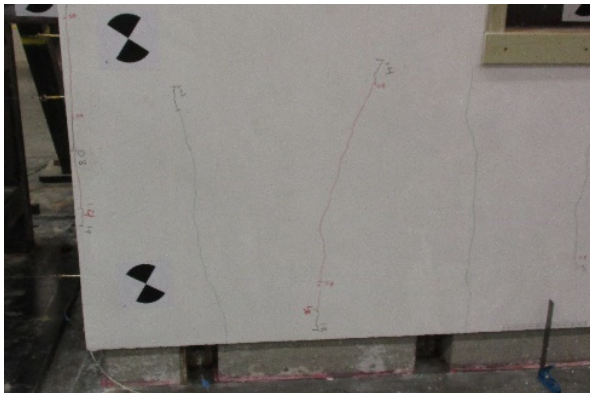
Figure 5.9 shows the damage state of Specimen AL-2 at a drift ratio of 1.4%. Cracking was first observed at the west and east end walls near the framed floor level at 0.8% drift. At 1.4% drift the cracking at the end walls and corners was observed to spread up and down from the floor level. At the north and south walls modest spreading and new hairline cracks were observed in the field of the wall. Unlike Specimen AL-1, the cracking that initiated at the specimen corners and extended into the north and south walls was much more limited. Like Specimen AL-1, at this drift ratio the bond between the stucco and foundation was still intact, with no measurable relative movement.



(a)



(b)



(c)



(d)

**Figure 5.9** Specimen AL-2 damage state at 1.4% drift ratio: (a) bottom of northwest corner; (b) bottom of southwest corner; (c) bottom of south-end of wall; and (d) middle of southeast corner.

#### **5.1.2.4 Discussion of Observations and Damage for Test Specimens with Retrofit at 0.0% to 1.4% Drift Ratio**

Both retrofitted small- and large-component specimens experienced less damage at a drift ratio of 1.4% than the similar unretrofitted components. In the small-component specimens, this resulted in greatly reducing the extent of damage. In the large-component specimen, this resulted in a modest reduction in the extent of stucco cracking with smaller crack widths. In both retrofitted large and small specimens, the lateral force level was significantly higher at a drift ratio of 1.4% than it was without retrofit. This shows the combined benefits of retrofit of both higher seismic force level and reduced damage.

For the large-component specimen, the corner stucco damage was greatest at the floor level, whereas for the small-component specimens, it was greatest at the bottom of the cripple wall where it bore on the foundation.

## **5.2 COMPARISON OF OBSERVATIONS AND DAMAGE AT LATERAL STRENGTH**

Beyond the low levels of drift, another key damage state occurs when the cripple wall attains lateral strength. Thus, the damage features presented in this section are those that occurred following attainment of the cripple walls' lateral strength. Beyond this, larger imposed drifts resulted in a loss of load capacity. Examining the damage states at this level provides insight into how and why failure is occurring in a cripple wall. It is noted that lateral strength for all unretrofitted cripple walls tested occurred between global drift ratios of 2.8 to 5.0% and relative drift ratios of 2.4 to 3.7%. For the retrofitted cripple walls, lateral strength was achieved between global drift ratios of 2.8 to 8.0% and relative drift ratios of 2.8 to 5.3%. The relative drift is defined as the drift of the cripple wall only, absent displacement of the sill plate relative to the foundation. Unretrofitted test specimens are discussed first, followed by retrofitted test specimens.

### **5.2.1 Comparison of Damage at Lateral Strength for Unretrofitted Specimens**

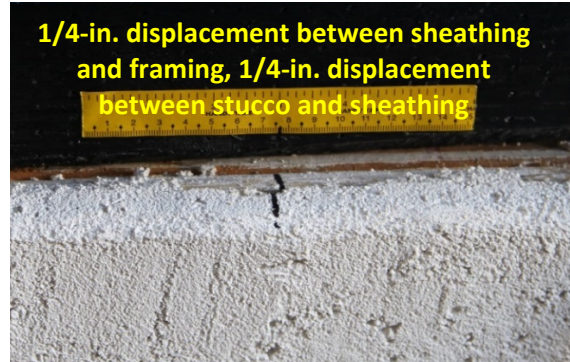
#### **5.2.1.1 Specimen A-1 Observations and Damage at Lateral Strength**

Figures 5.10(a) to (f) show the damage state of Specimen A-1 at lateral strength, which occurred at 3% global and relative drift ratio in both the push and pull loading directions. Due to its lower capacity, Specimen A-1 did not experience any sill displacement relative to the foundation. At strength, there were still no visible cracks on the face of the stucco. Figure 5.10(e) shows a 3/16-in. separation between the stucco and sheathing. This occurred as the furring nails detached from the framing and started to work their way out of the sheathing (nail withdrawal), or the furring nails have detached from the stucco (nail head pullout). Both conditions can occur, and their occurrence is dependent on how well the furring nails were fastened to the wire lath and how well they were fastened to the sheathing. Whichever condition has the least capacity determines what mechanism will occur first. It should be noted that only 1/8 in. of the 1-1/2-in furring nails would be driven into the framing because the nails were furred out 1/4 in. and penetrated through the 7/8-in.-thick horizontal sheathing.

The displacement between the base of the stucco and the foundation increased to 1/2 in., and a gap between the stucco and foundation face became more pronounced. Figure 5.10(f) shows that at the top of the cripple wall, a 1/4-in. relative displacement between the stucco finish and the sheathing developed as well as a 1/4-in. relative displacement between the sheathing and framing. In addition, a small gap opened up between the sheathing and framing, indicating that the small amount of embedment that the furring nails had into the framing was now gone. On the interior of the cripple walls, the uplift of the studs was more pronounced, while the rotation of the studs was similar to that at the service-level drift ratio. Some of the studs began splitting at both the connection to the sill plate and top plate. Lastly, cracks had begun to form on the ends of the sheathing boards, concentrated near the location that the boards are nailed to the studs.



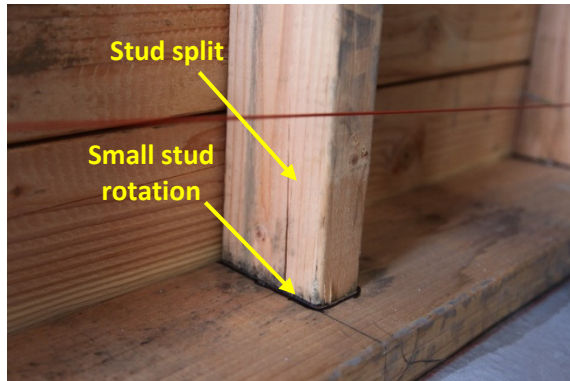
(a)



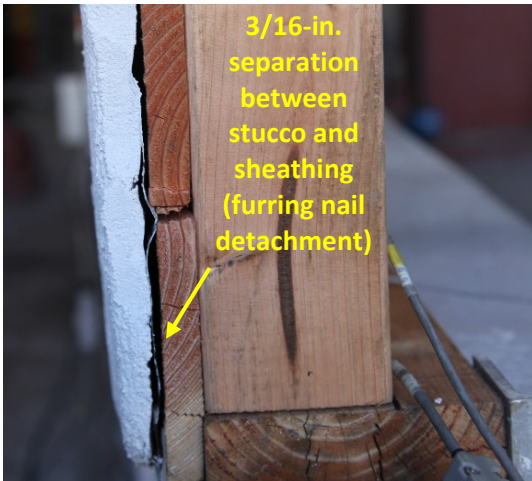
(b)



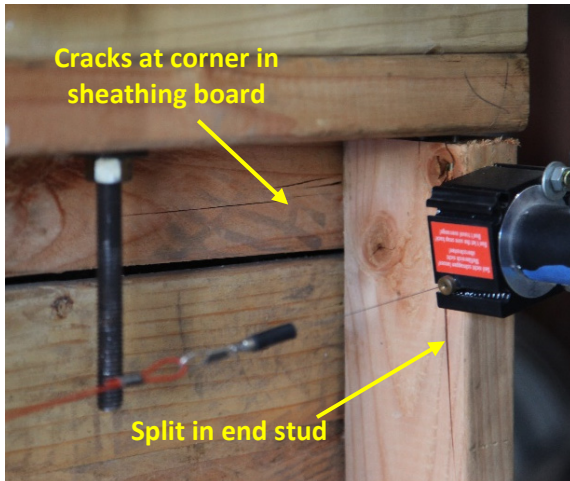
(c)



(d)



(e)



(f)

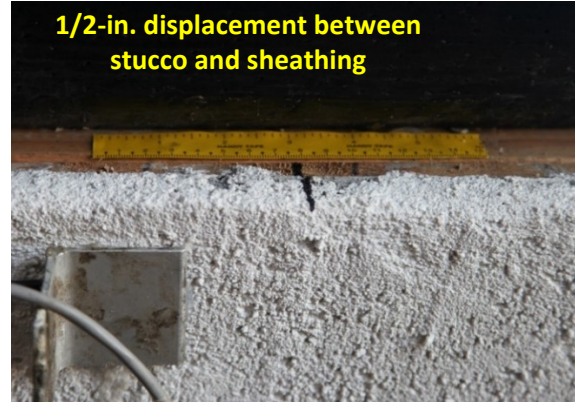
**Figure 5.10** Specimen A-1 damage state of at lateral strength @ +3% drift,  $\Delta = +0.72$  in.: (a) exterior elevation; (b) top of the exterior wall; (c) bottom of exterior wall; (d) close-up of stud; (e) north-end corner of wall; and (f) close-up of top of south-end interior corner.

### **5.2.1.2 Specimen A-2 Observations and Damage at Lateral Strength**

Figure 5.11(a) to (f) show the damage state of Specimen A-2 at lateral strength. The lateral strength occurred at 5% global drift ratio in the push loading direction and 4% in the pull loading direction. The corresponding relative drift ratio was 4.3% in the push direction and 3.1% in the pull direction. At lateral strength, additional vertical cracks began propagating along the face of the stucco. The formation of a 1/2-in. gap occurred at the base of the stucco, which is evident from Figures 5.11(c) and (e). At this point, the stucco had detached from most of the furring nails at the base, but in some cases, the furring nails remained attached to the stucco and had withdrawn significantly from the sheathing. The former being the more common occurrence. This same gap was not evident at the top of the cripple wall because of the increased pullout resistance due to the significantly denser furring nail arrangement on the upper top plates. The displacement of the stucco at the base and the foundation has increased to 7/8 in., while the only apparent relative displacement at the top of the cripple wall was a 1/4-in. displacement between the stucco and sheathing, as shown in Figure 5.11(d). This is due to the rotation of the furring nails at the top of the wall. At the exterior corners, major cracking ran in all directions and was heavily concentrated at the corner edge; see Figure 5.11(f). Crushing and spalling of the stucco was extensive at the corner faces due to the heavy bearing of the stucco finish on the foundation. On the interior face, some of the studs had split at the connection to the sill plate. In addition, a slight lateral movement occurred on the studs. This lateral movement can be attributed to the horizontal sheathing and stucco finish moving out laterally due to the nails being pulled out as they rotated back and forward during each cycle.



(a)



(b)



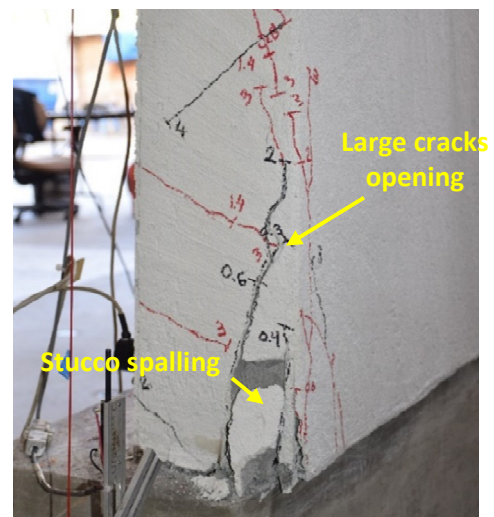
(c)



(d)



(e)

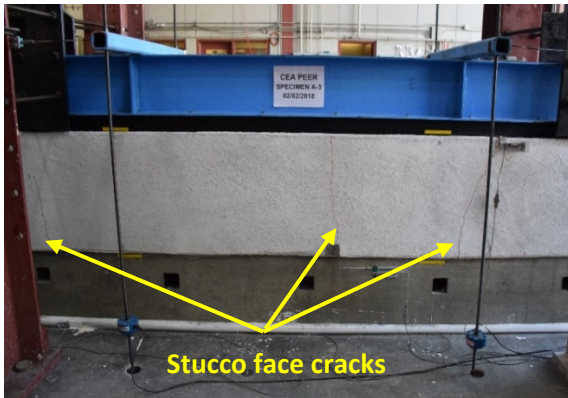


(f)

**Figure 5.11** Specimen A-2 damage state at lateral strength @ -4% drift,  $\Delta = -0.96$  in.: (a) exterior elevation; (b) top of exterior wall; (c) bottom of exterior wall; (d) close-up of studs; (e) close-up of north-end corner; and (f) close-up of bottom south-end exterior corner.

### **5.2.1.3 Specimen A-3 Observations and Damage at Lateral Strength**

Figures 5.12(a) to (f) show the damage state of Specimen A-3 at lateral strength. The lateral strength occurred at 4% global drift ratio in the push loading direction and 3% in the pull loading direction. The corresponding relative drift ratio was 2.9% in the push direction and 2.0% in the pull direction. At lateral strength, cracks had propagated vertically along the face of the stucco. As seen in Figure 5.12(c), the displacement between the base of the stucco and the foundation had increased to 1 in., and a large gap had formed between the stucco and the foundation face, evidence that the furring nails had completely detached from the stucco along bottom of the stucco face. This is confirmed by large cracks running vertically from the base of the stucco at the corners. In addition to the vertical cracks at the corners, diagonal cracks were propagating along the face of the return walls. At the top of the cripple wall, the displacement between the sheathing and framing did not expand, and there was no presence of displacement between the stucco and sheathing. This is both due to the dense furring nail arrangement on the upper top plates as well as the extended corner return walls resisting these relative displacements. Figure 5.12(e) shows that a gap formed at the base of the return walls as the furring nails detached from the stucco. On the interior of the wall, more pronounced uplift of the studs occurred. Again, some of the studs had split near the connection to the sill plate; see Figure 5.12(b). This splitting occurred in the South return wall sill plate due to the rocking motion of the return walls during cyclic loading.



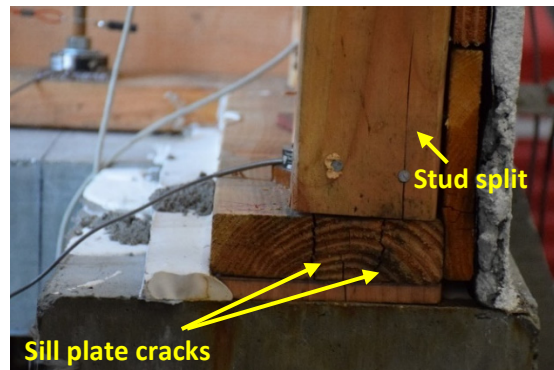
(a)



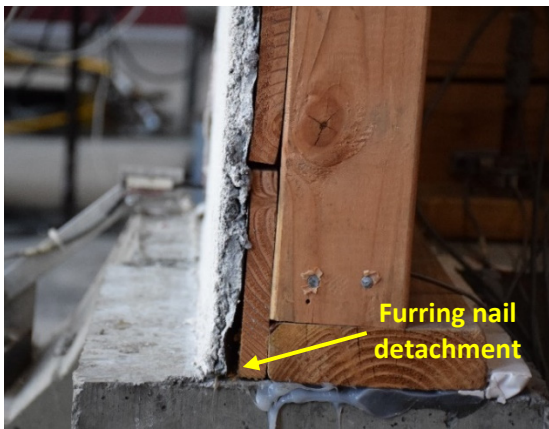
(b)



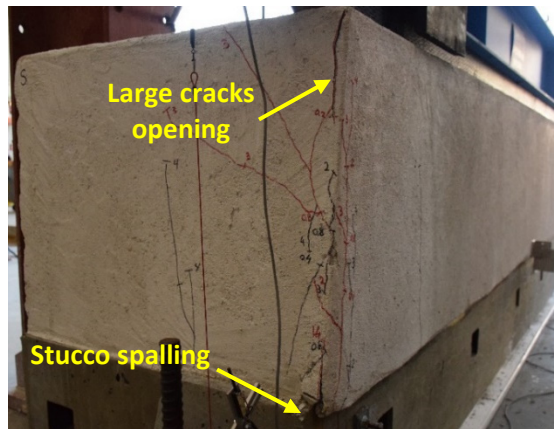
(c)



(d)



(e)



(f)

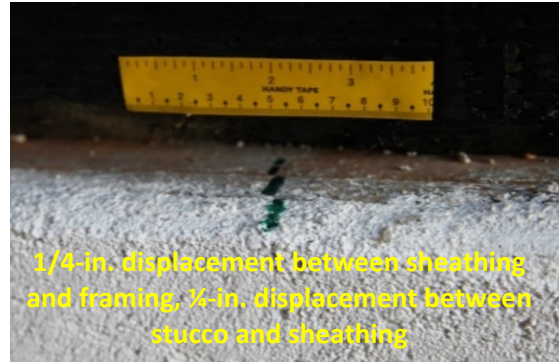
**Figure 5.12** Specimen A-3 damage state of at lateral strength @ +4% drift,  $\Delta = +0.96$  in.: (a) exterior elevation; (b) top of exterior wall (c) bottom of exterior wall; (d) close-up of south-end wall; (e) close-up of north-end corner of wall; and (f) north-end exterior corner.

#### **5.2.1.4 Specimen A-4 Observations and Damage at Lateral Strength**

Figure 5.13(a) to (f) show the damage state of Specimen A-4 at lateral strength. The lateral strength occurred at 5% global drift ratio in the push loading direction and 5% in the pull loading direction. The corresponding relative drift ratio was 3.9% in the push direction and 3.5% in the pull direction. At lateral strength, an additional crack in the stucco formed, running from the top of the cripple wall to the base. The displacement between the base of the stucco and the foundation increased to 3/4 in. Figure 5.13(e) shows that large cracks opened up near the bottom at the corner of the wall, indicating that the stucco had moved laterally away from the sheathing, confirmed by the furring nails having become detached from the stucco at the base of the wall. Because the stucco was bearing on the foundation, the rotation was inhibited unlike the previous specimens. This led to an increased capacity of the cripple wall and drift ratio at strength for the cripple wall because the separation between the stucco finish and the sheathing occurs as a lateral movement of the stucco away from the sheathing or an uplift of the stucco. The stucco nails detached primarily from the wire lath in the stucco; however, more commonly compared to the previous tests, the furring nails withdrew from the sheathing boards. At the top of the cripple wall, a 1/4-in. displacement occurred between the stucco and the sheathing, accompanied by a 1/4-in. displacement occurring between the sheathing and framing. Both the nails in the sheathing and the furring nails exhibited significant bending leading to these displacements. As shown in Figure 5.13(f), extensive cracking occurred at the exterior on the corners, extending vertically and diagonally on the corner faces. In addition, significant crushing and spalling of the stucco occurred on the corner faces. On the interior, the uplift of the studs was more pronounced, with was no visible rotation of the studs.



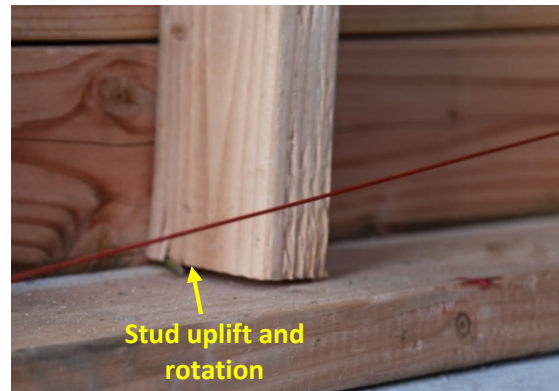
(a)



(b)



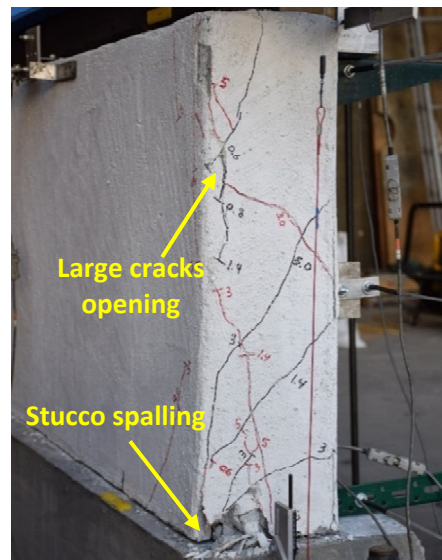
(c)



(d)



(e)



(f)

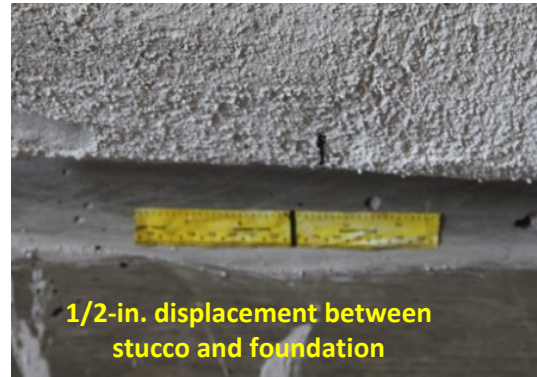
Figure 5.13 Specimen A-4 damage state of at lateral strength @-5% drift,  $\Delta = -1.20$  in.: (a) exterior elevation; (b) top of exterior wall; (c) bottom of exterior wall; (d) close-up of stud; (e) close-up of exterior south-end corner; and (f) north-end exterior corner.

### **5.2.1.5 Specimen A-20 Observations and Damage at Lateral Strength**

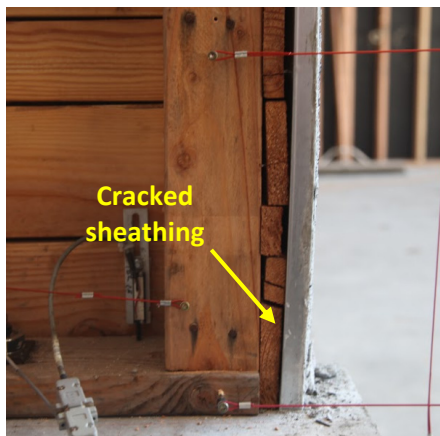
Figure 5.14 shows the damage state of Specimen A-20 at lateral strength. Lateral strength occurred at 3% global drift ratio in the push loading direction and 3% global drift ratio in the pull loading direction. The relative drift ratio at strength was 2.4% in the push direction and 2.4% in the pull direction. At strength, the stucco had detached from the furring nails at the sill plate and bottom of the studs, a common occurrence for all wet finished (stucco) cripple walls. This can be seen by the gap that formed between the stucco extension and the footing in Figure 5.14(f). At the top of the cripple wall, the stucco and sheathing had displaced 1/4 in. relative to the framing, and at the bottom, a 1/2-in. displacement of the finish material and the foundation occurred; see Figure 5.14(a) and (b). Many of the sheathing board at the corners split due to the bearing of the finish materials at the corners on the foundation; see Figure 5.14(c). The stucco detached from the sheathing nails as well but remained attached to the furring nails; see Figure 5.14(d). For most specimens, the furring nails would stay attached to the sheathing/framing, but due to the cracks in the sheathing boards, there was less resistance to the furring nails withdrawing from the sheathing/framing.



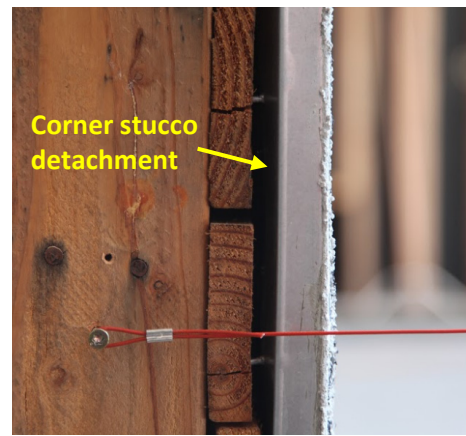
(a)



(b)



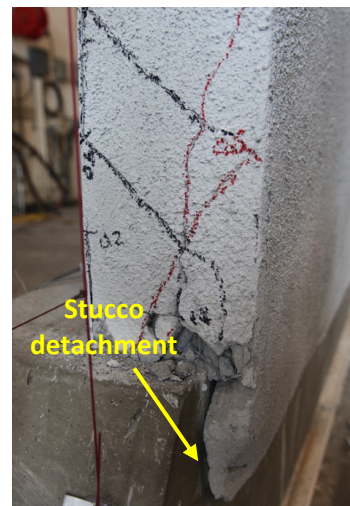
(c)



(d)



(e)



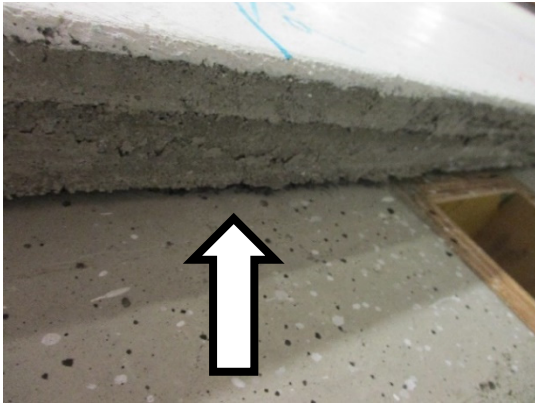
(f)

**Figure 5.14** Specimen A-20 damage state of at lateral strength @ +3% drift ratio,  $\Delta = +0.72$  in.: (a) top of north-end exterior of wall; (b) bottom of north-end exterior of wall; (c) bottom of south-end interior corner of wall; (d) middle of south-end interior corner of wall; (e) south-end corner of wall; and (f) bottom of south-end corner of wall.

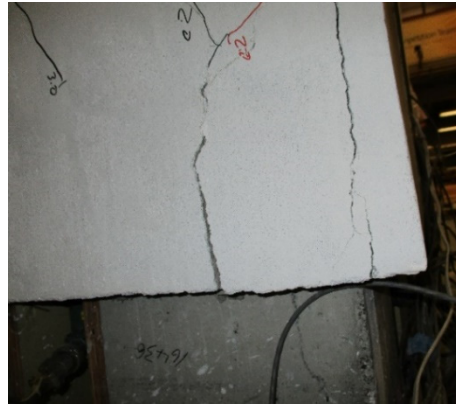
### **5.2.1.6 Specimen AL-1 Observations and Damage at Lateral Strength**

Prior to reaching lateral strength, the stucco continued to deteriorate, with the stucco being pushed off the east- and west-end wall framing clearly visible. Small chunks of stucco started to work loose, and stucco cracks up to 3/16 in. wide were measured. On the north and south walls, 1/4-in. slip occurred between stucco and lumber sheathing at floor line while stucco cracking on north and south faces remained near hairline.

Figure 5.15 shows the damage state of Specimen AL-2 at lateral strength. As Specimen AL-1 reached lateral strength at approximately 3% drift, the end-wall stucco continued to deteriorate and pushed off of the framing, leading to the damage patterns seen in Figure 5.15(b) and (c). On the north and south walls, the stucco had developed an extensive network of cracks, but they remained near hairline; see Figure 5.15(e). A 1/8-in. out-of-plane gap opened between the stucco and sheathing at the floor line; see Figure 5.15(f). Following popping noises, visible out-of-plane gaps opened up between the stucco and the concrete foundation; see Figure 5.15(a). This is understood to have been the stucco debonding from the foundation. The gaps were estimated to be 1/16 in. wide. During selective demolition following testing, it was observed that all of the furring nail heads at the foundation sill plate has been pulled out of the stucco. This head pull-out is believed to have occurred at the same time as the stucco debonded from the foundation.



(a)



(b)



(c)



(d)



(e)



(f)

**Figure 5.15 Specimen AL-1 damage state of at lateral strength @ 3% drift ratio,  $\Delta = +0.72$  in.: (a) gap between stucco and foundation; (b) cracking and flaring of stucco; (c) bottom of northwest corner; (d) stucco spall at floor line; (e) bottom of south-west end of wall; and (f) separation of stucco and lumber sheathing.**

### **5.2.1.7 Discussion of Observations and Damage for Test Specimens without Retrofit at Lateral Strength**

For all specimens, the lateral strength was associated with detachment of the stucco from the foundation sill plate (and stucco debonding from the foundation in the case of Specimen AL-1). As the small-component test specimens were loaded up to lateral strength, there were numerous locations where slip could be seen, including between the stucco and the foundation and between the stucco and the horizontal lumber sheathing. In sharp contrast, the visible indicators of drift being imposed on the large-component specimen did not include this type of slip. This is in large part because the stucco remained bonded to the foundation on the large-component specimen up until lateral strength. Had this bonding not occurred, it is anticipated that slip similar to the small-component tests would have been seen.

The lack of visible slip at the same imposed drift ratio suggests that the drift was being accommodated by other mechanisms in the large-component test. Some portion of the slip occurred between the stucco and the framing in the vicinity of the floor. A number of other potential slip locations can be identified.

The damage observed for Specimen A-1 was notably different than the other specimens, with much less visible damage up to lateral strength. The damage observed for Specimen A-4 was also notably different, with more cracking on the face of the stucco and at the cripple wall base. It is suggested that testing using these configurations should be limited to studies where these configurations exist in the building population.

## **5.2.2 Comparison of Damage at Lateral Strength for Specimens with Retrofit**

### **5.2.2.1 Specimen A-5 Observations and Damage at Lateral Strength**

Figure 5.16(a) to (f) show the damage state of Specimen A-5 at lateral strength. The lateral strength occurred at 5% global drift ratio in the push loading direction and 5% in the pull loading direction. The corresponding relative drift ratio was 3.6% in the push direction and 2.8% in the pull direction. At strength, multiple cracks had propagated vertically from across the entire face of the stucco. The displacement between the stucco base and the foundation had increased to almost 5/8 in., which is around half of total displacement imposed on the wall. Again, this correlates to a complete detachment of stucco from the sheathing at the base of the wall. Most of this detachment came in the form of the furring nails detaching from the wire lath in the stucco. As shown in Figure 5.16(e), significant uplift (3/8 in.) occurred at the ends of the cripple walls, which can be attributed to the strength of the plywood panels causing the sill plate to bend.

At the top of the cripple wall, there was a 3/16-in. relative displacement between the sheathing and the framing, which was due to the increased stiffness of the framing from the plywood attachment resisting displacement. Figure 5.16(f) shows the damage state of the interior at the corner. Evident is uplift of the corner studs, uplift of the sill plate, splitting of the added blocking that the plywood is nailed to, and partial pull-through of the nails attaching the plywood panels to the blocking. In addition, the displacement between the plywood panels was more pronounced as the panel rotations increased. All nails on the plywood panels had begun to either withdraw or pull through. Any nail that was slightly overdriven falls into the latter category, while the other nails fall into both categories. The majority of nails pulling out were located at the base

where they caused the blocking to split, thus freeing the nails. Both the withdrawal out and pulling through of the nails is attributed to the back and forward bending of the nails during each cycle.

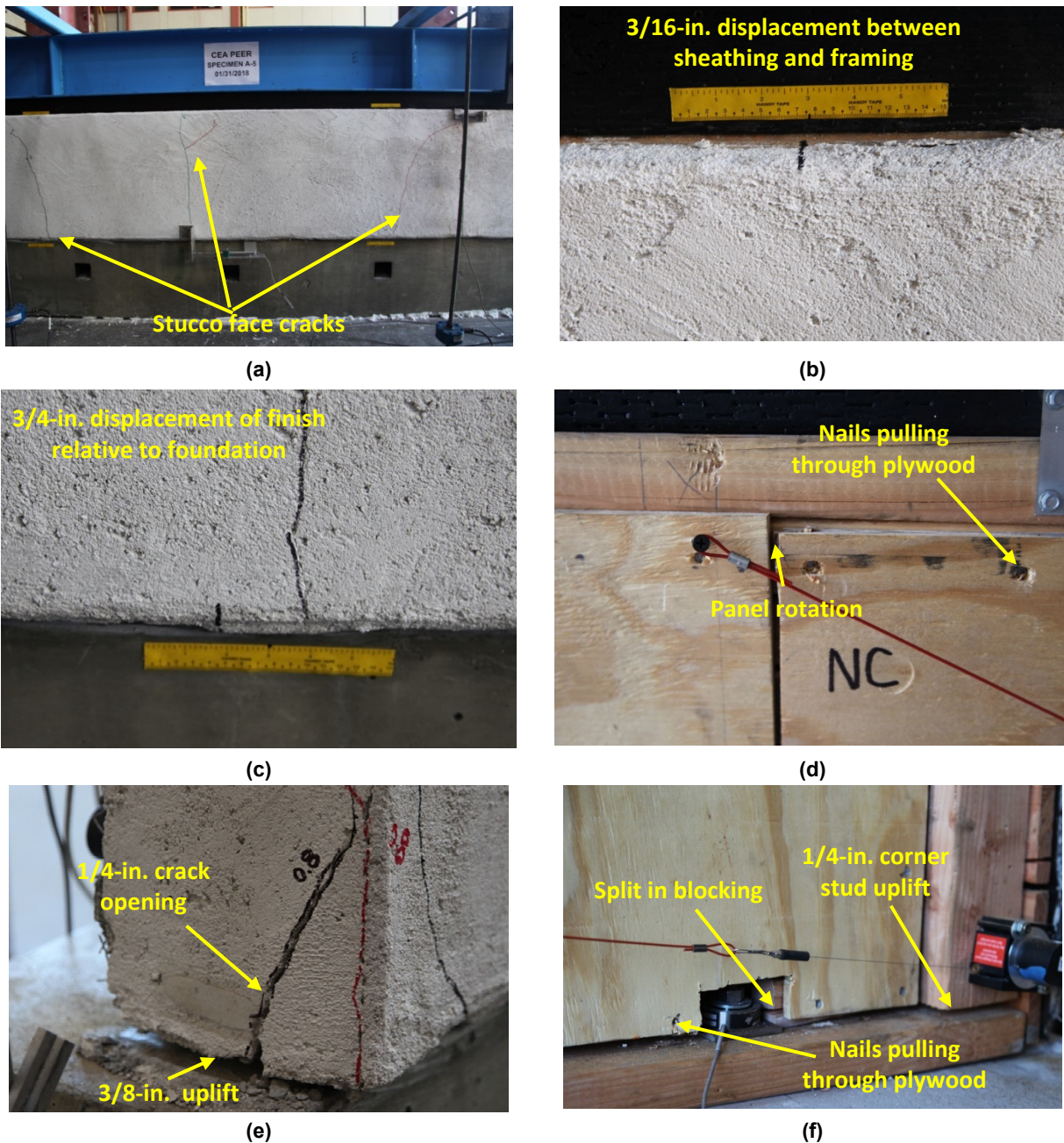


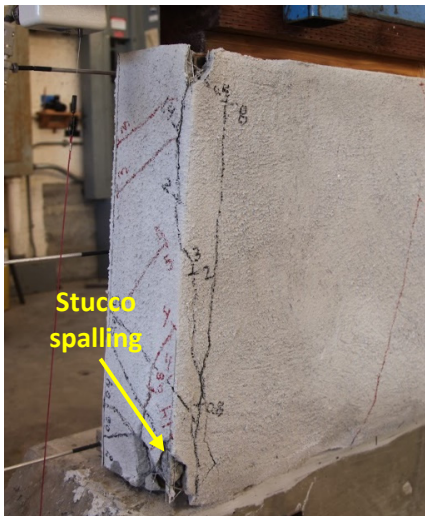
**Figure 5.16** Specimen A-5 damage state of at lateral strength @ +5% drift,  $\Delta = +1.20$  in.: (a) exterior elevation; (b) top of exterior wall; (c) bottom of exterior wall; (d) close-up of plywood panel joint; (e) close-up of south-end exterior corner; (f) bottom of south-end interior wall corner.

### **5.2.2.2 Specimen A-19 Observations and Damage at Lateral Strength**

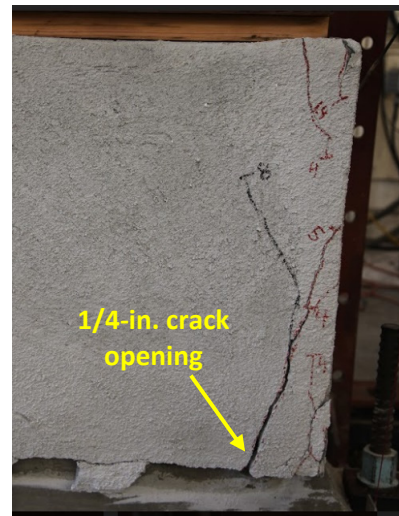
Figure 5.17 shows the damage state of Specimen A-19 at lateral strength. Lateral strength occurred at 8% global drift ratio in the push loading direction and 8% global drift ratio in the pull loading direction. The relative drift ratio at strength was 5.3% in the push direction and 5.3% in the pull direction. At strength, multiple cracks had formed in the stucco along the exterior face of the specimen; see Figure 5.17(a). Most of the cracks propagated vertically, and the largest crack openings occurred near both corners of the cripple wall; see Figure 5.17(b) and (c). The crack openings were as large as a 1/4-in. thick, indicating that the stucco had detached from the furring nails at the sill plate and bottom of the studs. On the interior of the cripple wall, 1/2-in. uplift of the plywood and corner studs occurred at the ends of the specimens. The uplift caused splitting of the blocking at the end stud bays; see Figure 5.17(d). The plywood panels were crushed due to their bearing on the flat studs at both ends of the specimen; see Figure 5.17(e). The panels exhibited large rotations; see Figure 5.17(f). Many of the nails showed partial pull through at the bottom and sides of the panels, and some of the nails had torn through the edges near the locations of the anchor bolts; see Figure 5.17(g).



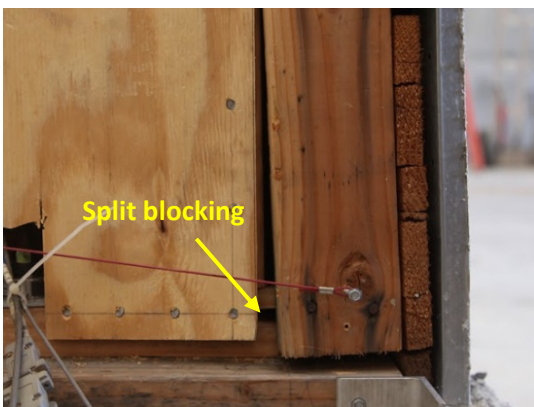
(a)



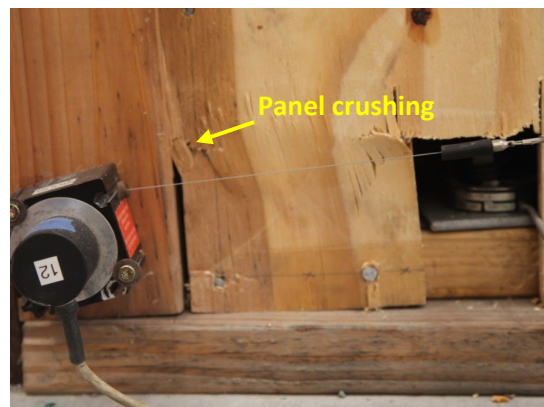
(b)



(c)

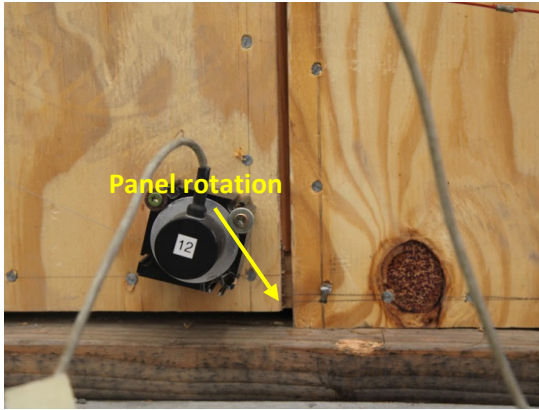


(d)



(e)

**Figure 5.17** Specimen A-19 damage state of at lateral strength @ +8% drift ratio,  $\Delta = +1.92$  in.: (a) exterior elevation; (b) south-end exterior corner of wall; (c) north-end exterior of wall; (d) bottom interior of wall (south and middle panels); (e) bottom interior of wall (north panel); (f) bottom interior of wall (south and middle panels); and (g) bottom interior of wall (north panel).



(f)



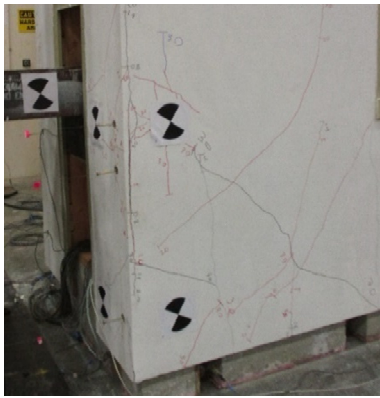
(g)

Figure 5.18 (continued).

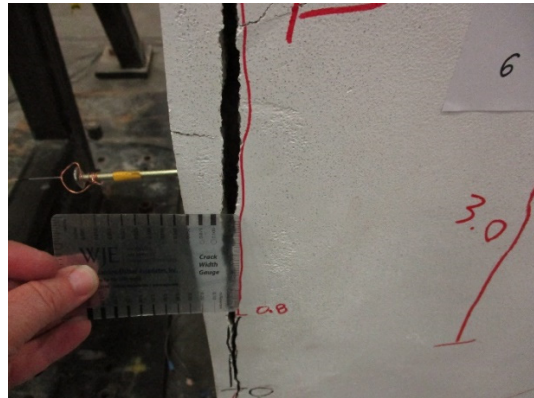
### 5.2.2.3 Specimen AL-2 Observations and Damage at Lateral Strength

Prior to reaching lateral strength, limited spread of stucco cracking was observed on the end walls and corners. Cracks opened to a maximum measured crack width of 0.050 in. At the north and south walls, limited spreading of cracks was observed.

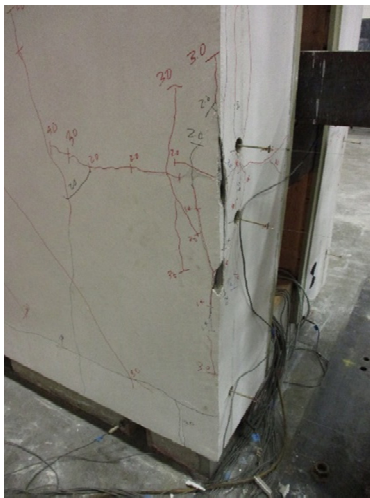
Specimen AL-2 reached lateral strength at approximately 3% drift; see Figure 5.18 damage state at this drift level. At the end walls and corners, cracks at the floor line widened to approximately 1/8 in.; see Figure 5.18(a) and (b). The stucco was pushed off of the end walls, and limited small pieces of stucco started falling off at corners; see Figure 5.18(c) and (d). At the north and south walls, popping noises were heard, corresponding to debonding of the stucco from the foundation. A gap of approximately 1/16 in. was measured between the foundation and the stucco; see Figure 5.18(e). Like Specimen AL-1, later selective demolition identified that furring nails at the foundation sill plate had been pulled out of the stucco; it is believed that this occurred at the time the stucco debonded from the foundation. There was no observable damage to the retrofit; see Figure 5.18(f). No uplift of the cripple wall relative to the foundation was observed.



(a)



(b)



(c)



(d)



(e)



(f)

**Figure 5.19 Specimen AL-2 damage state of at lateral strength @ 3% drift ratio,  $\Delta = +0.72$  in.:** (a) bottom of southwest corner; (b) southwest corner detail; (c) bottom of northwest corner; (d) middle of southwest corner; (e) gap between stucco and foundation; and (f) middle of north-end of crawlspace.

#### **5.2.2.4 Discussion of Observations and Damage for Specimens with Retrofit at Lateral Strength**

As noted for the unretrofitted test specimens, the retrofitted small-component test specimens exhibited more noticeable signs of slip and uplift compared to the large-component specimens. This is particularly true of the retrofit sheathing and nailing; Specimen AL-2 did not show signs of deterioration (i.e., partial nail withdrawal and partial nail head pull through). Figure 3.9 shows that after the initial lateral strength occurred at a drift ratio of approximately 3%, a second peak occurred near 7%. This second peak is associated with the specimen reaching lateral strength of the retrofit plywood.

### **5.3 COMPARISON OF OBSERVATIONS AND DAMAGE AT 20% RESIDUAL LATERAL FORCE**

This section discusses observations and damage at a point in the load-deflection response when the displacement is well beyond lateral strength and the lateral force has dropped to a residual lateral force level of approximately 20% of the lateral strength (i.e., an 80% drop in lateral force). This occurred at very significant drift ratios and represents a high level of deterioration. When testing stopped before a 20% residual strength level occurred, discussion is provided of the observations and damage at the final recorded displacement cycle. The unretrofitted specimens are discussed first, followed up the retrofitted specimens.

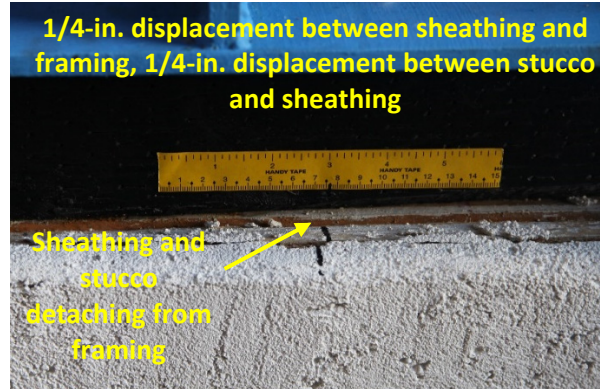
#### **5.3.1 Comparison of Observations and Damage at 20% Residual Lateral Force for Unretrofitted Specimens**

##### **5.3.1.1 Specimen A-1 Observations and Damage at 20% Residual Lateral Force**

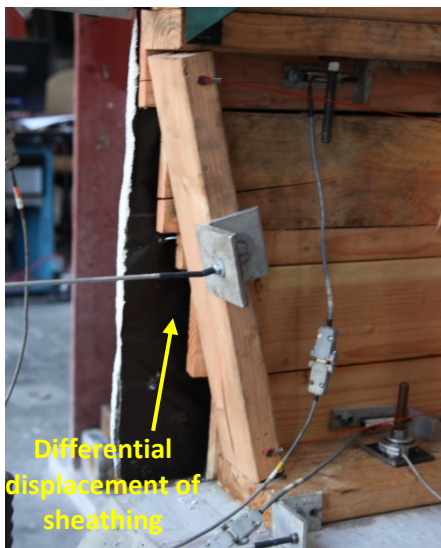
Figure 5.19(a) to (d) shows the damage state of Specimen A-1 at +12% drift ratio. Specimen A-1 never reached an 80% drop in lateral strength. The damage state at 12% correlates closer to a 60% drop in lateral strength. At this stage, the stucco is connected only to the top plate and top row of furring nails on the studs. As shown in Figure 5.19 (c) and (d), almost all of the furring nails remained attached to the sheathing and pulled away from the wire lath in the stucco. At the top of the wall, the displacement between the stucco and sheathing was 1/4 in. and between the sheathing and the framing had grown to 1/4 in. In addition, the gaps occurred at the interface of both the stucco and sheathing as well as sheathing and framing. At this point, the stucco provided negligible lateral resistance. The source of capacity was due to the stacking of (bearing between) the horizontal sheathing boards bearing on the foundation. In Figure 5.20(c), the gaps between all but the top sheathing board had closed. Cracks formed on the corners of the sheathing boards where the nails were located. Figure 5.20 shows photographs of the cripple wall in its residual state at the end of testing after a +5.0 in. (+20% drift ratio) monotonic push. There was a residual displacement of +4.90 in. (+20.4% drift ratio) once the load was removed.



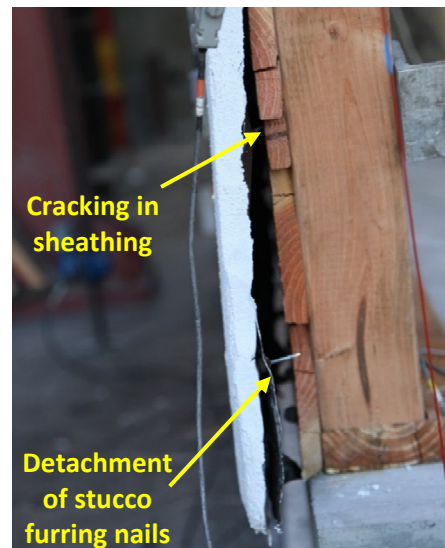
(a)



(b)



(c)



(d)

**Figure 5.20** Specimen A-1 damage state at 60% post-peak reduction of lateral strength @ +12% drift,  $\Delta = +2.88$  in.: (a) close-up of studs and sill plate; (b) exterior top of the wall; (c) north-end interior corner; and (d) north-end bottom of corner.



(a)



(b)



(c)



(d)

**Figure 5.21 Specimen A-1 post-test photographs (lateral load = 0 kips, residual displacement = +4.90 in. @ +20.4% drift): (a) exterior elevation of cripple wall; (b) interior elevation of cripple wall; (c) north-end exterior corner view; and (d) south-end interior corner view.**

### 5.3.1.2 Specimen A-2 Observations and Damage at 20% Residual Lateral Strength

Figure 5.21(a) to (d) shows the damage state of Specimen A-2 at +12% drift ratio. Specimen A-2 never reached an 80% drop in lateral strength. The damage state at 12% correlates closer to a 70% drop in lateral strength. The stucco completely detached over the majority of the wall. The only attachment was at the dense furring nail arrangement at top. Figure 5.21(d) shows extensive movement of the stucco away from the sheathing at the base as well as around a 1/4 in. of movement of the sheathing board away from the framing. Much of the stucco had spalled off of the corners, coming off in large chunks. Sheathing boards on the corners had mostly split. A 3/8-in. gap had formed between the top two sheathing boards, which was due to the top sheathing board being fastened to the top plates while the other sheathing boards were attached to the studs. The capacity of the wall is attributed again the sheathing boards stacking (bearing) on each other and bearing on the foundation. Figure 5.22 shows photographs of the cripple wall in its residual state at the end of testing, after a +4.50 in. (+18.8% drift ratio) monotonic push. There was a residual displacement of +3.45 in. (+14.4% drift ratio) once the load was removed.

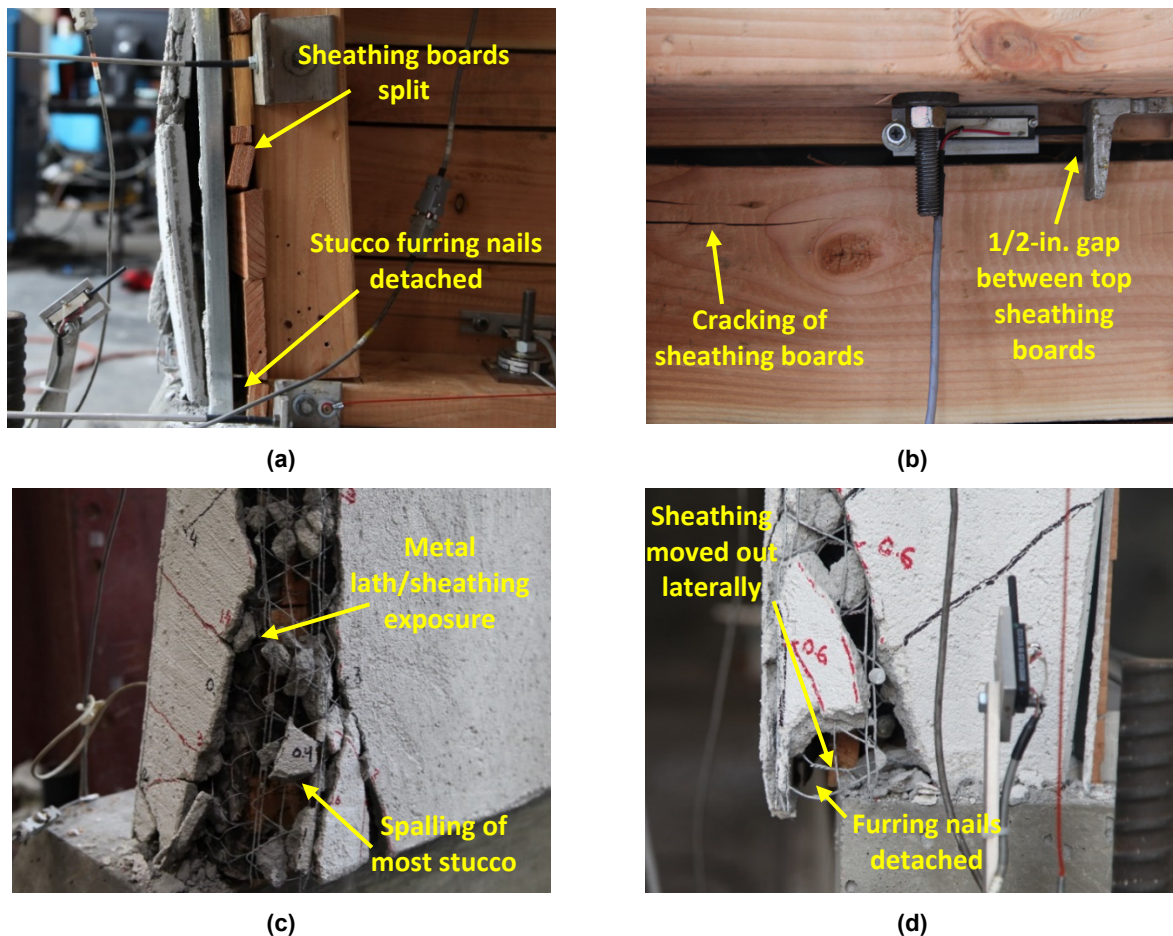


**Figure 5.22** Specimen A-2 damage state of at 70% post-peak reduction of lateral strength @ +12% drift,  $\Delta = +2.88$  in.: (a) north-end of interior corner bottom; (b) close-up of top of interior wall; (c) south-end of exterior bottom corner; and (d) north-end of bottom corner.



(a)



(b)



(c)



(d)

**Figure 5.23** Specimen A-2 post-test photographs (lateral load = 0 kips, residual displacement = +3.45 in @ +14.4% drift): (a) exterior elevation of cripple wall; (b) interior elevation of cripple wall; (c) south-end exterior corner view; (d) north-end interior view.

### 5.3.1.3 Specimen A-3 Observations and Damage at 20% Residual Lateral Force

Figure 5.23(a) to (d) shows the damage state of Specimen A-3 at -12% drift ratio. Specimen A-3 never reached an 80% drop in lateral strength. The damage state at 12% correlates closer to a 60% drop in lateral strength. Extensive horizontal cracks had propagated across the return walls; a massive gap between the return wall and stucco face is clearly visible. Again, the only attachment of the stucco on the face remained at the top plates. The face stucco acted as a rigid body, providing little lateral resistance. Like Specimen A-2, the sheathing boards stacked (bore) on each other, providing the majority of the remaining strength in the wall. This stacking caused the sheathing nails to pull away from the framing, which is evident in Figure 5.23(d). Significant rotation of the studs on the return walls occurred; see Figure 5.23(b). Figure 5.24 shows the cripple wall in its residual state at the end of testing, after a +5.0 in. (+20.8% drift ratio) monotonic push. There was a residual displacement of +4.51 in. (+18.8% drift ratio) once the load was removed.

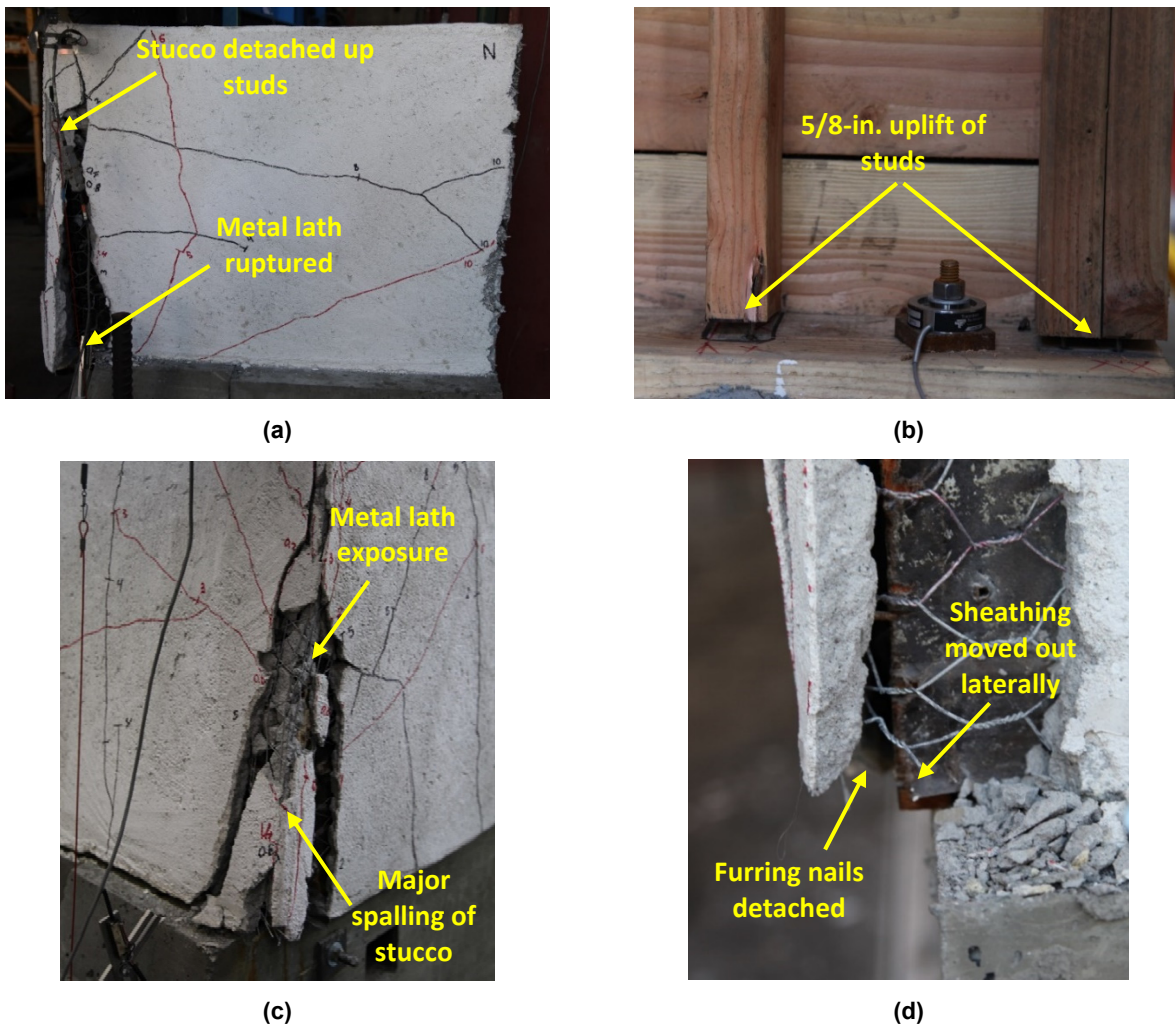


**Figure 5.24** Specimen A-3 damage state at 60% post-peak reduction of lateral strength @ -12% drift,  $\Delta = -2.88$  in.: (a) exterior view of north-end return wall; (b) interior of bottom of south-end return wall; (c) bottom of south-end exterior corner; (d) bottom of north-end corner.



(a)



(b)



(c)



(d)

**Figure 5.25** Specimen A-3 damage state at 80% post-peak reduction of lateral strength @-12% drift,  $\Delta = -2.88$  in.: (a) exterior elevation (b) bottom of north-end interior corner; (c) north-end exterior corner; and (d) top-down view of exterior.

### 5.3.1.4 Specimen A-4 Observations and Damage at 20% Residual Lateral Force

Figure 5.25(a) to (d) shows the damage state of Specimen A-4 at -12% drift ratio. Specimen A-4 achieved an 80% loss of strength before the monotonic push was implemented. Unlike the previous three specimens, the stucco detached from both the bottom and top of the wall; see Figure 5.25(c) and (d). At this point, the stucco provided almost no lateral resistance. The stucco completely detached at the corners and many of the sheathing boards split; see Figure 5.25(b). Like the previous three tests, the majority of the lateral resistance can be attributed to the bearing of the sheathing boards on the foundation. Figure 5.26 shows photographs of the cripple wall in its residual state at the end of testing, after a +4.70 in. (+19.6% drift ratio) monotonic push. There was a residual displacement of +3.43 in. (+14.3% drift ratio) once the load was removed.

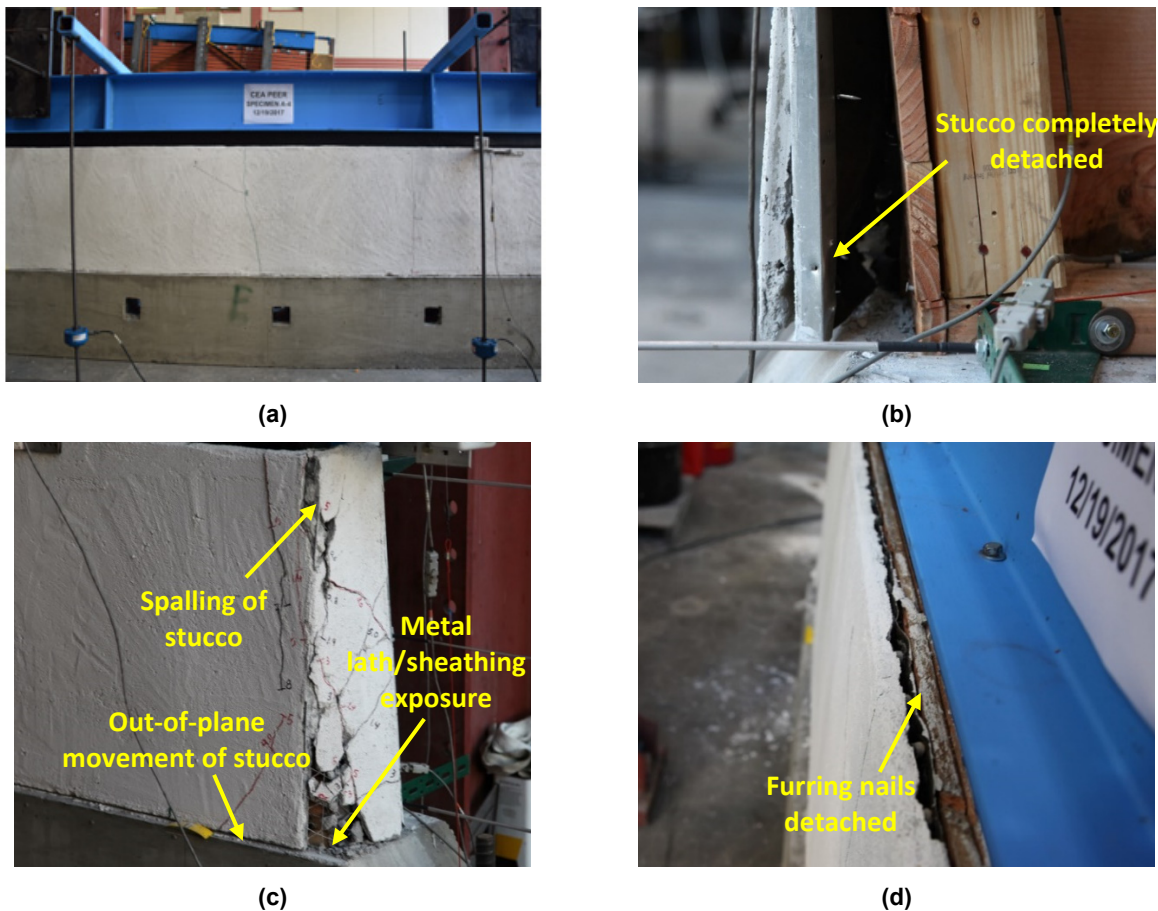


Figure 5.26 Specimen A-4 damage state at 80% post-peak reduction of lateral strength @ -12% drift,  $\Delta = -2.88$  in.: (a) exterior elevation; (b) bottom of north-end interior corner; (c) north-end exterior corner; and (d) bottom of north-end corner.



(a)



(b)



(c)



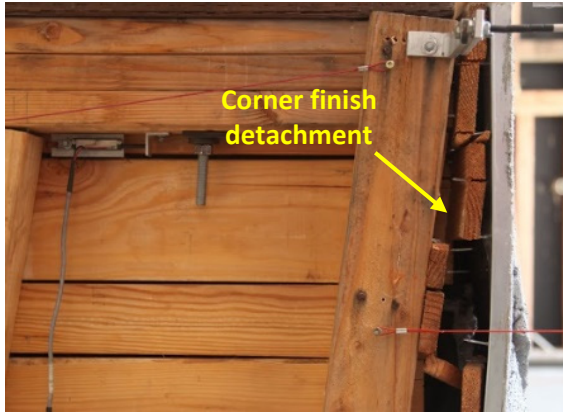
(d)

**Figure 5.27** Specimen A-4 post-test photographs at lateral load = 0 kips and residual displacement = +3.43 in. @ +14.3% drift: (a) exterior elevation of cripple wall; (b) interior elevation of cripple wall; (c) north-end exterior corner view; and (d) north-end interior view.

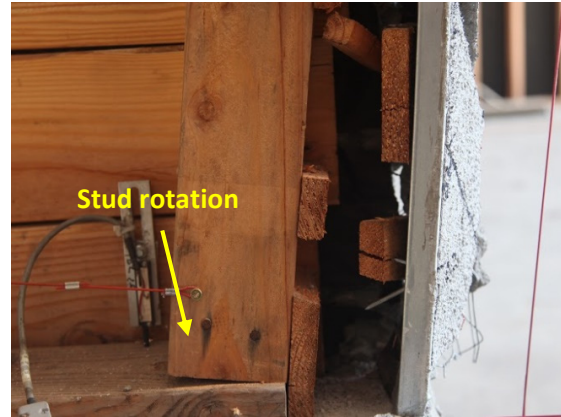
### **5.3.1.5 Specimen A-20 Observations and Damage at 20% Residual Lateral Force**

Figure 5.27 shows the state of Specimen A-20 at the -14% global drift ratio, corresponding to an 80% drop in lateral strength. Figure 5.27(c) and (d) shows large cracks and openings in the stucco, indicating that the stucco finish had detached from most of the furring nails on the studs and remained only attached to the furring nails at the top plates and the tops of the studs. The metal lath had ruptured at the bottom of the corners. Most of the sheathing boards at the corners had cracked and detached from the framing along with the stucco; see Figure 5.27(a) and (b). There was little damage to the sheathing boards spanning across the face of the cripple wall.

The loss of strength was primarily due to the detachment of the stucco from most of the cripple wall as the horizontal sheathing boards do not provide a large amount of lateral resistance relative to the contribution from the stucco. Figure 5.28 shows the residual state of the specimen is shown after a monotonic push to +5.0 in. (+20.8% drift ratio). The residual displacement was +4.81 in. (+20.0% drift ratio). Along the exterior face, no additional vertical cracks propagated post-strength, but the cracks at the edges had opened significantly; see Figure 5.28(a) and (c). At this point, the only remaining attachment of the stucco to the framing was at the top plates, while the stucco was nearly fully detached at the corners; see Figure 5.28(d). Along the interior of the cripple wall, there was little visible damage to both the framing and the sheathing boards; see Figure 5.28(b).



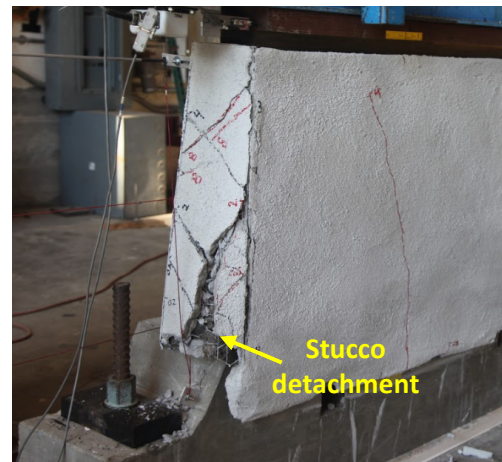
(a)



(b)



(c)



(d)

**Figure 5.28** Specimen A-20 damage state at 20% residual lateral strength at -14% drift ratio @  $\Delta = -3.36$  in. unless otherwise noted: (a) top of south-end interior of wall at +14% drift; (b) bottom of south-end interior of wall at +14% drift; (c) bottom of south-end exterior corner of wall; and (d) south-end exterior corner of wall.



(a)



(b)



(c)



(d)

**Figure 5.29** Specimen A-20 post-test photographs at lateral load = 0 kips, residual displacement = +4.81 in. (+20.0% drift ratio) after monotonic push to +5.0 in. (+20.8% drift ratio): (a) exterior elevation; (b) interior elevation; (c) north-end exterior corner of wall view; and (d) south-end interior corner of wall view.

### 5.3.1.6 Specimen AL-1 Observations and Damage at 20% Residual Lateral Force

Specimen AL-1 dropped to approximately 20% of the lateral strength at a drift ratio of between 6 and 7%; see damage state in Figure 5.29. At the end wall and corners, the stucco continued to deteriorate and be pushed off of end wall sheathing and framing. Gaps of up to approximately 1/2 in. were observed between stucco and sheathing at the end walls and corners. At the north and south walls for 4% drift and above, only very limited spreading or additional cracks were observed. At the end walls, the stucco cracked open at corners, exposing the wood sheathing below.

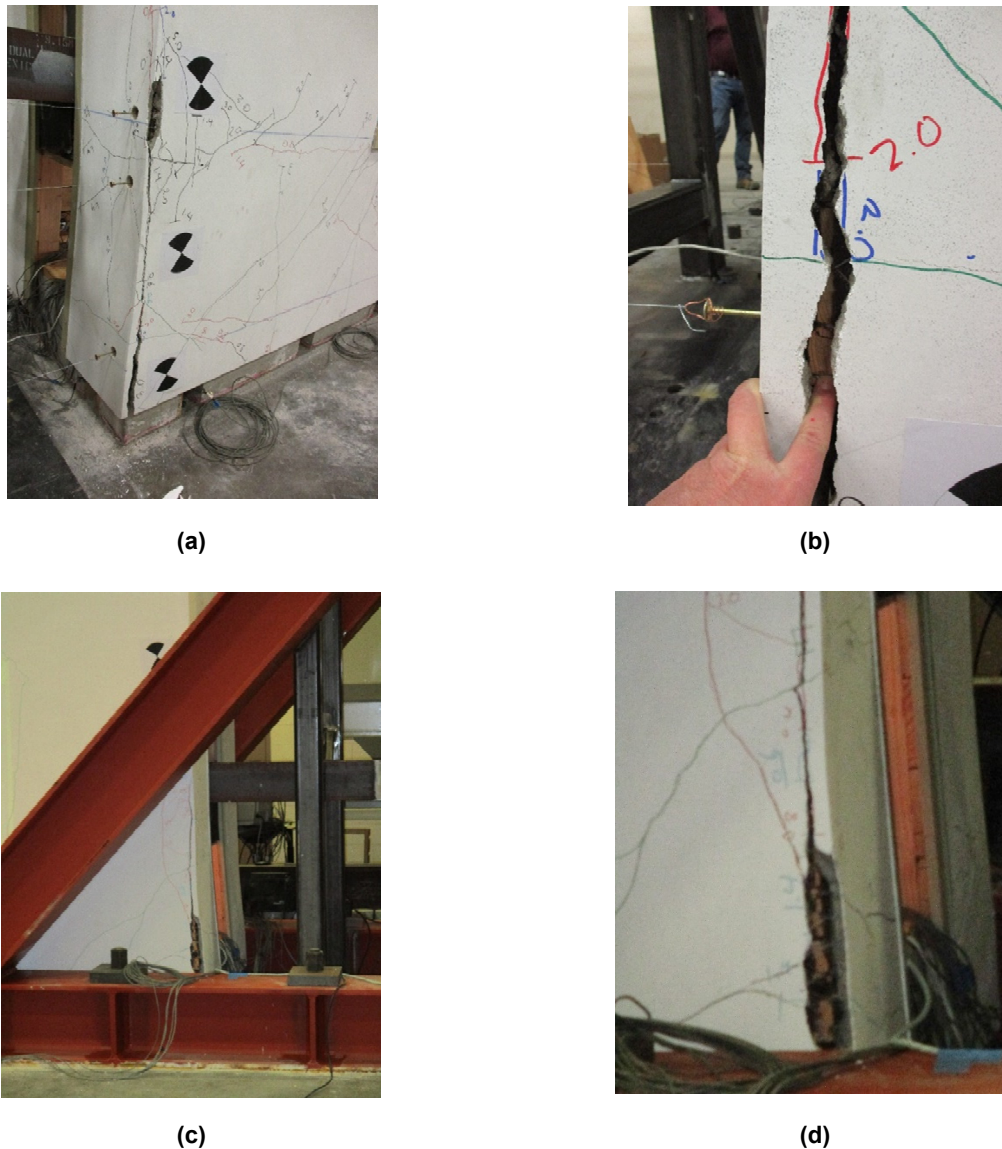


**Figure 5.30** Specimen AL-1 photographs after cyclic testing to 6 to 8% drift ratio: (a) bottom of southwest corner; (b) southwest corner detail; (c) bottom of northeast corner; and (d) bottom of southeast corner detail.

Specimen AL-1 continued to retain a lateral force of 10 to 20% of the lateral capacity well beyond 6 to 7% drift. At 8% drift, chunks of cripple wall stucco started falling off of the end walls at corners. At 8% drift ratio, clearly visible permanent flaring of the bottom of the stucco away from the underlying sheathing and framing occurred at the north and south walls. At 10% drift, at all walls the cripple wall stucco had detached from the underlying sheathing and framing over the full height of the cripple wall. The racking of the lumber sheathing below was observed.

Figure 5.30 shows the damage state of Specimen AL-1 at the end of the final monotonic push. The final monotonic push took the 24-in.-tall cripple wall to a 10-in. (40%) drift. The already separated stucco was pushed away at the east end and sucked under the cripple wall at the west end. Horizontal sliding of the lumber sheathing was clearly visible, with the sheathing nails being fully withdrawn from lower sheathing boards towards the end of the monotonic push. Even with the sheathing board nails being withdrawn, the overlying stucco tended to hold the lumber sheathing boards in place.

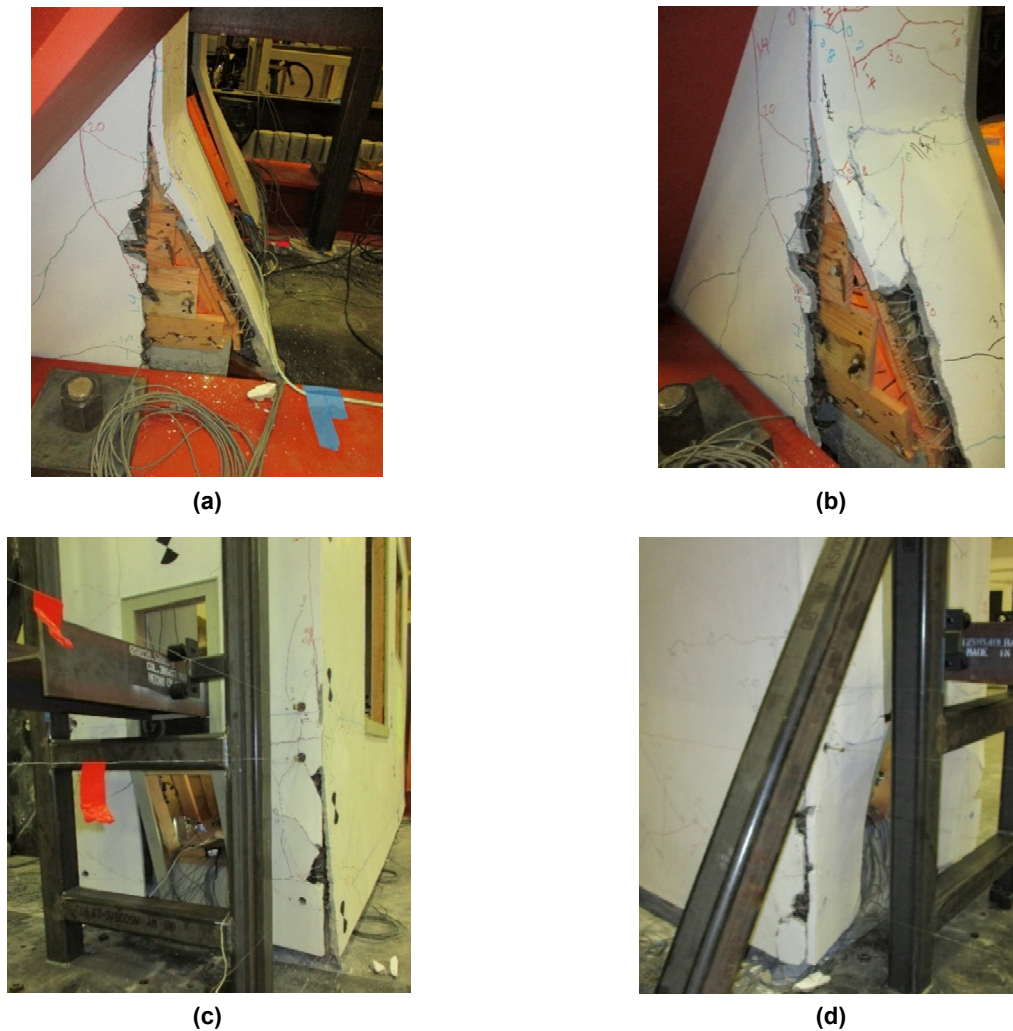
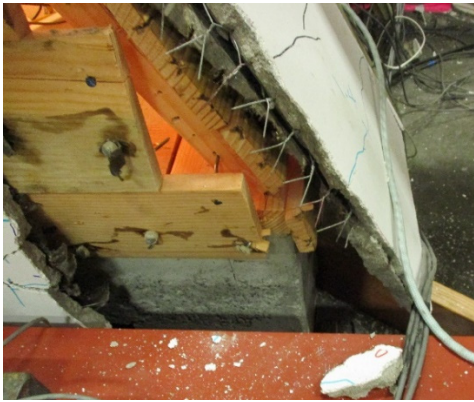


**Figure 5.31** Specimen AL-1 post-test photographs after monotonic push to 40% drift ratio: (a) bottom of northeast end; (b) bottom of southeast corner; (c) west-end; (d) bottom of northwest corner; (e) bottom of northeast corner; and (f) east-end of crawlspace interior.



(e)



(f)

**Figure 5.30 (continued).**

### **5.3.1.7 Discussion of Observations and Damage for Specimens without Retrofit at 20% Residual Lateral Force**

In all existing test specimens, the stucco was no longer attached to the sheathing and framing in a way that could contribute strength. In Specimens A-1, A-2, A-3, and A-20, the stucco was only still attached to the specimen top plate. Similarly, in Specimen AL-1 the stucco remained attached in the vicinity of the floor framing level but was no longer attached below. The stucco in Specimen A-4 was noted to be substantially detached from both the top and bottom plates.

Significant deterioration occurred at the stucco corners in all specimens, including both rupture of the stucco and fracture of the wire lath. In all cases damage to the horizontal wood sheathing occurred. For the group of unretrofitted specimens, the extent and types of damage to the small- and large-component specimens at this displacement level were similar. The superstructure story in the large-component specimen permitted the additional observation that only very limited stucco cracking occurred above the framed floor.

## **5.3.2 Comparison of Observations and Damage at 20% Residual Lateral Strength for Specimens with Retrofit**

### **5.3.2.1 Specimen A-5 Observations and Damage at 20% Residual Lateral Strength**

Figure 5.31(a) to (d) shows the damage state of Specimen A-5 at -11% drift ratio. The data for this test stopped being accurately recorded at 7% drift ratio amplitude due to the loss of the control displacement potentiometer. Higher amplitudes were however imposed to obtain a visual of the damage state of the failed wall. All plywood panels had become nearly completely detached (two to three nails remain attached) on the top, bottom, and one side, providing no lateral resistance. The south-end plywood panel was only attached with two nails; see Figure 5.31(a). Most of the nails at the top failed in edge tear-out or head pull-through. At the bottom of the plywood panels, many of the nails withdrew from the block, and much of the blocking either uplifted off of the sill plate or split where the plywood was nailed. The corner flat studs split due to the abutting plywood. The damage to the stucco had the same characteristics as the existing condition replica, Specimen

A-2. Figure 5.32 shows photographs of the cripple wall in its residual state at the end of testing, after the end of the 11% drift ratio cycle group. After the wall was unloaded at -11% drift ratio (-2.64 in.), a residual displacement of -1.74 in. (-7.3% drift ratio) remained.

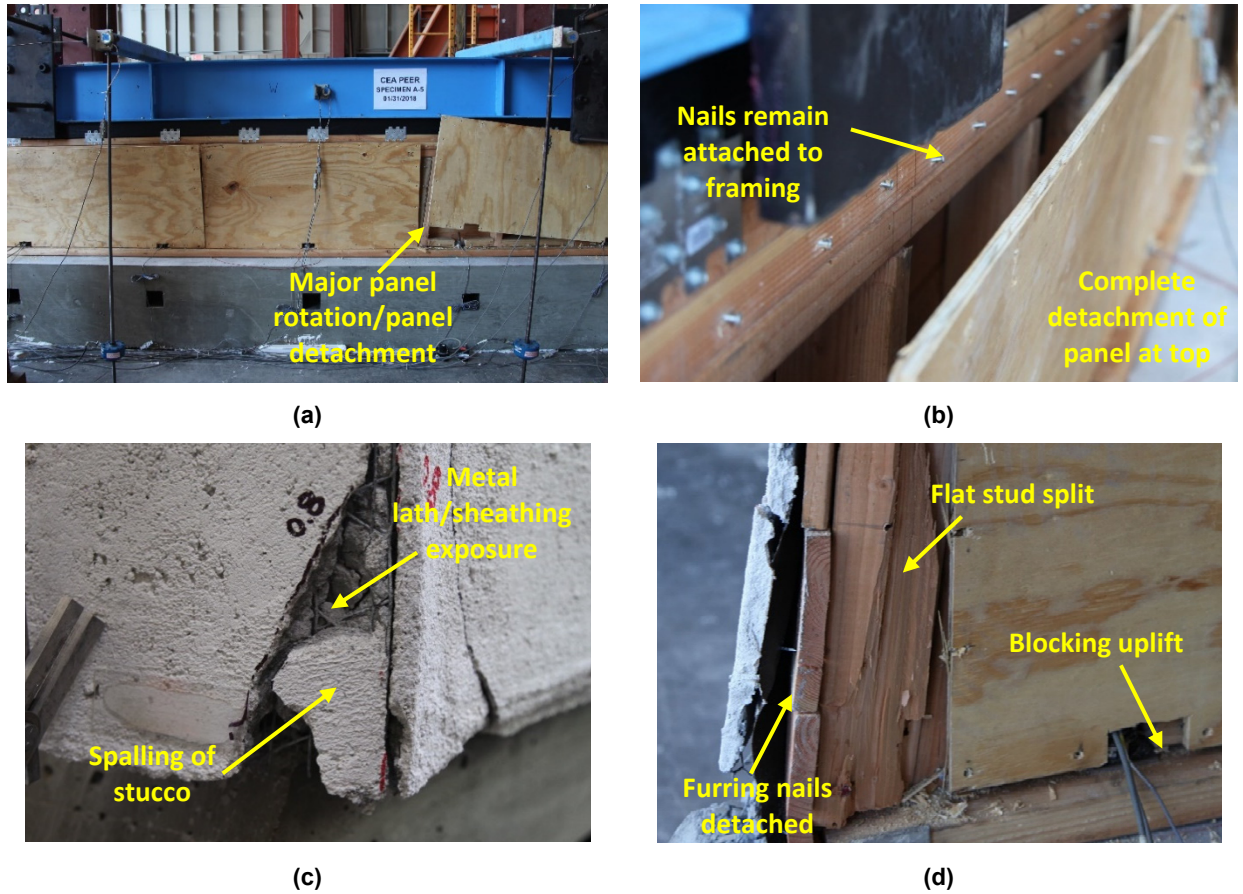


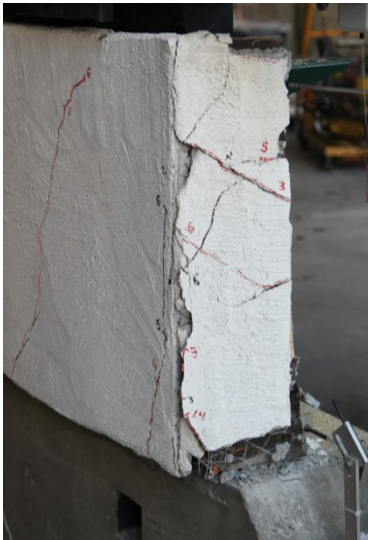
**Figure 5.32** Specimen A-5 damage state at 80% post-peak reduction of lateral strength @ -11% drift,  $\Delta = -2.64$  in.: (a) interior elevation; (b) top-down view of interior; (c) close-up of exterior south-end corner; and (d) close-up of interior north-end corner.



(a)



(b)



(c)



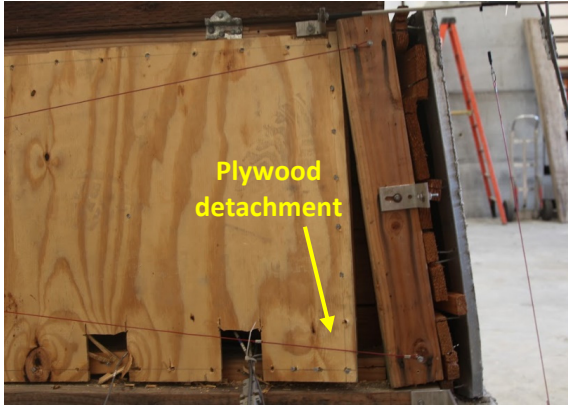
(d)

**Figure 5.33** Specimen A-5 post-test photographs at lateral load = 0 kips and residual displacement = -1.74 in. @ -7.3% drift: (a) exterior elevation of cripple wall; (b) interior elevation of cripple wall; (c) north-end exterior corner view; and (d) south-end interior corner view.

### **5.3.2.2 Specimen A-19 Observations and Damage at 20% Residual Lateral Force**

Figure 5.33 shows the state of Specimen A-10 at -12% global drift ratio, corresponding to an 80% drop in lateral strength. The stucco finish had detached from most of the furring nails on the studs and remained only attached to the furring nails at the top plates and the tops of the studs, a response similar to that of all wet finished (stucco) specimens. This is indicated by the large cracks in the stucco at the corners; see Figure 5.33(d). Along the interior, the plywood panels had rotated heavily and were detached from the framing at many locations; see Figure 5.33(a) and (c). Most of the nails at the bottom of panels failed either through edge tear-out or head pull-through; see Figure 5.33(b). At the corners, most of the sheathing boards had split. Many of the sheathing boards also detached from the framing when the stucco had fully detached from the framing, as seen in Figure 5.33(a).

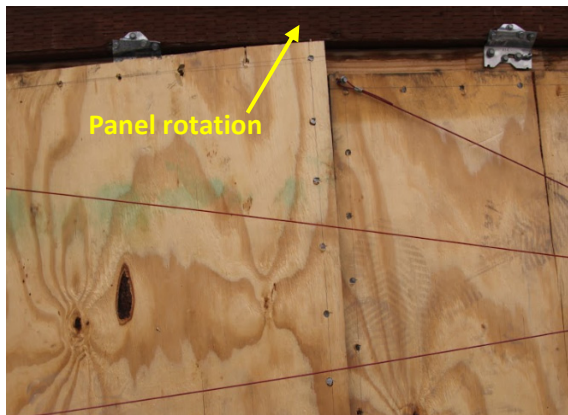
In Figure 5.34, the residual state of the specimen is shown after a monotonic push to +5.0 in. (+20.8% drift ratio) for a residual displacement of +4.26 in. (+17.8% drift ratio). Along the exterior face, no additional vertical cracks propagated post-strength, but the cracks at the edges had opened significantly; see Figure 5.34(a) and (c). The metal lath at the north corner had ruptured from the bottom of the wall all the way to the bottom of the top plates. The only remaining attachment of the plywood panels was at the top of the cripple walls. The north panel had nearly completely detached; see Figure 5.34(b). In addition, the plywood panels had crushed against the flat end studs. The blocking remained relatively intact.



(a)



(b)



(c)



(d)

**Figure 5.34** Specimen A-19 damage state at 20% residual lateral strength @ -11% drift,  $\Delta = -2.64$  in.: (a) interior elevation; (b) top-down view of interior; (c) close-up of exterior south-end corner; and (d) close-up of interior north-end corner.



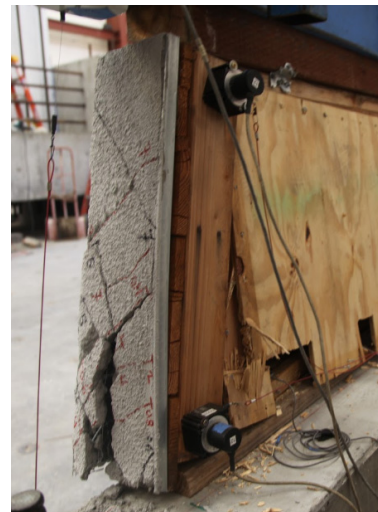
(a)



(b)



(c)



(d)

**Figure 5.35** Specimen A-19 post-test photographs at lateral load = 0 kips and residual displacement = +4.26 in. (+17.8% drift ratio) after monotonic push to +5.0 in. (+20.8% drift ratio): (a) exterior elevation; (b) interior elevation; (c) north-end exterior of wall view; and (d) north-end interior corner of wall view.

### **5.3.2.3 Specimen AL-2 Observations and Damage at 20% Residual Lateral Force**

Specimen AL-2 did not drop to below 20% of peak capacity until a drift ratio of approximately 16% was reached in the final monotonic push. At 6% drift, nearly complete fracture of the stucco at the corners was observed over the height of the cripple wall end walls and corners. Gaps of up to 1 in. opened between end wall stucco and the stucco on the north and south walls. The north and south walls exhibited very modest progression of cracking. The stucco continued to flare further at the base of the walls. The gap between stucco and foundation increased to approximately 1/2 in. For the retrofitted specimen, further rotation of the plywood panels was seen, with vertical sliding of the plywood panels estimated to be up to 1/4 in. at the specimen's east and west ends and 1/8 in. at interior panel joints. There was no observable damage to the clip angles (shear clips).

At 8% drift, separation of stucco at the corners and breaking of the stucco wire lath continued to increase. At the north and south walls there was no significant progression of cracking. Flaring of stucco away from the cripple wall framing and sheathing at the base increased to approximately 3/4 in. For the retrofitted cripple wall, the framing at the end walls began to lean to the point where it was visible. Rotation of the panels continued to increase. Nails in the upper top plate were withdrawn up to 1/8 to 1/4 in.; however, the retrofitted specimen remained functional. No observable damage occurred to the clip angles.

At 10% drift, the stucco at the end walls showed significant detachment, having separated from underlying sheathing and framing, and the wood siding was visible below. The north and south walls had negligible new cracking. The stucco flare was measured up to 1 in. For the retrofitted specimen, some nails in the upper top plate were observed to be withdrawn up to 1 in. and had deformed (bending with limited change in angle). In limited locations at the top and bottom corners of the sheathing, sheathing nail heads were observed to pull through. Some limited gapping between the sheathing and underlying framing was observed.

At 14% drift, the stucco at the end walls continued to deteriorate, and spalling of the stucco occurred. The north and south walls had negligible new cracking. Flaring at stucco base up to almost 2 in. occurred for the retrofitted specimen, and the diaphragm and upper top plate started to push off from the lower top plate and cripple wall. This caused the top of the east wall rim joist to roll towards the west as the top of the rim joist was pulled along with the displacement of the diaphragm sheathing.

In the final monotonic push, the diaphragm and upper top plate were pushed off from the lower top plate and cripple walls. The cripple walls remained at a very low drift, while the majority of the actuator displacement was taken up in diaphragm sliding.



(a)



(b)



(c)



(d)

**Figure 5.36** Specimen AL-2 during the final monotonic push to 40% drift ratio: (a) bottom of northwest corner; (b) bottom of southwest corner; (c) east-end of wall; and (d) northeast-end of wall.

#### **5.3.2.4 Discussion of Observations and Damage for Specimens with Retrofit at 20% Residual Lateral Force**

A comparison among retrofitted Specimens, A-5, A-19, and AL-2 showed similar damage mechanisms: (1) the stucco was no longer attached to the sheathing and framing in a way that could contribute strength; (2) the stucco at the corners had been substantially deteriorated, including rupture of the stucco and fracture of the stucco wire lath, such that the lumber sheathing could be seen below; and (3) damage to the retrofit plywood was extensive, indicating that the plywood strength and deformation capacity had been substantially developed without any premature weak links. The one notable difference is that at the end of the large-component test, the horizontal lumber sheathing showed little damage, while it was extensively damaged in the small-component tests.



## 6 Discussion

As noted in Section 1.2, the pairing of small- and large-component tests was included in the PEER–CEA Project test plan so that direct comparison could be made regarding (1) how closely small-component testing could emulate the response seen in the large-component tests, and (2) what boundary conditions in the small-component testing leads to the best match with large-component tests. A group of seven small-component and two large-component test specimens were used to study these questions. All of the specimens were constructed with stucco installed over horizontal lumber sheathing and tested with the same protocol and similar superimposed loads. The following discusses what has been learned in response to these questions.

### 6.1 CRIPPLE WALL LATERAL STRENGTH

When considering the lateral strength (peak capacity) of cripple walls without retrofit (see Section 3.1), the lateral strength of the large-component test ranged from 1.8 to 2.8 times the lateral strength of the small-component tests. The only exception was Specimen A-4, with the stucco and horizontal lumber sheathing seated directly on top of the foundation (the large-component lateral strength was 1.4 times small-component Specimen A-4); because Specimen A-4 was seen to have different response behavior in a number of aspects, it was considered a poor candidate for comparison. Based on this data, it is judged that large-component Specimen AL-1 is representative of an upper bound of capacity. This is due to a combination of the larger test specimen with its more realistic boundary conditions and the very high bond strength that developed between the stucco and the concrete foundation, which was not present in any of the small-component tests. Based on the limited data set currently available, it is assumed that large-component tests will provide higher lateral strengths.

When considering the lateral strength of the retrofitted cripple walls, the lateral strength of the two small-component and one large-component test specimens were remarkably similar. This may have been in part due to an unexpected weak link in the large-component test that is thought to have reduced peak capacity; however, the comparable lateral strengths show that the retrofit significantly increased the lateral strength of the specimens. When the bond between the stucco and the foundation broke in the large-component test, there was a limited but noticeable drop in capacity in the subsequent drift cycle. In this drift cycle, the capacity of small-component Specimen A-19 and large-component Specimen AL-2 were nearly the same, although it was post-peak for the large-component test and pre-peak for the small-component test. In the same drift cycle that Specimen A-19 reached strength, the large-component specimen reached a second peak, although around 15% lower than Specimen A-19. The staggered nailing of the plywood on the top

plates as well as slip plane developed between the top plates of the large-component test likely resulted in decreased strength capacity of the specimen at this drift cycle. Based on the limited data currently available, it is assumed that testing of small-component test specimens will predict with reasonable accuracy the peak lateral strength of retrofitted large-component specimens.

## **6.2 CRIPPLE WALL DRIFT AT LATERAL CAPACITY**

The relative drift at lateral capacity for the cripple walls without retrofit (see Section 3.2) were wide ranging, with the drift ratio for Specimens A-3 and A-20 being moderately smaller, Specimen A-1 being moderately larger, and the balance notably larger than Specimen AL-1. It is noted that the small-component test specimen with the closest matching boundary conditions to Specimen AL-1 had the smallest drift ratio at lateral strength of the group. The relative drift ratio at lateral strength of Specimen A-20 was 2.4%, and the relative drift ratio at lateral strength for Specimen AL-1 was 2.8%. It is believed that the superstructure used in large-component Specimen AL-1 helped to limit the in-plane rotation of the stucco on the longitudinal walls, thereby reducing the drift ratios; it is possible that the 2-ft returns on Specimen A-3 similarly restrained stucco rotation. The lower drift ratios for Specimen A-20 were due to both the outboard orientation of the stucco which allowed for increased in-plane rotation as well as the decreased lateral strength which reduced the displacement of the sill plate relative to the foundation.

The relative drift at lateral capacity for the retrofitted cripple walls were also wide ranging, with the drift ratio for Specimens A-5 and A-19 being 3.2 and 5.3%, respectively, while the drift ratio for Specimen AL-2 was 2.8%. Specimen A-19 was constructed with boundary conditions most closely resembling Specimen AL-2. The higher drift ratios associated with the small-component specimen were likely due to the difference in failure modes between it and the large-component test.

During testing, Specimen AL-2 developed a slip plane between its top plates, which did not occur with any of the small-component tests due to the top plates being connected by both nails as well as through bolts connecting the testing apparatus to the cripple wall. While the impact of this detail was most clearly seen in the final monotonic push, it is likely that it contributed additional deflection in prior displacement cycles. In addition, the rotation and uplift of the plywood was restrained in the large-component specimen from the sill plate and floor joists, whereas in the small-component tests, the plywood could more easily rotate and uplift since there were no floor joists restraining upward displacement.

## **6.3 CRIPPLE WALL POST-PEAK LOAD-DEFLECTION BEHAVIOR**

Among the test specimens without retrofit, the post-peak load-deflection behavior was quite similar (see Section 3.3), particularly for drift ratios of 6% or higher. All specimens retained residual capacities of 15–20% out to very significant drift ratios. At the conclusion of testing, the large-component specimen had a comparable residual strength to all unretrofitted specimens despite its lateral strength being more than double that of the small-component specimen with matching boundary conditions. This shows that at large displacement amplitudes, the majority of the residual strength could be attributed to the horizontal lumber sheathing boards as the stucco

had detached from most of the cripple wall. While there is some variation, numerical modeling parameters could reasonably be assigned from any of the tests.

Among the test specimens with retrofit the post-peak load-deflection behavior differed considerably; see Figure 3.25. The post-peak envelope curves are different enough that they would lead to notably different models for numerical modeling. During testing, the displacement control transducer for Specimen A-5 was knocked out of place, causing the imposed displacement to be much higher than the target displacement per the loading protocol; therefore, it is a poor indicator of the post-peak behavior of the retrofitted specimens. The post-peak load-deflection behavior of Specimen A-19 and Specimen AL-2 were much more closely matched. By the end of the cyclic portion of the test, the residual strength of the large-component test was around 30% higher than the small-component test. When the monotonic push was implemented, the residual strength at 20% drift ratio was nearly identical for the two specimens.

#### **6.4 CRIPPLE WALL BOUNDARY CONDITIONS FOR FUTURE TESTING**

For future testing, it is suggested that the best choice of boundary conditions for similar small-component testing would be the combination of top condition B and bottom condition a (used in Specimens A-2 and A-5), or top condition C and bottom condition a (used in Specimen A-3). Top boundary condition B and C were intended to mimic the continuity of the stucco into the first floor of the superstructure through a denser configuration of the furring nails at the top plates. For future testing, modifications to the top boundary condition could be explored in order to better mimic this continuity, as this was likely a major contributor to the decreased strength capacity of the unretrofitted small-component tests when compared with Specimen AL-1.

While the tests without retrofit were noted to have lower lateral strengths than the large-component specimen, these lower lateral strengths were observed for all small-component tests without retrofit. Of these two sets of boundary conditions, top boundary condition C and bottom boundary condition a (Specimen A-3) provided a drift at peak capacity most similar to the large-component tests. The small-component specimen with boundary condition detailing most similar to Specimen AL-1 (Specimen A-20), which had top boundary condition B and bottom boundary condition c, had a similar drift at lateral strength as well. With the small number of tests performed, the choice of best boundary conditions should be revisited in the future, specifically with addressing the increased strength of the large-component specimens associated with the continuity of the stucco from the cripple wall into the first floor of the superstructure.

#### **6.5 CRIPPLE WALL UPLIFT BEHAVIOR**

The discussion in Chapter 4 demonstrates that the small-component test specimens experienced much higher anchor bolt tension forces and damage associated with uplift. The uplift forces were lower in the large-component tests, and there was no damage due to the uplift. The uplift-related damage that occurred in the small-component tests considered herein is not believed to have reduced the lateral strength; therefore, it is not considered significant; however, the uplift and sliding at anchor bolts did increase the global drift ratios.

## **6.6 COMPARISON OF OBSERVED DAMAGE**

The discussion in Chapter 5 demonstrates the significant differences in damage mechanisms between the small- and large-component tests up to lateral strength. This was often seen in much higher levels of slip and damage in the small-component tests compared to the large-component tests. This would tend to make the small-component tests a conservative predictor of damage level and repair cost when compared to the large-component tests. At 20% residual strength, the damage observed in small- and large-component specimens was much more similar, with some minor differences.

## 7 Conclusions

This section discusses overarching conclusions drawn from comparison of the response of small- and large-component cripple wall specimens with stucco over horizontal lumber sheathing. This section also provides recommendations for future testing; these recommendations address the full scope of the PEER–CEA Project Working Group 4 (WG4) testing, rather than just cripple walls with stucco over horizontal lumber sheathing.

Specimens constructed with other materials were included in the WG4 tests but are outside of the scope of this report (see Schiller et al. [2020a-d] and Cobeen et al. [2020]). The intent of the UC Berkeley large-component cripple wall tests (Specimens AL-1 and AL-2) was to capture the effect of boundary conditions as closely as possible to those that would occur in a complete house. This included providing continuity of the exterior stucco around corners, continuity of the stucco into the superstructure story above, and continuity of the stucco down the face of the foundation (a common detail in existing homes). The UC San Diego small-component tests (Specimens A-1, A-2, A-3, A-4, A-5, A-19, and A-20) explored the effects of a range of boundary conditions applied to 12-ft-long cripple wall (only) components. All cripple walls considered in this report were 2 ft high.

### 7.1 OVERARCHING CONCLUSIONS

This section provides overarching conclusions from the comparison of small- and large-component specimen responses. These are organized by focusing on the load-deflection as well as damage characteristics similarities and differences, with particular regard to cripple walls finished with stucco over horizontal lumber sheathing. First, notable commonalities are as follows:

- For both small- and large-component test specimens, drift ratios at lateral strength were significantly higher in cripple walls compared with similar full-story-height walls. This confirms the pattern previously suggested by the cripple wall tests of Chai et al. [2002]; and
- Another commonality seen in the small- and large-component test specimens is an ability to retain 10 to 20% of their lateral strength out to large drift ratios (between 10 and 40%). This is a significant new finding as past testing was not conducted to such large drift ratios. This information is important for numerical modeling intending to identify the probability of collapse. It is recommended that future testing extend to insipient collapse or as close to insipient collapse as permitted by the test setup.

For specimens *without retrofit*, key conclusions include the following:

- The lateral strength (peak capacity) of the large-component specimen was significantly higher than that of the small-component specimens. This is largely attributed to a combination of the continuity of the stucco from the cripple wall to the first floor, the excellent construction quality of the bond between the stucco and the foundation, and the continuity of the stucco around the entire large-component specimen. Therefore, the large-component specimen is viewed as representing a high but achievable upper bound of lateral strength;
- The drift at lateral strength of the small-component specimens had notable variations. Small-component Specimen A-3, with 2-ft-long return walls reached lateral strength at a 2.5% drift ratio, which appears to agree with the large-component specimen that reached lateral strength at a 2.8% drift ratio with comparable damage mechanisms. Specimen A-20, which best matched the boundary conditions of Specimen AL-1, was also a close match to the large-component specimen with a drift ratio at lateral strength of 2.4% with comparable damage mechanisms; and
- Although the extent and location of damage varied between the small- and large-component specimens, the mechanisms of damage remained similar.

The following are primary conclusions regarding the *retrofitted* specimens:

- The lateral strength of the small- and large-component specimens was quite similar. This may be due in part to detailing of the large-component specimen retrofit plywood, which may have prevented the retrofit sheathing from achieving full capacity;
- The drift at lateral strength varied notably, with the drifts of the small-component specimens being larger than that of the large-component specimen. Significant uplift at the ends of the small-component specimens may be one source of the larger drift. This uplift may have been suppressed for the large-component specimens due to the size of these specimens and presence of the upper floors. Another source of the discrepancy might be due to the plywood panels in the small-component tests being free to move upward, i.e., free from partial constraint against rotation and uplift as opposed to the large-component tests. Lastly, a slip plane developed between the top plates of the large-component test, which did not occur with the small-component tests due to the presence of through bolts extending from the load transfer system through the top plates thus preventing any slip from occurring; and
- The physical damage at a drift ratio of 1.4% was more extensive in the large-component specimen than the small-component specimens. At lateral strength, the small-component specimens experienced notably more deterioration in the retrofit plywood than the large-component specimen. At 20% residual strength, the damage to the small- and large-component specimens was similar.

The following are overarching conclusions regarding the benefits of retrofit:

- The increase in lateral strength with the addition of cripple wall retrofit was significant for both small- and large-component specimens;
- The energy absorption capacity is significantly increased;
- The ratio of lateral strength with retrofit to without was higher for the small-component tests; and
- At 1.4% drift, both the retrofitted small- and large-component specimens consistently experienced less damage than the corresponding specimens without having been retrofitted.

## 7.2 FUTURE RESEARCH NEEDS

A key goal of the testing phase of PEER–CEA Project was, physical testing was conducted to expand the limited available load-deflection information from which numerical models could be generated [Welch and Deierlein 2020]. Although this testing program contributed extensively to the currently available test data, there are still notable ways in which the numerical modeling, damage assessment, and loss estimation could benefit from additional test information. This section discusses how the testing program of PEER–CEA Project raised issues that should be addressed. The following are recommendations for future testing of cripple walls based on knowledge gained from the PEER–CEA Project testing:

1. The pairing of small- and large-component specimens is encouraged where practical because the results can complement each other and provide a more complete picture. It is notable that the large-component specimen provided upper bound lateral strength. Moreover, the complementary large-component specimens offered a more complete system and thus identified additional damage patterns and weak links, e.g., as the slip between upper and lower top plates in Specimen AL-2.
2. If future testing incorporates smaller components, the boundary conditions used in the PEER–CEA Project small-component test specimens may be useful when attempting to capture conditions occurring in complete houses. These boundary conditions include: (1) additional fasteners between the stucco and the cripple wall top plates; (2) finish materials orientated outboard of (overhanging) the foundation; and (3) the wrapping of the stucco around the wall end for stucco returns of between 6 in. and 2 ft.
3. Lastly, for a small-component specimen, the foundation could be modified such that finish materials on return walls are placed outboard of the foundation (i.e., overhanging), essentially matching the orientation on the long face of the cripple wall. This would better mimic house construction and a configuration also achievable with a larger component specimen.

The PEER–CEA Project testing program considered both small- and large-test specimens, with a wide range of sheathing and finish materials, and load path details. The broad scope of this Project meant that there was only a single specimen for each unique configuration tested. The

following suggestions for future testing protocol might add to the robustness of the PEER–CEA data and help to better identify the variation of response that might occur for a given configuration.

- Additional tests are recommended for the subset of the small-component test specimens that are deemed of high importance for numerical modeling. It is recommended providing an additional two to four replications of the test;
- An additional replication of Specimen AL-1 might be conducted without an extension of the stucco down the face of the footing. Although this detail is commonly seen in dwellings with stucco finishes, cracks can develop in the stucco along the sill plate causing the bond between the stucco and foundation could potentially be weakened due to the deterioration associated with a dwelling's age. This would aid in identifying how closely the peak capacities of the small- and large-component tests might resemble each other with this variation in boundary conditions; and
- Replicating the testing of Specimen AL-2 might be conducted with the revised detail for retrofit plywood sheathing nailed into the uppermost top plate. This would help identify whether or not the peak capacity had been increased with this revised detail, enhancing the understanding of the response mechanisms when comparing the response of small- and large-component specimens.

The PEER–CEA Project tests focused primarily on houses having cripple walls of uniform heights; it did not address stepped cripple walls or the case where the lowest floor framing sits directly on top of concrete or masonry foundation stem walls. These conditions can occur alone or in combination with level cripple walls. The following are additional configurations for which testing is recommended:

- Additional tests with stepped cripple walls and representative boundary conditions are recommended to complement the testing already conducted by Chai et al. [2001]; and
- Tests with floor framing supported on a foundation sill plate sitting directly on the foundation are recommended to better understand this common configuration. It is suggested that these be tested alone and in combination with cripple walls, both level and stepped.

The PEER–CEA Project focused primarily on cripple walls with foundation sill plates fastened to the foundation with anchor bolts for cripple walls with and without retrofit. Several tests were conducted with wet-set foundation sill plates having nails partially embedded into the sill plate and nail heads cast into the concrete. This is believed to have been a common method of fastening foundation sill plates prior to widespread use of anchor bolts. The capacity of the wet set connection was larger than expected. Listed below is additional testing that would address the wet set sill configuration.

- It is recommended that there be additional research into the range of fastening conditions that occur with wet set foundation sill plates, such as existence of, number of, and spacing of fasteners cast into the concrete;
- It is recommended that additional specimens be testing with wet set sills, including a range of finish and sheathing materials and representative variation

in the wet set fastening. Wet set sill plates tested were encased in concrete at the ends. It is recommended that the future tests extend the sill plate the entire length of the foundation; and

- It is also recommended that future foundations for cripple wall or like foundation components representative of older construction consider using rough float finish if warranted to mimic standards of practice at that time.

The testing results of the PEER–CEA Project contributed greatly to the available test data; however, there are still notable ways in which the numerical modeling could benefit from additional experimental information. As much of the testing to date has been conducted on small (isolated) components, questions as to how well load-deflection parameters derived from small-component data serve as a predictor of the performance of the full house remain. Listed below are recommendations for additional testing to better understand the ability of component testing to predict the response and performance of the full house.

- It is recommended that full-house shake table testing be conducted in order to demonstrate the improved performance resulting from cripple wall retrofit, as well as to allow interpretation of PEER–CEA numerical modeling, damage assessment, and loss modeling. See Appendix B to this report for a more detailed discussion of possible full-house testing; and
- It is recommended that additional large-component testing be conducted to better bridge the gaps between small-component tests and the performance of full houses. This might be a particularly effective way to further study the stepped and zero-height cripple wall configurations previously discussed and the combinations of cripple wall configurations within a house.

The PEER–CEA Project focused on houses with crawlspaces and cripple walls. The houses studied were modeled to have crawlspaces extending under the full building footprint. There are a notable number of California houses, however, in which a portion of the house is over a crawlspace with cripple walls, while the balance is constructed with a slab on grade foundation. These can extend to split-level crawlspace houses with a living-space-over-garage configuration. The following is additional testing that might be conducted to investigate these buildings with a more complex geometry:

- It is recommended that additional testing be conducted to support analytical modeling of these more complex house configurations.

In addition to conducting testing to generate data for numerical modeling of cripple walls, the PEER–CEA Project also conducted tests of superstructure walls that occur in occupied stories. The project was able to conduct two tests to generate data for two of the highest priority combinations of wall sheathing and finish materials. Future numerical modeling efforts would benefit from a more robust set of test data for superstructure walls including additional replications of key tests, additional combinations of sheathing, interior finishes and exterior finishes, and additional variations in detailing (i.e., conventional construction detailing and engineered detailing).



## REFERENCES

- Arnold A.E., Uang C., Filiatrault A. (2003a). Cyclic behavior and repair of stucco and gypsum woodframe walls: Phase I, *CUREE -Caltech Woodframe Project Publication No. EDA-03*, Department of Structural Engineering, University of California, San Diego, CA.
- Arnold A.E., Uang C., Filiatrault A. (2003b). Cyclic behavior and repair of stucco and gypsum woodframe walls: Phase II, *CUREE -Caltech Woodframe Project Publication No. EDA-07*, Department of Structural Engineering, University of California, San Diego, CA.
- Chai Y.H., Hutchinson T.C., Vukazich S.M. (2002). Seismic behavior of level and stepped cripple walls, *CUREE - Caltech Woodframe Project Publication No. W-17*, Division of Civil and Environmental Engineering, University of California, Davis, CA.
- Cobeen K., MahdaviFar, V., Hutchinson, T., Schiller, B., Welch, D. P., Kang, G. S., and Bozorgnia, Y. (2020). Large-component seismic testing for existing and retrofit single-family wood frame dwellings, *PEER Report No 2020/20*, Pacific Earthquake Engineering Research Center, Berkeley, CA.
- FEMA (2018). *Vulnerability-Based Seismic Assessment and Retrofit of One- and Two-Family Dwellings, FEMA P-1100*, Vol. 1, Prestandard, Federal Emergency Management Agency, Washington, DC.
- Osteraas J. et al. (2010). General guidelines for the assessment and repair of earthquake damage in residential woodframe buildings. *CUREE -Caltech Woodframe Project Publication No. EDA-02*, Consortium of Universities for Research in Earthquake Engineering, Richmond, CA.
- Schiller B., Hutchinson T.C., Cobeen K. (2020a). Cripple wall small-component test program: Wet specimens I, *PEER Report No. 2020/16*, Pacific Earthquake Engineering Research Center, University of California, Berkeley, CA.
- Schiller B., Hutchinson T.C., Cobeen K. (2020b). Cripple wall small-component test program: Dry specimens, *PEER Report No. 2020/17*, Pacific Earthquake Engineering Research Center, University of California, Berkeley, CA.
- Schiller B., Hutchinson T.C., Cobeen K. (2020c). Cripple wall small-component test program: Wet specimens II, *PEER Report No. 2020/18*, Pacific Earthquake Engineering Research Center, University of California, Berkeley, CA.
- Schiller B., Hutchinson T.C., Cobeen K. (2020d). Cripple wall small-component test program: Comparisons, *PEER Report No. 2020/19*, Pacific Earthquake Engineering Research Center, University of California, Berkeley, CA.
- Vail K., Lizundia B., Welch D., Reis E. (2020). Earthquake damage workshop. *PEER Report No. 2020/23*, Pacific Earthquake Engineering Research Center, University of California, Berkeley, CA.
- Welch D.P., Deierlein G. (2020). Technical background report for structural analysis and performance assessment, *PEER Report No. 2020/22*, Pacific Earthquake Engineering Research Center, University of California, Berkeley, CA.



# APPENDIX A      Working Group 4 Plan for Experimental Program

## A.1 INTRODUCTION

This appendix summarizes the test plan established in early 2017 to guide the PEER–CEA Project Working Group 4 testing. This information is included to provide information on the overall experimental testing scope, objectives, and approach. Some aspects of the testing plan were revised during implementation. In particular, this is true of the small-component tests detailed in the following section, in which choice of test specimens further evolved as testing was being conducted.

The primary objectives of the proposed testing are to:

- Develop descriptions of load-deflection behavior of components and connections that can be used by Task 5 in development of analytical modeling; and
- Collect data on descriptions of damage at varying levels of peak transient drift that can be used by Task 6 in development of loss modeling.

The testing descriptions in this appendix are developed to a conceptual level. Full details of testing will be developed incorporating research on details of construction applicable to the year of construction ranges of interest.

## A.2 TESTING GROUP A: CRIPPLE WALL COMPONENTS

**What:** Testing of cripple wall components to develop load-deflection behavior for analytical modeling and loss modeling; these tests will also serve to identify characteristics of damage evolution to the cripple wall component during combined lateral and vertical (gravity) loading.

**Why:** The load-deflection behavior of cripple walls is key to predicting seismic response of cripple wall dwellings and related damage. Existing data is very limited.

**Approach:** Small-component testing as described below for finish materials with limited continuity and for correlation studies with large-component testing.

Large-component testing as described below to capture influence of component size, boundary conditions, and continuity of finish materials to occupied story wall

above. Intent is to use limited number of tests for comparison to small-component tests. This will determine whether it is possible to capture response in small-component tests, or larger component is required.

### A.3.1 Testing Group A: Small Components

**Tests:** Twenty-eight tests with varying materials, condition, year of construction, and load path connections (consistent with year of construction); see Table A.1 and Figures A.1 and A.2. It is noted that the setup adopted in the UC Davis cripple wall test program [Chai et al. 2002] is proposed with modified edge conditions for specimens finished in stucco to capture the additional restraint anticipated at the floor and end-wall boundaries.

**Test Location:** UC San Diego

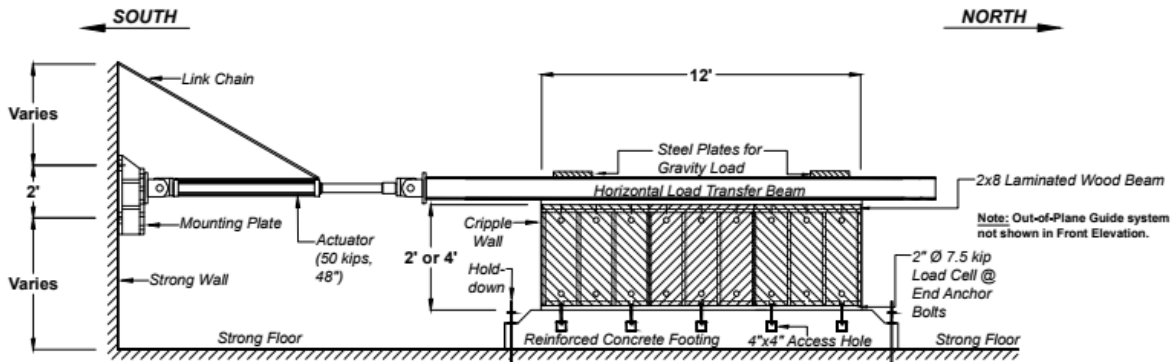


Figure A.1 Group A small-component test setup (2 ft and 4 ft CW) is proposed to be similar to that used in CUREE testing by Chai et al. [2002].

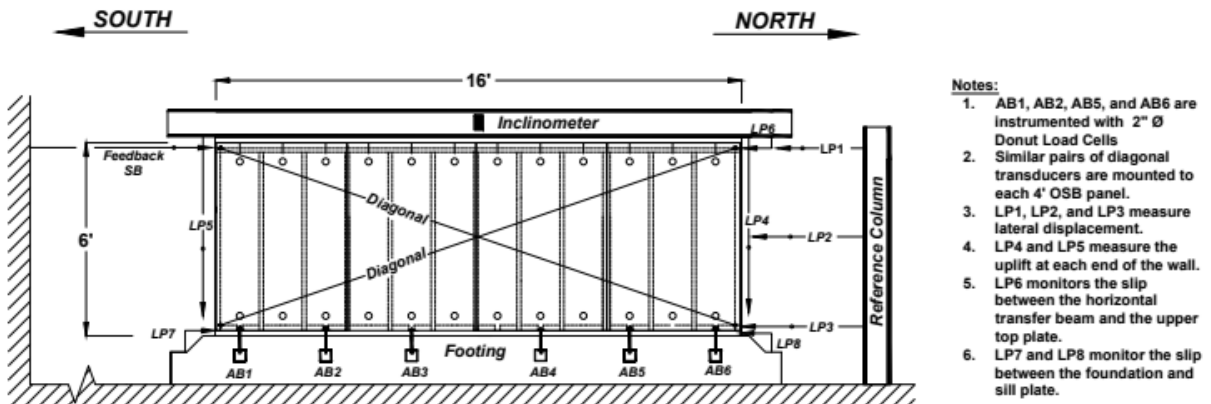


Figure A.2 Group A small-component instrumentation setup (6 ft CW) is proposed to be similar to that used in CUREE testing by Chai et al. [2002].

Table A.3 Small-component complete testing matrix.

Testing phase	Report no.†	Specimen	Test no. (date)	Existing or retrofitted	Era	Vertical load	CW height (ft)	Anchorage	Exterior finish	Top BC	Bottom BC	Loading	Test date
1	1	A-1	4	E	Pre-1945	H	2	S(64 in.)	S+HSh	A	a	C	1/26/2018
		A-2	3	E	Pre-1945	H	2	S(64 in.)	S+HSh	B	a	C	1/18/2018
		A-3	6	E	Pre-1945	H	2	S(64 in.)	S+HSh	C	a	C	2/2/2018
		A-4	1	E	Pre-1945	H	2	S(64 in.)	S+HSh	B	b	C	12/18/2017
		A-5	5	R	Pre-1945	H	2	S(32 in.)	S+HSh	B	a	C	1/31/2018
		A-6	2	E	Pre-1945	H	2	WS	S+HSh	B	b	C	12/22/2017
2	2	A-7	7	E	1945–1955	H	2	S(64 in.)	HS	B	c	C	5/11/2018
		A-8	8	R	1945–1955	H	2	S(32 in.)	HS	B	c	C	5/22/2018
		A-9	11	E	1945–1955	H	2	S(64 in.)	HS+DSh	B	c	C	7/19/2018
		A-10	12	R	1945–1955	H	2	S(32 in.)	HS+DSh	B	c	C	7/26/2018
		A-11	9	E	1956–1970	H	2	S(64 in.)	T	B	c	C	6/15/2018
		A-12	10	R	1956–1970	H	2	S(32 in.)	T	B	c	C	6/28/2018
		A-13	13	E	1945–1955	H	6	S(64 in.)	HS	B	c	C	8/26/2018
		A-14	14	R	1945–1955	H	6	S(32 in.)	HS	B	c	C	8/30/2018
3	3	A-15	20	E	Pre-1945	H	2	S(64 in.)	S+DSh	B	c	C	11/20/2018
		A-16	21	R	Pre-1945	H	2	S(32 in.)	S+DSh	B	c	C	2/5/2019
		A-17	18	E	Pre-1945	H	2	S(64 in.)	S	B	d	C	11/5/2018
		A-18	22	R	Pre-1945	H	2	S(32 in.)	S	B	d	C	11/13/2018
		A-19	19	R	Pre-1945	H	2	S(32 in.)	S+HSh	B	c	C	10/22/2018
		A-20	15	E	Pre-1945	H	2	S(64 in.)	S+HSh	B	d	C	10/31/2018
		A-21	17	E	Pre-1945	H	2	WS	S+HSh	B	c	C	10/26/2018
		A-22	16	E	Pre-1945	H	2	S(64 in.)	S	B	c	C	10/29/2018
4	2	A-23	23	E	1956–1970	H	6	S(64 in.)	T	B	c	C	9/16/2019
		A-24	24	R	1956–1970	H	6	S(32 in.)	T	B	c	C	10/3/2019
	3	A-25	27	E	Pre-1945	H	6	S(64 in.)	S	B	c	C	10/29/2019
		A-26	28	R	Pre-1945	H	6	S(32 in.)	S	B	c	C	11/7/2019
		A-27	26	E	Pre-1945	H	2	S(64 in.)	S+HSh	B	c	M	10/25/2019
	2	A-28	25	E	1945–1955	L	2	S(64 in.)	HS+DSh	B	c	C	10/10/2019
Denotes Pre-1945 Era				Retrofitted		Low Vertical Load		Wet set sill or retrofitted	Dry finish materials	Case A,C	Case a,b,d	Monotonic loading	
Denotes 1945–1955 Era													
Denotes 1956–1970 Era													

Notes: E = existing R = retrofitted, S = anchor bolt spacing, H = heavy vertical load (450 plf), L = light vertical load (150 plf), S = stucco, HS = horizontal siding, HSh = horizontal sheathing, DSh = diagonal sheathing, T = T1-11 wood structural panels, BC = boundary condition, uppercase letters = top boundary conditions, lowercase letters = bottom boundary condition, C = cyclic, and M = monotonic.

†Reports are as follows: Report 1: Schiller et al. [2020(a)], Report 2: Schiller et al. [2020(b)], and Report 3: Schiller et al. [2020(c)].

### A.3.2 Testing Group A: Large Components

**Tests:** Two tests including two different exterior finish materials and with and without retrofit; see Figure A.3.

**Table A.2 Large-component test matrix.**

Specimen	Existing (E) of retrofit (R)	Exterior finish	Interior finish
AL-1	E	Stucco over horizontal sheathing	Gypsum wallboard
AL-2	R	Stucco + S+HS	Gypsum wallboard

**Test Location** UC Berkeley

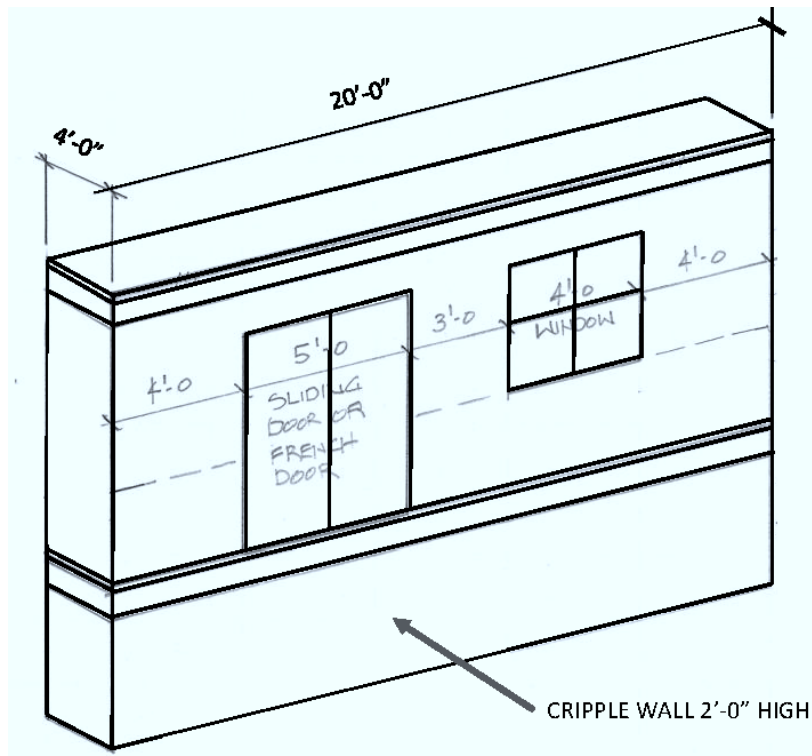


**Figure A.3** Group A large-component test setup is proposed to be similar to that used in CUREE-CEA testing by Arnold et al. [2003] i.e., *CUREE EDA-03* and *CUREE EDA-07*.

#### A.4 TESTING GROUP B: LOAD PATH CONNECTIONS

**What:** Testing of load path connections between foundation sill plate and foundation and connections between cripple wall top plate and floor framing above. These tests will include retrofit conditions.

**Why:** These connections are critical to the performance of cripple walls and anchorage, and there is little or no publicly available information on performance, especially performance within representative cripple wall assemblies.

**Approach:** Testing of retrofit anchors to foundations, used where there is not enough height to use roto-hammer in installation of anchor bolts. These retrofit anchors are bolted to the face of the foundation rather than the top and will be tested in a 2-ft-high cripple wall assembly.

Testing with retrofit anchors will include representative connections from cripple wall top plate to floor framing above.

**Tests:** One tests of back-to-back cripple walls, with retrofit

**Table A.3 Load path connection test matrix.**

Specimen	Existing (E) or Retrofit (R)	Left Side		Right Side	
		Top Connection	Bottom Connection	Top Connection	Bottom Connection
B-1	R	A35	URFP	A35	URFP

**Test Location:** UC Berkeley

## A.5 TESTING GROUP C: COMBINED MATERIALS IN OCCUPIED STORIES

**What:** Limited testing of full story-height walls in occupied stories with key combinations of interior and exterior finish materials.

**Why:** The only combination of materials with substantial test information that includes appropriate wall configuration, boundary conditions, and loading protocol is the CUREE-CEA testing of combined stucco and gypsum wallboard. Rules currently used to combine finish material hysteretic behavior is known to be very approximate. Description of the combined finishes is key to study of propagation of damage into the occupied stories and resulting losses.

**Approach:** Tests of priority combinations of materials using wall configuration and boundary conditions similar to the CUREE-EDA testing. Priority will be given to material combinations thought to be most damageable and therefore more critical to estimating losses.

**Tests:** Two tests of back-to-back walls.

**Table A.4 Combined materials in occupied stories test matrix.**

Specimen	Existing (E) or Retrofit (R)	Exterior Finish	Interior Finish	Matching Small-Component Specimen
C-1	E	Horizontal wood siding (shiplap)	Plaster on wood lath	A-9
C-2	E	T1-11 sheathing with typical non-shear wall installation	1/2-in. gypsum wallboard installed per conventional construction	A-25

**Test Location:** UC Berkeley

## A.6 FUTURE TESTING

The following were identified as testing of interest that did not rise to the level of priority or fit within the available budget. These are provided for consideration for future testing:

- Further testing of combined materials in occupied stories to better describe performance of the superstructure.
- Systematic testing of cripple walls with deteriorated materials or fastening in order to further expand the limited testing recommended to be conducted under Group AS. Discussion is needed of types and extents of deterioration can reasonably be studied through physical testing.

- Testing of large subassemblies using box configurations rather than planar walls to inform analytical modeling of three-dimensional structures. Additionally, this may inform concerns that cripple walls can fail due to excessive out of plane movement of the wall top, creating a P-delta condition that overcomes the stud top and bottom connection capacities.
- Hybrid testing combining a large-scale cripple wall test with an analytical model of a full building in to allow understanding of differences and possible model calibration required to capture response.
- Full-dwelling shake table tests of dwellings with and without cripple wall retrofit as a proof of concept and to allow modeling validation/calibration. It is noted that this type of test specimen is the focus of planning for the final year of the project, as requested in the CEA RFQ.

# **APPENDIX B      Recommendations for Future Full-Scale Testing (PEER–CEA Project Task 4.5)**

## **B.1    INTRODUCTION**

The PEER–CEA Project scope of work included the development of recommendations for future full-scale testing of cripple wall houses, denoted as Task 4.5. This appendix chapter provides Task 4.5 recommendations, including an overview of the benefits of providing such testing and discussion of what such testing might entail.

It is anticipated that, should CEA wish to pursue this testing, requests for research proposals would be a natural future step. In drafting this appendix chapter, it was recognized that in coordination with physical testing, it would be highly desirable to have concurrent and related research activities to interpret the test data utilizing both numerical modeling and loss estimation tools, and the results of the PEER–CEA Project. Included in this appendix chapter is discussion of how these related activities might be incorporated.

## **B.2    FOREWORD**

During the course of the PEER–CEA Project, physical testing was conducted in order to expand the limited available load-deflection information from which numerical models could be generated. In spite of the expansion of available test data that occurred during the project, there are still notable ways in which the numerical modeling could benefit from additional test information. Among these, much of the testing to date has been conducted on small (isolated) components, leaving questions as to how well load-deflection parameters derived from small component data serves as a predictor of the performance of the full house. Considerations include the additional complexity and perceived redundancy of the full house.

## **B.3    OBJECTIVES AND BENEFITS**

Full-scale house testing would be a very significant and beneficial expansion of current testing data and knowledge, generating a wide variety of benefits. The following are a few of the potential objectives and benefits of conducting full house testing.

- **Demonstration of Improved Performance.** A primary and highly visible benefit of full house testing would be demonstration of the vulnerability of cripple wall houses without retrofit, and of the significantly improved performance with retrofits installed; the use of realistic earthquake ground motions including ground motion scaling and dynamic rates of loading would offer this further credibility. This would be of benefit to homeowners, retrofit designers and installers, and communities considering retrofit ordinances, in that they would have a very real and relatable demonstration of the benefits of retrofit. This could contribute to an increased rate of voluntary and mandatory retrofit and an overall increase in resilience of the California housing stock;
- **Numerical Modeling.** A significant benefit to numerical modelers would be the availability of full house data to interpret relative to results of currently used modeling assumptions and tools, affording an opportunity to investigate load-deflection behavior, behavior mechanisms, three dimensional effects, etc. This would be a quantum leap forward from the current reliance on two-dimensional small (isolated) component data to model the three-dimensional response of much more complicated structures. This could lead to improvements in future modeling efforts, resulting in improved prediction of performance and loss estimation. There is currently believed to be a bias of the numerical modeling towards overpredicting the seismic response and resulting damage, relative to observed earthquake damage. Full house testing could provide additional data points from which the numerical modeling results could be better understood;
- **Loss Modeling.** A significant benefit to those involved in loss modeling would be observation and documentation of system level damage to interpret relative to damage scenarios used in developing PEER–CEA Project loss estimation information. This would allow interpretation relative to damage and repair descriptions from the PEER–CEA Project workshop, looking at both methodology and results. This testing might also provide an opportunity to test-run the newly updated *General Guidelines for Assessment and Repair and Engineering Guidelines for Assessment and Repair* [Osteraas et al. 2010]; and
- **Educational Materials.** Full-scale building testing could also provide a wealth of information for incorporation into educational materials targeted at a wide range of users.

#### B.4 PHYSICAL TESTING RECOMMENDATIONS

The following provides recommendations for the design and conduct of full-scale house testing. The focus of this discussion is on the construction of one or more houses in a laboratory for purposes of testing; an alternative approach would be to conduct *in situ* testing of one or more existing houses. The following discussion is also based on the assumption that shake table testing will be conducted; while this is the most desirable test method, it is possible that other testing methods might be used. It is recommended that the pros and cons of both the type of test specimen (new versus an existing house) and the testing method be considered before moving forward with a testing program.

### B.4.1 Test House Configuration

While a large variety of full house testing could be conducted and would be of interest, the recommended first priority is testing of mainstream house configurations at full scale and using shake-table testing. Within the building materials and geometries included in the PEER–CEA Project numerical studies, a large number of full-scale house permutations of interest for testing could be identified. While even one full-scale house test would be of considerable benefit, it would be desirable to have not less than four tests.

- If one house were to be tested, we would recommend it be a house with horizontal wood siding and with retrofit cripple walls;
- If two houses could be tested, we would recommend a pair of matching houses one with and the other without retrofit; and
- If four houses could be tested, we would recommend two pairs of houses, one pair with horizontal wood siding and the other pair with another exterior finish material (likely stucco).

Working Group 4 findings demonstrate the vast difference in in-plane seismic behavior across the range of cripple wall finish materials encountered in California housing stock. The purpose of considering a pair of finish materials would be to encapsulate the upper and lower bound of this range in strength and stiffness.

It is recommended that test houses include both the cripple walls and most or all of the superstructure, using building plan dimensions as near as possible to those of full houses. This will afford the best opportunity to understand performance of these complex three-dimensional structures. It is suggested that the case study houses models developed and used by the PEER–CEA Project Earthquake Damage Workshop [Vail et al. 2020] be considered for testing, as this will provide the benefit of continuity with numerical and loss estimation studies just completed. During the Earthquake Damage Workshop, damage assessment professionals provided estimates of the cost of repairing damage to houses with and without retrofits. Three buildings were provided for the workshop: two single story, 40-ft × 30-ft dwellings (Case Study Building 1 and Case Study Building 2) and one two-story dwelling with 40-ft × 30-ft stories (Case Study Building 3). Note that if used, plans and details of the full house configuration and materials of construction have been developed and could be used as a starting point. The plan for Case Study Buildings 1 and 2 is provided in Figure B.1, and elevations are provided in Figures B.2 and B.3. Although one-story houses are shown in these figures, either one- or two-story houses or both could be selected for testing.

It is recommended that the test houses have interior and exterior bracing and finish materials installed throughout to best emulate the seismic response of complete houses. One important consideration is the inclusion of gypsum wallboard and similar interior finish materials that are known to greatly affect seismic response. Common finish materials highly recommended for inclusion include cement plaster (stucco) and horizontal wood siding exterior finishes, and gypsum wallboard and plaster on wood lath interior finishes; Figure 4 illustrates cyclic testing data for the 2-ft-high cripple walls for these two exterior finish materials, illustrating the dramatically different load-deflection behaviors that are of interest to study. The full-scale house testing could also be used as an opportunity to observe performance of some of the more brittle materials that

are often installed in kitchen and bathrooms; interior finishes such as tile were identified in the Earthquake Damage Workshop to play an important role in estimated repair costs.

While testing could include a range of cripple wall heights, as well as stepped and level configurations, it is recommended that 2-ft-high cripple walls be prioritized. This cripple wall height is the most common in the California housing stock and is the most studied in both physical testing and numerical studies to date. As a result, it would provide an important point of comparison to work done to date. Testing of the buildings should include existing and retrofit pairs in order to demonstrate the vulnerability of cripple wall houses pre-retrofit and the improved performance post-retrofit. Another key outcome would be to see how increased strength and stiffness of the added retrofit affects the repair costs of the superstructure.

It is recommended that consideration be given to the base condition for the test houses. While laboratory testing typically uses foundations rigidly connected to the laboratory floor or the shake table, consideration should be given to test configurations that would allow uplift at the foundation or base. At the same time, the potential impact of soil–structure interaction should be considered. It is not known whether it would be feasible to modify the test house details in response to these considerations, but consideration is encouraged.

Although masonry chimneys are common in single-family houses, it is recommended that chimneys not be included in the full-scale test houses. Creating tests from which meaningful conclusions could be drawn regarding damage to chimneys would be difficult at best and would greatly distract from the purpose of studying the effect of cripple wall retrofits. Contributing to this are the variability in construction and condition of chimneys, the variability of base fixity conditions, and the very complex interaction that is thought to occur between chimneys and houses.

#### **B.4.2 Pre-Test Survey**

Prior to start of testing, an effort might be made to review existing house construction to identify the details that are most prevalent. This might be done in the field or from existing databases such as the photo database collected by the CEA from the Earthquake Brace and Bolt project. This information might be used in selection of most appropriate construction details for the test houses.

#### **B.4.3 Documentation of Full-Scale Test House Design**

Detailed structural and architectural construction documents will need to be developed for the test houses. These documents will serve a dual purpose: (a) allowing the development of consensus regarding appropriate design and detailing of the test houses, informing those interested in the loss estimations aspects; and (b) serving as a record of the tested configuration following testing. As previously noted, there are plans prepared for the PEER–CEA Project Loss Estimation Workshop that could serve as a starting point; see Figures B.1, B.2, and B.3. The workshop brought to light the significant amount of detail needed to adequately communicate with loss estimation professionals; this documentation will help serve that need.

#### **B.4.4 Damage States of Interest**

Other recommendations for future full house testing include developing descriptions of the damage states to be studied in the testing. This effort could start from the damage states developed for the PEER–CEA Project Earthquake Damage Workshop. This included four damage states ranging from minor cosmetic repairs to total loss of the dwelling.

#### **B.4.5 Testing Protocol**

It is important that detailed consideration be given to the testing protocol. Items for consideration include the selection, scaling, quantity, and sequence of ground motions. Decisions regarding the protocol will be critical in deciding how many test houses are needed or what extent of testing can be conducted with the available house or houses. It is desirable to collect performance information for a range of ground-motion levels, starting with very moderate levels and extending through incipient collapse. It is important to consider whether it is appropriate to use a series of increasing ground-motion levels on a single house; while this is convenient to do so, it means that the house will incur incremental damage rather than starting each shake from an undamaged condition. Also important is the decision of whether or not to test to incipient collapse. Once this level has been reached, it is generally impractical to conduct further testing on that specimen.

#### **B.4.6 Documentation of Testing**

It is recommended that extensive instrumentation and photographic and video documentation be collected during the course of the testing. In order to have video of most use to the CEA for education and outreach activities, it is suggested that the involvement of professional videographers be considered. Photographic and video documentation might include a combination of overall house response and detailed documentation of damage behaviors such as cracking on finish materials.

### **B.5 RECOMMENDED CONCURRENT WORK**

The primary objective of testing conducted as part of the PEER–CEA Project was to provide information to WG5’s numerical modeling efforts and WG6’s loss modeling efforts. The benefits of physical testing of full-scale houses could be significantly amplified by including concurrent work to interpret the results of the physical testing relative to the numerical modeling and loss estimation studies. Following are elements that we recommend be included to complete the research.

#### **B.5.1 Numerical Modeling**

It is recommended that a numerical modeling component be included. This would include both pre-test predictions of load deflection behavior and damage states, and post-test numerical comparisons. Pre-test modeling would be useful to help guide the selection of shake table test motions, while post-test modeling offers an important step in interpretation of the new data relative to the PEER—CEA Project numerical modeling. As part of a numerical modeling component, it

is recommended that a blind-prediction competition be considered; this can be an effective way to get broader engagement in the testing and numerical modeling efforts.

### **B.5.2 Damage Assessment**

It is recommended that a damage assessment component be included. This could include revisiting a number of steps in the process of identifying damage and developing repair costs. It could involve damage assessment of the test houses by damage assessment professionals. It could also potentially involve trial use of newly revised damage assessment guidelines. During the Earthquake Damage Workshop, it was learned that insurance adjusters will generally seek very detailed information (photographs, etc.) on the damage conditions as a basis for their repair estimates. Full-scale building testing would afford an opportunity for either a very detailed set of photographs to be developed, or for some of the adjusters to observe the damage firsthand. Full building testing might also afford a case study to revisit the topic of the ability to repair severely racked cripple walls, which received significant consideration during the PEER–CEA Project.

### **B.5.3 Loss Modeling**

It is recommended that a loss modeling component be included. In parallel with the other two recommended activities, it is recommended that a component be included to obtain loss estimates and interpret these relative to the PEER–CEA Project developed loss estimation tools.

## **B.6 CONSIDERATIONS REGARDING COST AND SCHEDULE**

The full-scale house testing described in this appendix chapter is acknowledged to be a significant undertaking. It will be important that sufficient time be allotted for detailed planning of the testing program in order to get the best benefit from the efforts and investment. We recommend that this program be planned as a multi-year (two- to three-year) project. The cost of the project could vary significantly depending on what elements the CEA should choose to include. It is noted that physical testing costs may benefit from complementary donations (if available) from industry. Should all recommended elements be included, the costs could be roughly estimated to be on the order of the current PEER–CEA Project.

## **B.7 CONCLUSIONS**

There is significant benefit that could result from the conducting of full-scale house testing. Conducting of such testing would be very timely as a capstone to the large effort just invested in the PEER–CEA Project. There are significant synergies that could occur if testing is conducted soon, in that currently used analytical modeling methods and models, and loss estimation models could readily be reused and possibly further improved should full-scale house testing occur in the near future.

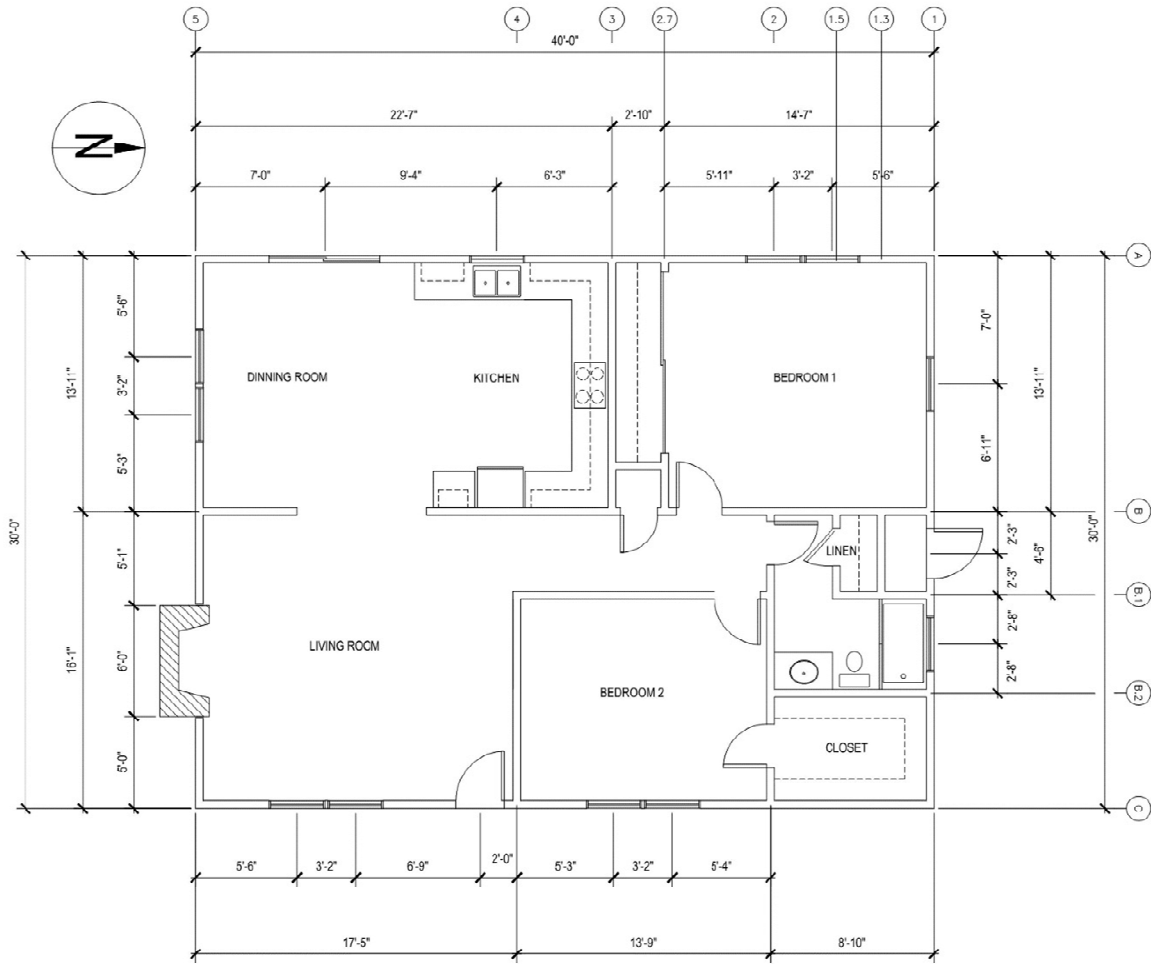


**Figure B.1 PEER-CEA Project Earthquake Damage Workshop Case Study Building 1 and Case Study Building 2 plan [Vail et al. 2020]**

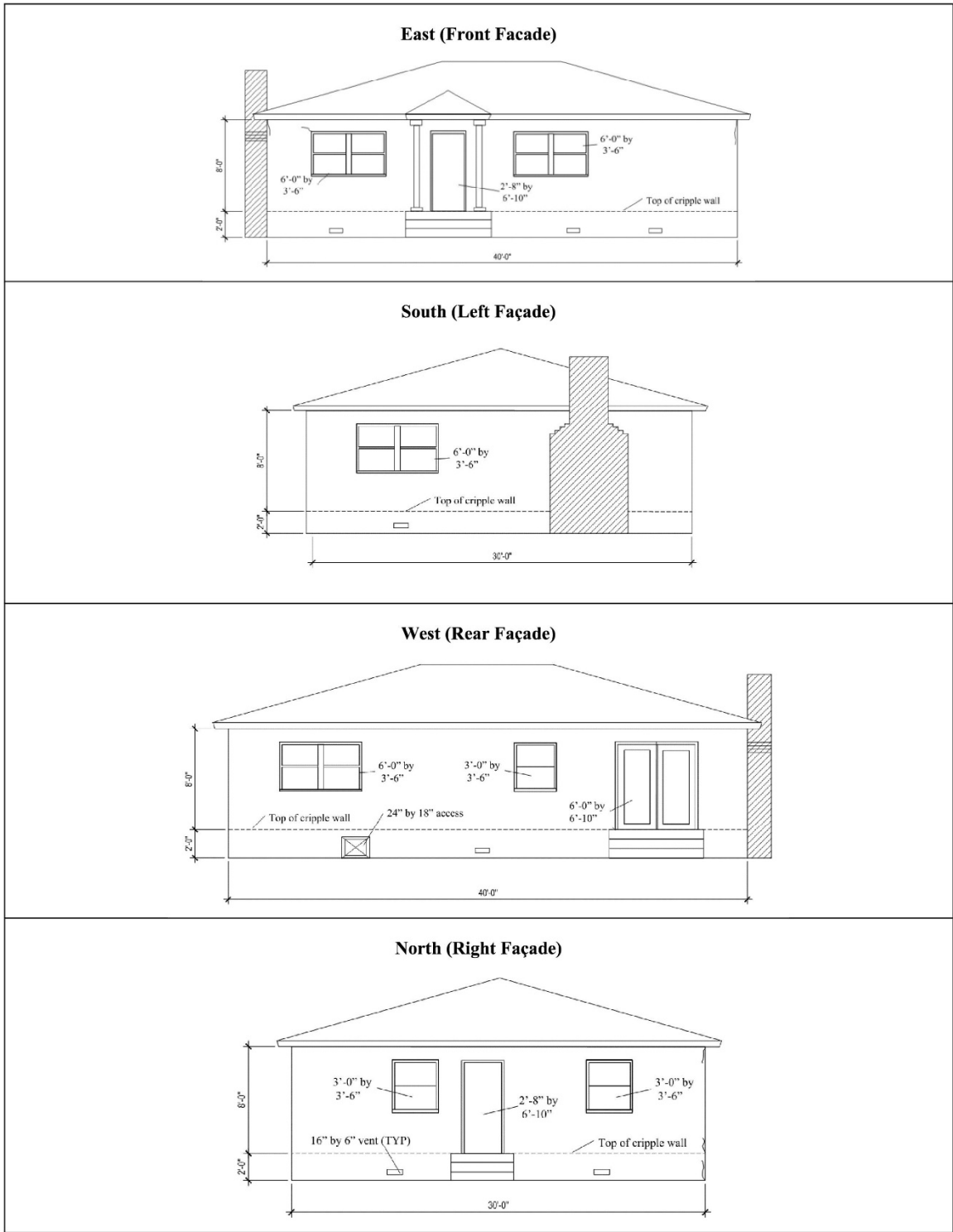


**Figure B.2 PEER-CEA Project Earthquake Damage Workshop Case Study Building 1 exterior elevations [Vail et al. 2020]**

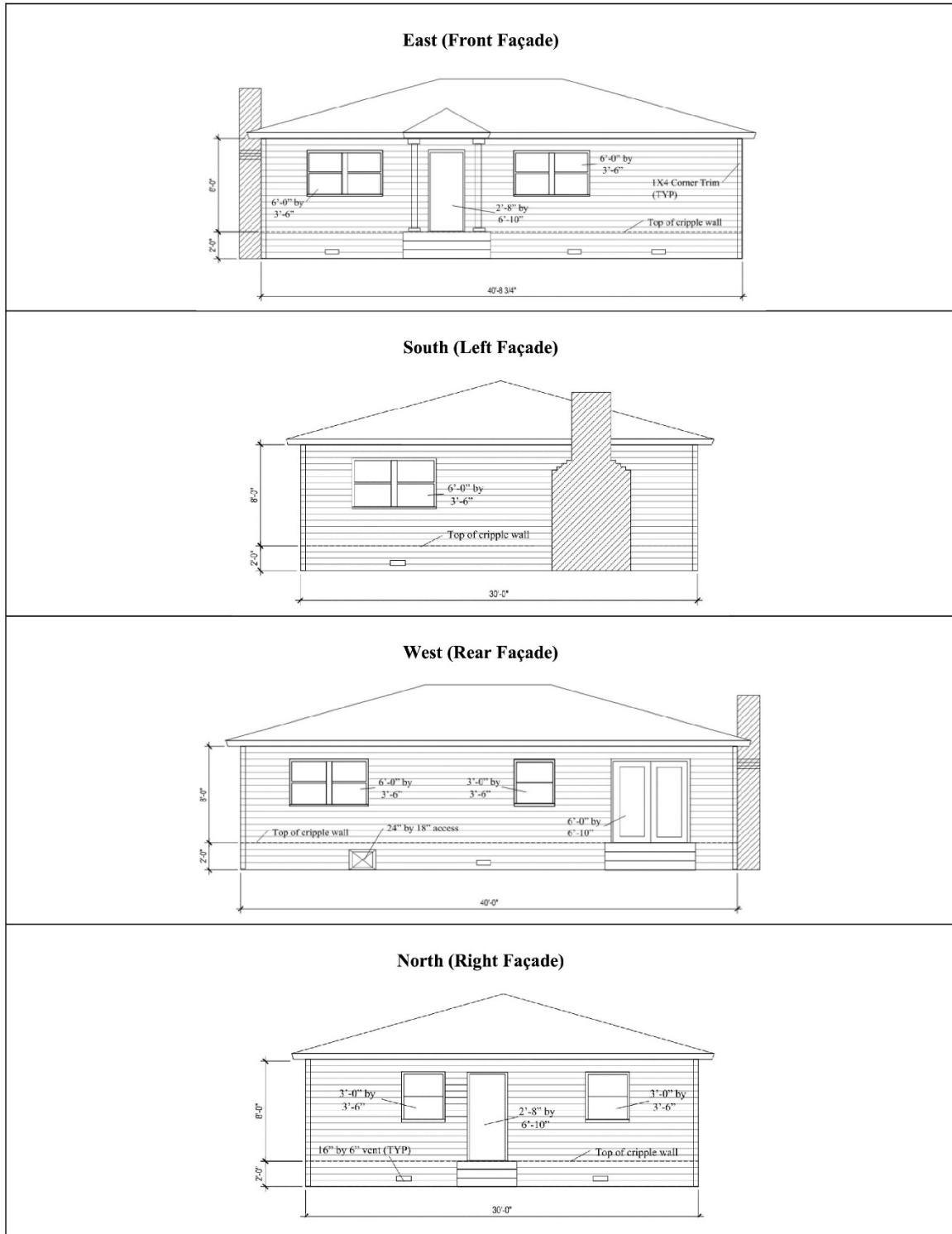


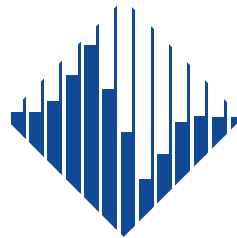
**Figure B.3 PEER-CEA Project Earthquake Damage Workshop Case Study Building 2 exterior elevations [Vail et al. 2020].**



The Pacific Earthquake Engineering Research Center (PEER) is a multi-institutional research and education center with headquarters at the University of California, Berkeley. Investigators from over 20 universities, several consulting companies, and researchers at various state and federal government agencies contribute to research programs focused on performance-based earthquake engineering.

These research programs aim to identify and reduce the risks from major earthquakes to life safety and to the economy by including research in a wide variety of disciplines including structural and geotechnical engineering, geology/seismology, lifelines, transportation, architecture, economics, risk management, and public policy.

PEER is supported by federal, state, local, and regional agencies, together with industry partners.



#### **PEER Core Institutions**

University of California, Berkeley (Lead Institution)  
California Institute of Technology  
Oregon State University  
Stanford University  
University of California, Davis  
University of California, Irvine  
University of California, Los Angeles  
University of California, San Diego  
University of Nevada, Reno  
University of Southern California  
University of Washington

PEER reports can be ordered at <https://peer.berkeley.edu/peer-reports> or by contacting

Pacific Earthquake Engineering Research Center  
University of California, Berkeley  
325 Davis Hall, Mail Code 1792  
Berkeley, CA 94720-1792  
Tel: 510-642-3437  
Email: [peer\\_center@berkeley.edu](mailto:peer_center@berkeley.edu)

ISSN 2770-8314  
<https://doi.org/10.55461/IYCA1674>